UNIVERSITY OF
BIRMINGHAM

Integrated Condition Monitoring of Industrial Wind Turbines

PhD Thesis

By

Siavash Hajiabady

A Thesis Submitted to the University of Birmingham

For the degree of

DOCTOR OF PHILOSOPHY

School of Metallurgy and Materials
College of Engineering and Physical Sciences
The University of Birmingham

November 2017

Abstract

The continuous growth in wind turbine power ratings and numbers has led to increased demands in inspection and maintenance due to the more significant financial and operational consequences of unexpected wind turbine failure. The fact that wind farms are commonly located at remote sites with potentially poor accessibility means it is necessary to reduce the need for corrective maintenance through evolution to preventive and prognostic maintenance activities. Prognostic repair schedules can be employed in order to optimise maintenance and contribute to the minimisation of the overall operational costs of wind farms.

The present study presents the development and qualitative evaluation of remote condition monitoring methodologies for the evaluation of the wind turbine power electronics and gearboxes. The failures of power converter and gearbox components result in significant wind turbine downtime and associated repair costs. Effective condition monitoring can enable the timely diagnosis of faults in order to prevent unexpected failures and loss of electricity production, contributing towards a noteworthy increase of the reliability, availability, maintainability and safety (RAMS) of wind farms. By understanding better the effect of various factors on the degradation rate of power converter and gearbox components prognosis of the remaining lifetime may be possible in the future helping wind farm operators to optimise Operation and Maintenance (O&M) expenditure.

Failure of the Insulated-Gate Bipolar Transistors (IGBT) leads to the overall power converter failure, causing the wind turbine to become inoperable unless more than one power converters are used in the design. There are many possible failure modes of IGBTs, but a common feature of many of the modes is that they are driven by a thermal cycling fatigue. Gearboxes can also fail through various failure modes affecting gears, bearing and shafts.

Within this study two customised test rigs have been employed to simulate various of faults and assess the capability of RCM in diagnosing these faults effectively. In addition field measurements have been carried out and correlated to the findings of the test rig experiments. From the results obtained it has been concluded that failures are highly random due to material-related factors in conjunction with the driving mechanisms of structural degradation. Although effective diagnosis is within reach, prognosis remains very difficult as a higher level of quantification of the variables influencing degradation is required. Moreover, the contributing levels of these variables to the overall gradual degradation of power converter electronic and gearboxes is not yet understood. In this study, it has been possible to identify these variables qualitatively, but the quantitative investigation is still pending and will be most likely the subject of several future studies in this field. The present thesis provides a compact summary of the analysis of the key findings of the experimental work performed within the context of the OPTIMUS FP7 European collaborative project.

Acknowledgments

I would like to express my deepest sincere appreciation to my supervisor, Dr Mayorkinos Papaelias for his valuable advices, suggestions, guidance, patience and constructive critics through the completion of my thesis work. Without his constant encouragement and support, this work would not have been possible and accomplished.

A very especial thank to Dr Stuart Hillmansen and Dr Farzad Hayati who have been supporting me all this time with their technical expertise. It is always a great feeling to have a knowledgeable and helpful person like you.

My sincerest thanks are extended to all my friends. Thanks for their constant support and contributions.

A very special note of appreciation to my supportive and understanding family, thanks for supporting me with all your love during the days of intensive work.

Table of Contents

List of Figures

List of Table

Symbols and Abbreviations

Symbol	Definition
A	Cross-sectional area of the wind being measured (m2)
AC	Alternating current
AE	Acoustic Emission
CM	Condition monitoring
CMS	Condition monitoring systems
CT	current transducer
DC	Direct Current
DFIG	Doubly- fed induction generators
EMI	Electromagnetic Interference
FFT	fast Fourier transform
GW	Gigawatt
GFRP	Glass-fiber reinforced plastic
GMF	Gear Mesh Frequency
Hz	Frequency
IGBT	Insulated-Gate Bipolar Transistors
kW	Kilowatts
KPIs	Key Parameter Indicators
LCOE	Levelised Cost of Electricity
MW	Megawatt
MV	Medium voltage
MCSA	Motor Current Signature Analysis
MOSFET	Metal Oxide Semiconductor Field Effect Transistor
NDT	Non-destructive testing
O&M	Operating and Maintenance
P	Power (W)
PWM	Pulse Width Modulation
RPM	Revolutions per minute
RCM	Remote Condition Monitoring
Rpm	Revolution per minute
RBSOA	Reverse Bias Safe Operating Area
SCSOA	Short Circuit Safe Operation Area
T	Temperature ℃
V_{cc}	Input voltage
Vout	Output voltage
V	Velocity of the wind within the measured cross section (m/s).
Vca	Voltage of generator and Voltage gird
P	Air density

List of publication

S. Hajiabady, S. Kerkyras, S. Hillmansen, P. Tricoli, M. Papaelias, Efficient diagnostic condition monitoring for industrial wind turbines, Conference: 3rd Renewable Power Generation Conference (RPG 2014), At Napoli, Italy

S. Hajiabady, S. Hillmansen, M. Papaelias, Condition Monitoring of Power Electronics in Wind Turbines, 11th International Conference on Condition Monitoring and Machinery Fault Prevention Technologies (CM2014), At Manchester, United Kingdom

Siavash Hajiabady, E.J. Camacho, F. Polo, Mayorkinos Papaelias, Integrated Condition Monitoring of Industrial Wind Turbines – The OPTIMUS project, The Twelfth International Conference on Condition Monitoring and Machinery Failure, Prevention Technologies, from sensors through diagnostics and prognostics to maintenance CM 2015, At Oxford, UK

V L Jantara Junior, J Zhou, S Roshanmanesh, F Hayati, **S Hajiabady**, H Dong, H Basoalto, X Y Li, F P Garcia Maquez, A P Marugan, V Kappatos, L Constantinou, Z Q Lang and M Papaelias. Driving forward wind turbine industrial standards on gearbox materials, maintenance, remaining lifetime assessment and condition monitoring methodologies, 56th Annual British Conference of Non-Destructive Testing, At the International Centre, Sep 2017, Telford, UK

Valter Jantara Junior, Jun Zhou, Sanaz Roshanmanesh, Farzad Hayati, **Siavash Hajiabady**, Xiao Ying Li, Hanshan Dong and Mayorkinos Papaelias, Evaluation of damage mechanics of industrial wind turbine gearboxes, Insight -Non-Destructive Testing and Condition Monitoring, August 2017, 59(8):410-414 ·

Valter Jantara Junior, Jun Zhou, Sanaz Roshanmanesh, Farzad Hayati, **Siavash Hajiabady**, Xiao Ying Li, Hanshan Dong and Mayorkinos Papaelias, New IoT technology set to maximise machine efficien**cy,** Insight • Vol 59 • No 8 • August 2017

Junior, Jun Zhou, Sanaz Roshanmanesh, Farzad Hayati, **Siavash Hajiabady**, Xiao Ying Li, Hanshan Dong and Mayorkinos Papaelias, Evaluation of Damage Mechanics of industrial wind turbine gearboxes**,** First World Congress on Condition Monitoring, June 2017,Valter Jantara

Jun Zhou, Sanaz Roshanmanesh, Farzad Hayati, Valter Jantara Junior, Taoran Wang, **Siavash Hajiabady**, Xiao Ying Li, Hector Basoalto, Hanshan Dong and Mayorkinos Papaelias, Improving the reliability of industrial multi-MW wind turbines, , Insight - Non-Destructive Testing and Condition Monitoring, April 2017, 59(4):189-195

Jun Zhou, Sanaz Roshanmanesh, Farzad Hayati, Valter Jantara Junior, Taoran Wang, **Siavash Hajiabady**, Xiao Ying Li, Hector Basoalto, Hanshan Dong and Mayorkinos Papaelias, Increasing the reliability of industrial multi-MW wind turbines, NDT 2016, East Midlands Conference Centre and Orchard Hotel, Nottingham, UK

J. Camacho Questa, V. Requena Montejano, F. Polo, L. Moreno, T. Vanhnonacker, B. Stalaart, A. Karyotakis, O. Panagoiliopoulos, V. Karakassidis, Z.-Q. Lang, C. Roldan De La Cuadra, M. Murillo Calleja Iosu, E. Oses, G. Auer, I. Zalacain, J. Errea Mugica, F. Garcia Marquez, D. Pedegral, D. Lee, S. Hillmansen, P. Tricoli, **S. Hajiabady**, G. Fernando and M. Papaelias, Optimisation of operational reliability of large-scale industrial wind turbines, Renewable energy offshore- guides sources (Ed), 2015 Taylor& Francis Group. London,

CHAPTER 1

INTRODUCTION

1.1 Introduction

Utility-scale wind turbines are very complex systems consisting of a variety of critical structural parts, such as the tower, blades, rotor hub and foundation and functional components including the main shaft, gearbox, generator, power electronics, yaw, sensors, brake mechanism, controller, anemometer and others. Development of faults in any of the aforementioned sub-systems or components can result in unnecessary downtime and associated costs due to the loss of production and emergency maintenance requirements. Depending on the type of component and developing fault, the effect on the overall downtime, repair timescale and financial losses can vary significantly. Figure 1 shows different part of wind turbine.

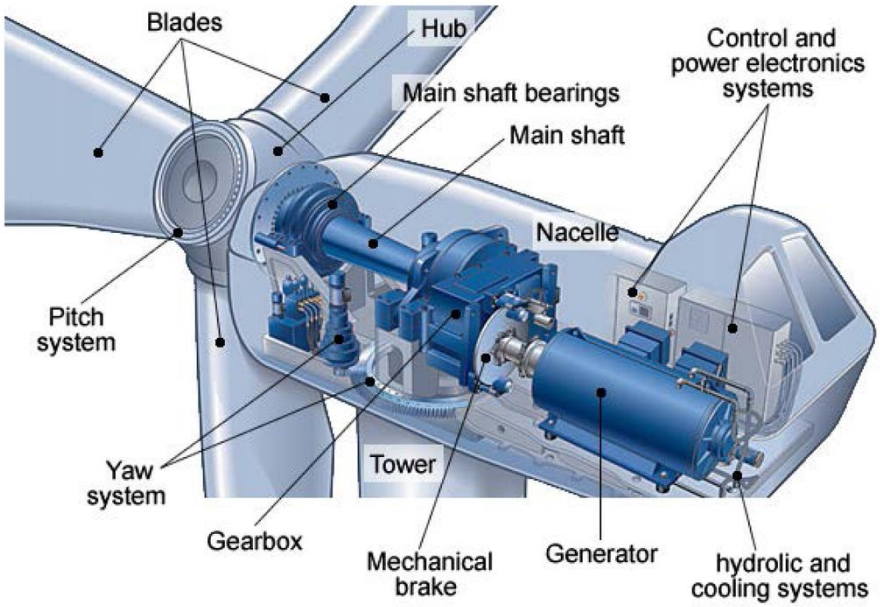

Figure 1 Wind turbine components [1]

Certain types of wind turbine faults can cause extensive collateral damage to other components or even result in complete loss of the wind turbine. More specifically a single overheating bearing in the gearbox or generator can lead to combustion of the lubricating oil. Consequently, the uncontrolled oil fire breakout will lead to catastrophic loss of a multi-MW wind turbine. Failure of the braking mechanism under windy conditions may also lead to catastrophic

structural failure of the blades and subsequently the wind turbine itself. Thus, gearbox faults may result in far longer downtime and maintenance costs than faults associated with power electronics or sensors. Although wind turbine manufacturers and operators demand that the gearboxes are designed for a minimum operational lifetime of twenty to twenty-five years, this target is rarely achieved. Therefore, wind turbine operators face gearbox refurbishment or even replacement costs at least twice or thrice within the anticipated design operational lifetime. For this reason, wind farms are financially planned taking into consideration gearbox replacement and associated downtime costs.

Although repair of faults in power electronics is less demanding, simpler and faster to repair, accessibility issues, particularly in the case of offshore or remotely located onshore wind farms, means that cumulative downtime can have significant contribution to the losses of power production occurring. As a result, there has been an ever-increasing requirement for remote condition monitoring and early prognosis of incipient faults in power electronic components. Although gearboxes are routinely monitored this is not a widespread practice in the case of power electronics.

The growing effects of global warming are a serious threat to the international economic and societal stability. The strong growth in the amount of energy provided by renewable energy sources and wind energy in particular contributes substantially into the meaningful reduction of greenhouse emissions as a primary tool for mitigating climate change [2]. Over the last three decades, wind energy has experienced substantial growth rates becoming the most important renewable energy source [3]. As of late 2017, more than 500 GW of wind energy projects had been installed worldwide with more projects being constructed both onshore and offshore. Wind energy industry has seen strong annual growth trends since the Kyoto Protocol was

signed in Japan, 1997 [4]. The decisions of the Kyoto Protocol were promoted further during the United Nations Bali Convention in 2007 emphasising the need for the decarbonisation of the international economy before the end of the twenty-first century and further enhancing investments in the wind energy industry [5].

The majority of wind turbines are built currently onshore. However, since the beginning of the new millennium more and more wind farms are built in offshore locations. Europe has so far been the leader of exploitation of offshore wind energy. More recently, other countries, including China, the U.S., Brazil and Korea, have also begun looking into offshore projects more closely.

Industrial scale wind turbines have traditionally been based on the three-blade horizontal axis geared design. However, due to the gearbox problems that have not been fully resolved to date, the industry has also been investing considerably in direct-drive designs which do not employ gearboxes. However, direct-drive wind turbines tend to have more complex power electronics which is currently also a part of the turbine prone to frequent failure. Direct-drive designs have heavier nacelles since they employ up to ten times more magnets than geared designs. Magnets are a commodity, which is imported by several countries. Therefore, magnet prices can significantly influence the final price of a direct-drive wind turbine. In addition, the rotor of direct-drive wind turbines needs to spin faster in order to enable the generator to reach adequate revolutions per minute (RPM) for electricity production. This results in higher stresses being sustained by the rotor and more torque is passed directly to the rotor and generator bearings. Approximately 70-75% of all wind turbines are geared. However, due to the significant gearbox problems encountered in offshore wind farms located in the North Sea, several offshore wind farms have employed direct-drive designs instead. So far almost 15 GW of total

offshore wind energy cumulative capacity has been commissioned. The vast majority of the projects have been constructed in the North Sea with the UK being the world leader in this sector. Other countries with considerable investments in offshore wind energy include Denmark, Germany, Sweden, the Netherlands, Belgium and Norway. Offshore wind farms currently represented 7-8% of all annual wind energy projects constructed in Europe. However, the EU is unlikely to achieve the 40 GW installed capacity target set for 2020.

1.2 Operational principles of industrial wind turbines

Wind turbines are designed to harvest the kinetic energy of the wind through the rotational movement of the blades. Subsequently, the rotor rotates the shaft whose speed is multiplied through the gearbox. The wind turbine gearbox apart from increasing the rotational speed of the generator it also reduces the torque applied. Industrial wind turbines since they are supposed to be installed in remote and relatively inaccessible areas should be maintained as little as possible throughout their intended lifetime. Moreover, whenever maintenance is required, it should be planned well ahead minimising production disruption and ensuring all maintenance activities occur during periods of low wind speeds. Therefore, maintenance should be planned and to the extent that it is possible predictive. Unfortunately, this is far from being realised yet. At the moment, wind farm operators rely heavily on corrective and emergency maintenance approaches which result in much higher electricity production prices. However, as competition intensifies the gradual shift to planned and predictive maintenance will need to be realised sooner than later to ensure wind energy projects being realised in the future remain financially viable. Figure 2 shows how does a wind turbine work.

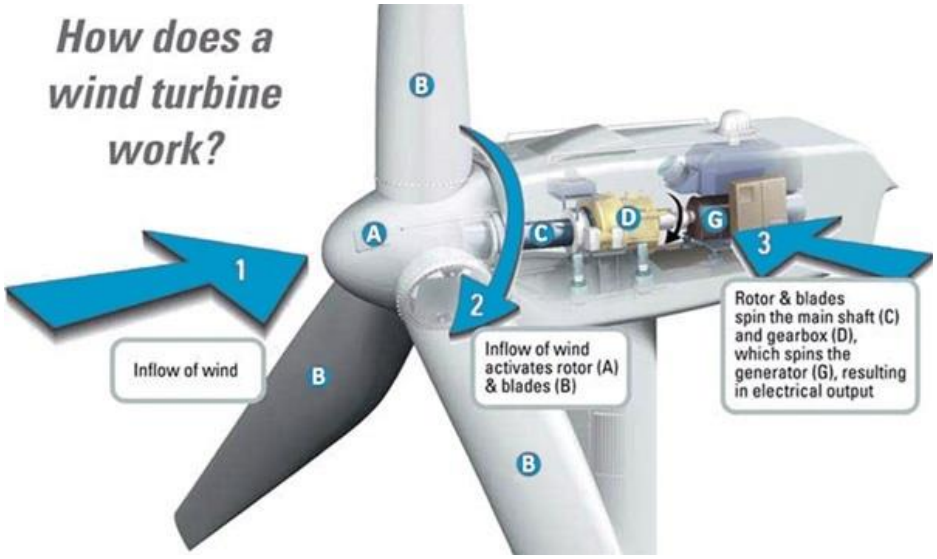

Figure 2 how does a wind turbine work [6]

Wind turbines operate under extremely adverse environments. Despite their simplistic appearance, they comprise numerous complex subsystems, rendering them also very complex as a global system. Maintenance activities are required to ensure that all parts of the wind turbine are healthy in order to enable it to operate as intended throughout its entire design lifetime. The fundamental principles of maintenance theory dictate that maintenance activities should make use of minimal resources, ensuring the highest possible level of reliability and hence availability and productivity [7] [8]. Corrective maintenance should be avoided as much as possible due to the location of wind farms and the accessibility issues associated with it.

Operating and Maintenance (O&M) costs of onshore wind farms normally do not exceed 20-25% of the overall project Levelised Cost of Electicity (LCOE) [7]. Unfortunately, in the case of the offshore wind farms O&M costs can exceed 40% of the LCOE. This has a significant impact on the profitability of offshore projects and subsequently the investment potential in new projects is curbed.

Certain types of failures may result in significant damage to other components or even complete loss of the wind turbine. Despite the fact that power electronics fail most often, they

can be fixed quicker than a gearbox. However, accessibility issues should also be taken into account in calculating the total effort required.

The drive-train and power electronics are critical for the operation of industrial wind turbines. Faults developing in these components can result in long downtime and expensive repair costs, particularly when offshore wind farms are concerned. Effective Remote Condition Monitoring (RCM) of these components can result in significant savings for wind farm operators and contribute to a substantial improvement of the operational reliability of wind turbines.

According to the findings of the RELIAWIND FP7 project failure of power converter components account for about 20% of all wind turbine faults leading to significant downtime and repair costs. Effective condition monitoring, in which a prognosis of remaining life is made will permit a noteworthy reduction in Operation and Maintenance (O&M) expenditure. Figure 3 shows the failure rate and downtime from two large European survey of wind turbines.

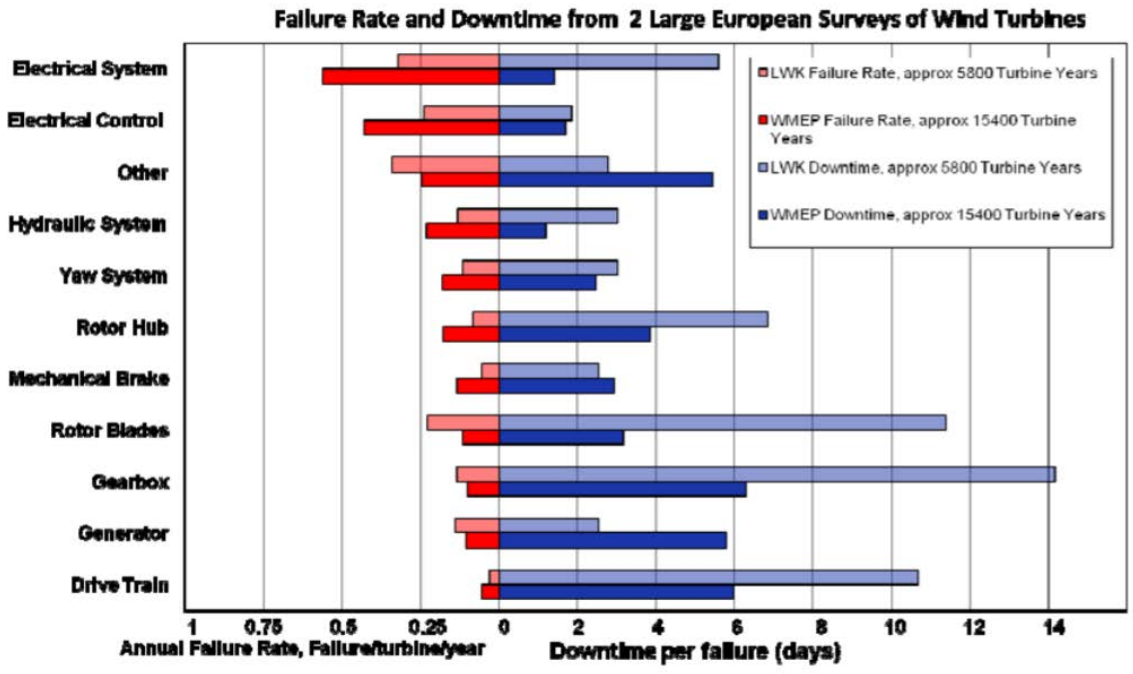

Figure 3 failure rate and downtime from two large European survey of wind turbines. [9]

Failure of the Insulated-Gate Bipolar Transistors (IGBT) leads to the overall power converter failure, causing the wind turbine to become operable unless more than one power converters are used in the design. There are many possible failure modes of IGBTs, but a common feature of many of the modes is that they are driven by a thermal cycling fatigue. One of the methods which can be utilised to estimate the life time of IGBTs is rainflow counting method. This algorithm coupled with an implementation of Miner's rule can be used to assess the remaining life of the component. There have been numerous advances to the rainflow algorithm with some going as far as to proposing certain modifications. Therefore, the rainflow algorithm can be used to estimate the IGBT remaining life time.

1.3 The importance of remote condition monitoring

For several years, RCM has been of utmost importance for the wind energy industry. Even insurance companies demand that some sort of RCM capability is present on each industrial wind turbine in order to accept their insurance. The readings of the RCM systems installed and the subsequent actions arising need to be presented to the insurance company when submitting a claim. This is to ensure that the wind turbine operators do all they can to prevent failure from occurring.

The gearbox has been one of the wind turbine sub-systems receiving the most interest from an RCM perspective. However, analysis of failure modes and downtimes of various wind turbine types and models has shown that other components can also have significant maintenance consequences resulting in loss of wind turbine availability and hence reduced capacity factor. As a result, there has been an increasing interest to monitor industrial wind turbines at a global level, i.e. evaluating remotely all critical components that can potentially cause downtime and result in reduced availability and productivity.

Power electronics are gradually increasing more interest due to the amount of downtime caused by faults of related subcomponents. However, monitoring systems for power electronics are yet to widely implemented. There is also a significant learning curve to be overcome in terms of identifying the exact reasons and mechanisms of failures and the different sub-components affected. Therefore, there is a clear need to identify the type of sensors, data acquisition strategy and signal processing methodology, which are appropriate for power electronics evaluation.

In the case of gearboxes, there is a strong need to translate the RCM data into exact damage level so maintenance scheduling can be optimised. However, due to the variability of loading conditions during wind turbine operation, this task is quite challenging. The fact that lubrication quality can also vary with time further varies to the complexity of the issue and enabling accurate trending of damage evolution with time.

Monitoring technologies play a crucial and necessary role in avoiding the possible evolution of faults to critical level resulting in unnecessary downtime, production losses and decreasing the potential risk of catastrophic failure [10].Hence, in recent years there has been a rapid growth in the use of RCM technologies for the purposes of fault detection, and diagnosis techniques in the industrial applications. This has not only been attributed to their usefulness in decreasing the likelihood of unexpected failure and improving maintenance planning capabilities, but also reducing O&M costs. The application of condition monitoring systems is also nowadays a basic requirement for insurance companies. The main advantages of the application of condition monitoring in wind turbines can be summarised to the contribution to the reduction of maintenance costs, enabling early fault detection, evolution prediction,

providing performance optimisation and improvements in reliability and minimising downtime leading to increased availability.

A wind turbine condition monitoring system must have capability of detection and evaluation of a fault being effectively precise and reliable. This enables the operator to order periodic maintenance or corrective maintenance based on feedback arising from condition monitoring system data [11]. Increasing the chance of fault detection as an early stage as possible along with identification of the faulty component has been an ongoing challenge in the industry while reducing false alarms to a satisfactory level [11]

1.4 Objectives and achievements

This PhD project presents the development of a novel methodology for condition monitoring of wind turbine power electronics and a novel modular CM system capable of diagnosing faults in the gearbox. The data analysis methodology and the key results arising from measurements on actual industrial wind turbines are also presented.

One of the primary objectives has been the evaluation of the types of faults affecting industrial wind turbine components and their relationship. Also to assess the mechanisms that lead to the occurrence of these faults, their nature and how they can interact with each other resulting into complex failure modes. It has also been of significant interest to obtain a good idea of the downtime caused by the different types of failure and the maintenance approaches currently employed by wind farm operators. The types of RCM systems used and the type of data generated as well as the reliability of the information gained in order to optimise maintenance activities and scheduling, i.e. how often false positive occurs in comparison with true positive cases.

As part of this project tests have been carried out on test rigs developed domestically as well as in collaboration with other researchers for simulating gearbox and power electronics faults. The data collected have been analysed using various algorithms and techniques which will be discussed subsequently in the present thesis. Furthermore, extensive tests and data have been collected from the actual wind turbines. A comparison between the knowledge gained from the test rig tests and the field data has been carried out. The instrumentation used, data acquisition parameters and signal processing algorithms employed are thoroughly presented and discussed together with the key results. The project has focused exclusively on the RCM of two key subcomponents of the wind turbine, namely the gearbox and power electronics.

The main results produced have proven that RCM techniques can be employed for the accurate analysis of the actual condition of the critical wind turbine components. Hence, RCM data can be used not only to avoid unexpected failures but also to plan maintenance based on the actual condition of the wind turbine. So far it has been shown that condition-based maintenance approaches can be successfully implemented. However, the reliable implementation of predictive maintenance strategies remains still elusive and there is a substantial amount of research required before such approaches can be adhered by the industry. This study has contributed towards understanding the requirements that will need to be addressed for predictive maintenance to be successfully employed by the wind energy sector in the future.

1.5Structure of the thesis

The present thesis is divided in eleven chapters. The present introductory chapter (Chapter 1) provides the general background behind this study and puts it in the context of the industrial need for the accurate online evaluation of multi-MW industrial wind turbines.

Chapter 2 discusses the main operational principles of industrial wind turbines, including various types and critical components. Chapter focuses on the power electronics employed in wind turbines, key subcomponents and modes of failure. Chapter 4 discusses the key operational principles of wind turbine gearboxes and the main types of failure modes. Chapter 5 presents the main approaches employed for remote condition monitoring of wind turbine power electronics and gearboxes. Chapter 6 discusses the experimental methodology employed for the tests carried out on the customised test rig developed as part of this study. Chapter 7 presents the main results acquired during the power converter tests and their analysis. Chapter 8 discusses the experiments carried out on the gearbox test rig together with the main results obtained. Chapter 9 presents the instrumentation employed for monitoring the power converter on actual industrial wind turbines together with the results obtained and analysis carried. Chapter 10 discusses the methodology used for monitoring industrial wind turbine gearboxes and the key results obtained together with the signal processing methodology employed. Finally, Chapter 11 presents the main conclusions drawn from the present study and proposes directions for future work to be carried out in this research field.

CHAPTER 2

WIND TURBINE OPERATIONAL PRINCIPLES

2.1 Wind energy for utility scale electricity production

Wind energy is one of the most beneficial, environmentally friendly and cost effective renewable energy sources. Provided suitable wind conditions are available and wind turbine operation is reliable without the occurrence of unexpected failures, wind energy projects can be profitable without the requirement for any governmental subsidisation. Wind energy is a true alternative to fossil-based energy production although the integration of large amounts of wind power in the energy mix due to the variability of production arising from fluctuations in the wind is still a hot topic which needs to be addressed in the foreseeable future [12]. Figure 4 shows the Average hourly wind power availability by season (averaged over 34 years of wind speed data). Wind energy is generated using large multi-MW onshore and offshore wind turbines which can be based on Vertical or Horizontal Axis designs. Three-bladed Horizontal Axis wind turbines are the most common and can be categorised to geared (design includes gearbox) and gearless (design is based on direct-drive) turbines.

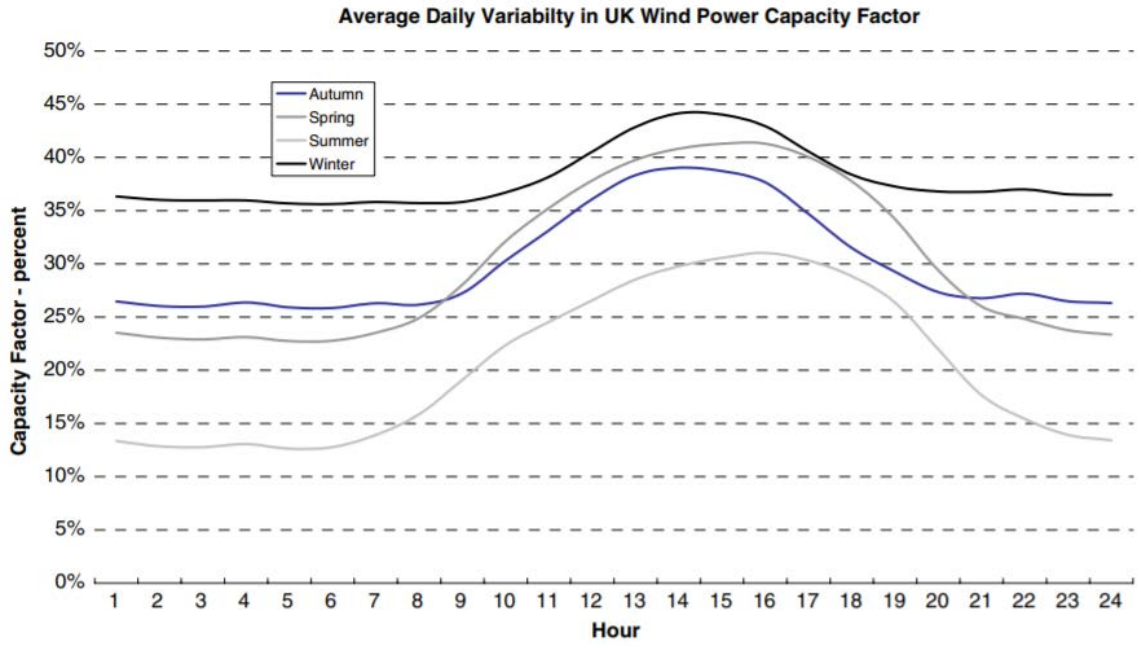

Figure 4 Average hourly wind power availability by season (averaged over 34 years of wind speed data). [13]

2.2 History of wind energy

The history of wind energy goes back to the antiquity where wind mills were used for grain-grinding and water pumping. Mathew [14] lists different concepts of using wind energy in order to generate mechanical power. Wind power has been considered to have been initially used for irrigation by the Babylonian Emperor Hammurabi in the seventeenth century B.C. Others argue that the birth place of wind mills was India [15]. A classic work shows that wind power was used for lifting water back in the fourth century B.C. In Persia wind mills have also been known to be used for grinding grains since 200 B.C. [14].

Wind mills of the antiquity were designed and built using basic materials, normally stones and bundles of reeds or wood. Their designs were simple based on vertical or horizontal axis machines. Stones or wood were used for the construction of the foundation, and bundles of reeds or wood were used to make sails for the rotor. The grinding stones were attached to the main shaft and rotated with the rotation of the rotor.

Figure 5 Old Wind Mill [15].

In mid-Eighteenth Century, wind turbines were applied for the first time to agricultural use [14]. The design involved smaller rotors using metallic blades, which were used for pumping water from several metres below the surface of the ground.

Wind energy in modern times is predominantly used for utility scale production of electricity. In 1887, Scottish Engineer James Blyth developed a prototype vertical axis wind turbine in order to generate the necessary power to charge a battery for lighting his summer house. During the same year, Charles F. Brush built the first automatic wind turbine in Cleveland, U.S. The Cleveland wind turbine was 18 metres tall, weighed 3.6 tonnes and had a maximum power rating of 12 kW (figure 6).

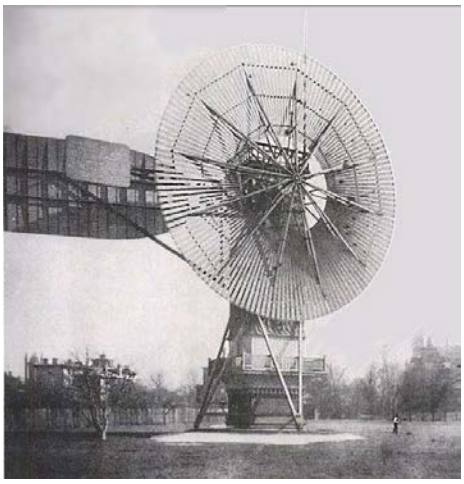

Figure 6 The Cleveland 12 kW wind turbine [16]

Another, large-scale for that time period, wind turbine used for electricity production, was constructed in Denmark in 1890. This wind turbine operated for 20 years, and its rated power was 12 kW [14]. Since then, more and more wind turbines with bigger power production capacity have been constructed. The first utility-scale system was a 100 kW turbine that was built in Russia in 1931. The Russian wind turbine generated the equivalent of about 20,000 kWh of electricity within two years.

The first MW-rated wind turbine was a 1941 Smith-Putnam model with a maximum power rating of 1250 kW which was installed in Vermont, U.S. The Smith-Putnam MW wind turbine was able to operate only for 1100 hours before suffering a critical failure [14]. As World War 2 was raging at the time, the necessary materials to repair the damage were deemed to be too

valuable to be sacrificed for the repair of the wind turbine. Therefore, it had to be subsequently decommissioned due to lack of the necessary raw material resources to repair the damage suffered.

Figure 7 The Smith-Putnam MW wind turbine built in Vermont, U.S.A. in 1941[Source: NREL].

After World War 2 wind energy production did not see much development until the early 1980s when the first small-scale utility wind farms begun to be constructed. These wind farms employed wind turbines capable of producing 15-20 kW. In 1982, the first hybrid power generation system in the world involving a wind farm, was built on the island of Kythnos in the Aegean Sea, Greece. It consisted of five 20 kW wind turbines, a 100 kW photovoltaic park and a diesel generator. The renewable energy component of the Kythnos hybrid power plant contributed up to 25% of the total energy mix of the island [17]. Subsequently, wind turbines begun to grow in size. As the surface area of the blades increases so the maximum amount of energy production potential. The first MW-rated wind turbines were commissioned in the 1990s. In 2017, the wind turbine with the highest power rating commercially available is the Vestas V-164 model which is capable of producing 9.5 MW of electricity. The V-164 model has a blade size of approximately 81 metres. Figure 8 shows Various models of modern

Horizontal Axis Industrial Wind Turbines used for electricity production in a utility-scale wind farm and figure 9 shows Growth of industrial scale wind turbines over the years.

Figure 8: Various models of modern Horizontal Axis Industrial Wind Turbines used for electricity production in a utility-scale wind farm [18].

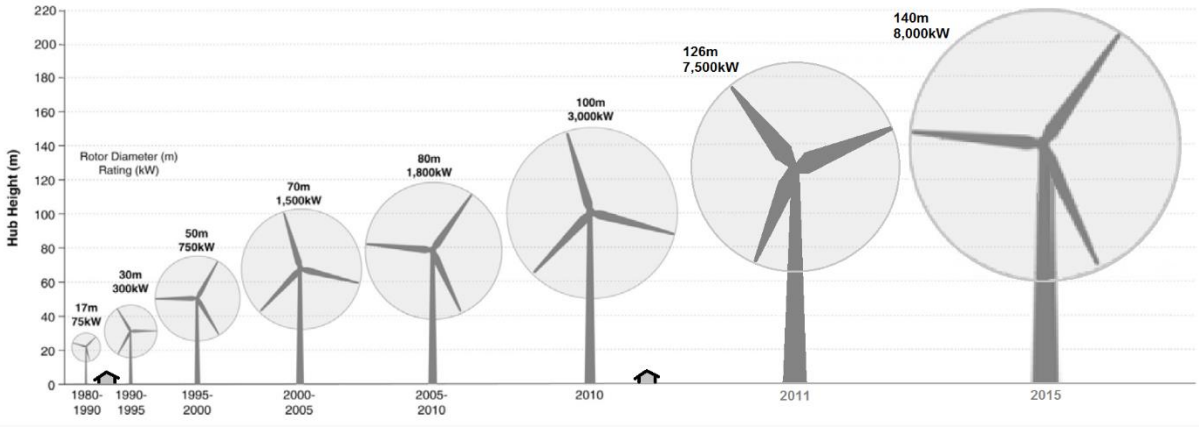

Figure 9 Growth of industrial scale wind turbines over the years [19]

The power generated from harvesting the kinetic energy of the wind is directly related to the wind's velocity. This relationship is represented mathematically as equation 2-1: [20] .

$$P = 1/2 \times p \times A \times V^3 \qquad (2\text{-}1)$$

P = wind power (W),

ρ = air density (typically 2.70 lb/m3 [1.225 kg/m3] at sea level and 59°F [15°C]),

A = cross-sectional area of the wind being measured (m2),

V = mean velocity of the wind within the measured cross section (m/s).

It is obvious from the equation that, wind power is affected by three main elements which are air density, cross-section area of the blade, and velocity of the wind.

2.3 Modern wind turbine design

Wind turbines are complex systems consisting of a variety of critical components as discussed previously. Depending on the type of component concerned type of fault occurring the total downtime and production losses caused, as well as the spare parts, equipment and human resources required to carry out the repair can vary significantly. Figure 10 shows the key components of a typical utility-scale wind turbine.

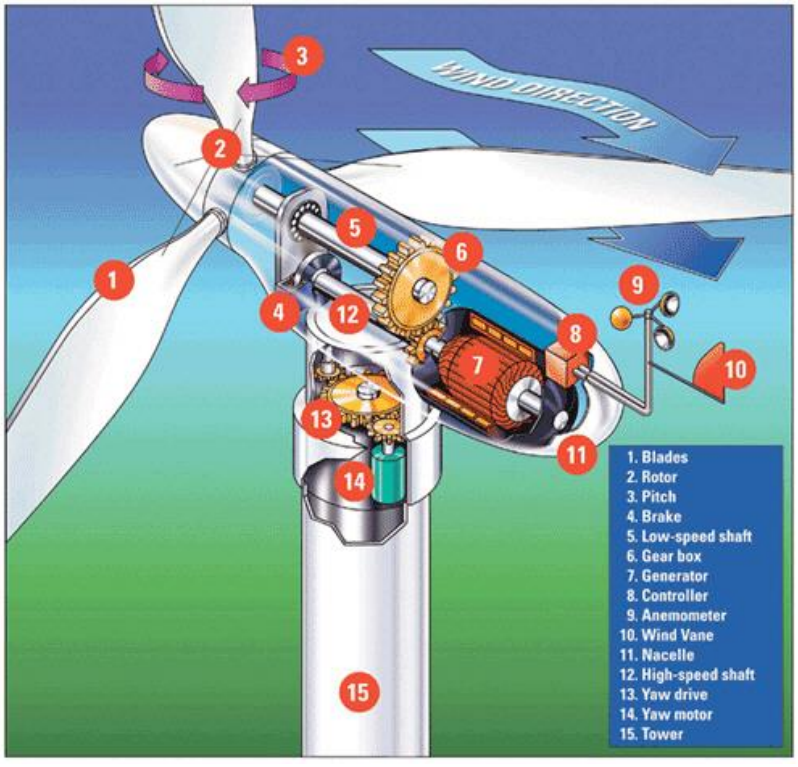

Figure 10 Wind turbine components [21].

2.3.1 Tower and foundation

The tower is the structure which supports the nacelle and rotor of the wind turbine. Its height is important as it allows the blades to be exposed to wind streams which are more consistent in quality. The thickness of the steel plate used for the construction of the tower depends on the power rating of the wind turbine. As wind turbines grow bigger and heavier, thicker plates are required. This makes the welding process more challenging.

The tower is installed on the foundation which is normally made of reinforced concrete. The foundation together with the tower, are responsible for ensuring the stability of the entire structure. Excessive vibrations or movement can cause deterioration of the performance of the wind turbine. In addition, they can result in fatigue cracks developing in the tower and less frequently to the foundation. The tower compartment undergoes variable loading arising from the rotation of the rotor, nacelle movement and wind turbulence [22]. In almost all cases steel is used in a form of a tubular construction for industrial wind turbine towers installed onshore or offshore. The initiation and subsequent propagation of fatigue cracks can result in structural failure and loss of the wind turbine as shown in figure 11.

Figure 11 Collapsed wind turbine in Scotland in 2008 [Image Source: The Guardian].

2.3.2 Wind turbine rotor

The kinetic energy of the wind is harvested by the blades converting it into circular mechanical motion which is then transferred into the gearbox and eventually to the generator. Wind turbine blades are usually made of glass-fibre reinforced plastic (GFRP) although carbon-fibre reinforced plastics (CFRP) are also used but to a much smaller extent due to their higher cost. Hybrid blade manufacturing based on the use of both materials is possible. In this case, the parts of the blade bearing the highest loads are made of CFRP and the rest of GFRP materials. The combination of wind forces, drag and pressure variations cause the blade to rotate. Up to the turn of the millennium, two types of blades were employed; stall and pitch-controlled. Stall tended to be inherently safer as they would break aerodynamically above a certain wind speed, normally in excess of 15 m/s. However, the stall design reduces the production potential of the wind turbine at favourable wind conditions and also allows for little control of the rotor. Pitch-controlled wind turbines are capable of adjusting their angle changing their exposure to the wind. Therefore, at high winds the wind turbine can still produce the power it is rated for by adjusting the pitch to a less favourable angle reducing the blade surface exposed to the wind.

Structural damage of the blades can arise due to fatigue-related issues, erosion (particularly in the leading edge due to impact with dust particles) or accidental impact damage and lightning.

2.3.3 Nacelle

The nacelle houses the key machinery of the wind turbine including the gearbox, generator, yaw system, rotor hub, breaking system, lubrication system, brake, etc. The nacelle is allowed to face at different directions through the yaw mechanism which consists of a bearing and gear. Nacelles are normally manufactured from GFRP due to the easiness moulding manufacturing offers, steel or aluminium alloys. With time fatigue cracks can develop, necessitating structural repairs. In the case of metallic-based nacelles corrosion can be a concern, predominantly in offshore environments.

2.3.3.1 Gearbox

The generator requires a minimum rotating speed of 1500 rpm to enable production of electricity. To convert the slow rotation of the blades (22 rpm) to 1500 rpm in the generator a three-stage gearbox is used in the majority of geared wind turbines. Larger machines such as the V-164 can make use of hybrid designs with intermediate operational speeds. Gearboxes consist of a variety of components including bearing, gears and shafts. The lubrication of the gearbox is a critical parameter affecting its overall operational lifetime and the intervals between maintenance.

2.3.3.2 Generator

In modern wind turbines two types of generators are commonly used, induction generators or synchronous with a full- scale of power factor and doubly- fed induction generators (DFIG) with a partially rated power converter. In those types of generators variable-speed reduces the

mechanical loading on the structural elements of the wind turbine [23]. Figure 12 shows simplified schematics of the wind turbine drive trains.

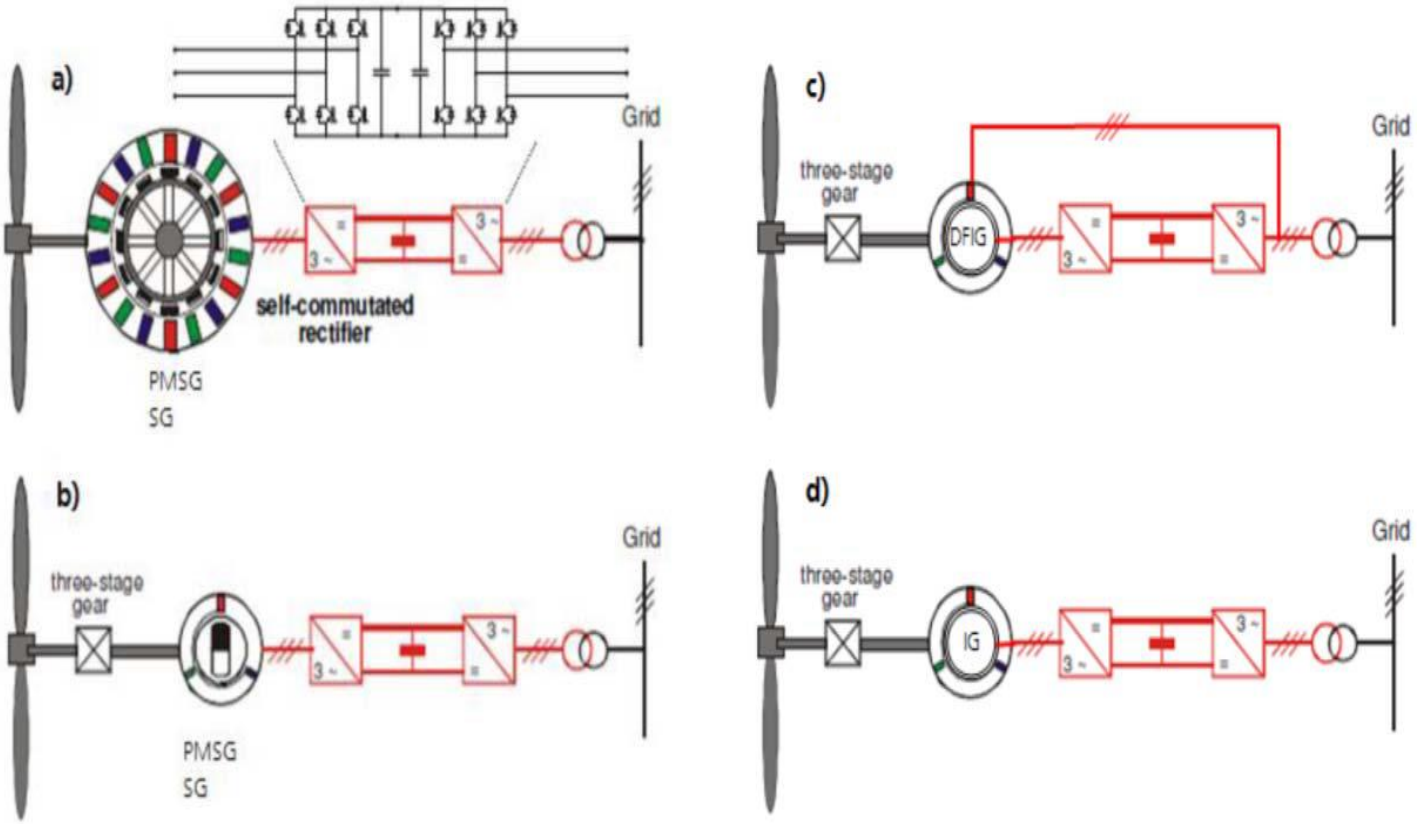

Figure 12 Common generator topologies: synchronous generator (left) or induction generator (right) with back-to-back voltage source converter [23].

2.3.3.3 Coupling and brake

A rigid connection exists between the transmission and the main shaft due to the massive torque sustained. The type of brake depends on the control mechanism for the blades, but they are usually based on hydraulic designs. The aerodynamic brakes at the tip of the blades should be considered separately.

2.3.4 Electronic equipment

Wind turbines have different types of electronic equipment consisting of sensors, the generator and power converter for feeding the electricity produced to the grid. Measurements of the wind speed, direction, operational temperature and several other parameters are performed using a variety of sensors which are normally placed inside or on the nacelle, and help control and monitor the basic operation of the wind turbine.

2.3.5 Supplementary components

Wind turbines contain various other components including sensors for following the wind direction, cooling, heating, lightning protection as well as lifting gear and fire extinguishing equipment.

2.4 State of the art

The growing effects of global warming are a serious threat to the global economic and societal stability. The strong growth in the amount of energy provided by renewable energy sources and wind energy in particular contributes substantially into the meaningful reduction of greenhouse emissions [24]. Wind is identified as the world's fastest growing energy source today and yet one of the most beneficial technologies and it has been used in different regions and several industrial countries in order to generate electricity. Figure 13 illustrates the top 10 of newly installed wind power capacity in 2015 in the world.

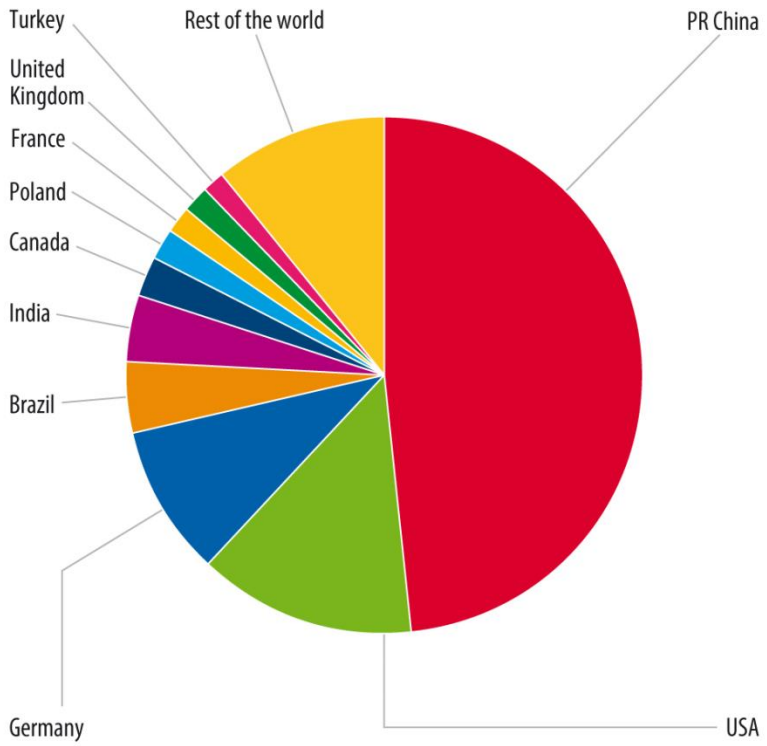

Country	MW	% Share
PR China**	30,500	48.4
USA	8,598	13.6
Germany	6,013	9.5
Brazil	2,754	4.4
India	2,623	4.2
Canada	1,506	2.4
Poland	1,266	2.0
France	1,073	1.7
United Kingdom	975	1.5
Turkey	956	1.5
Rest of the world	6,749	10.7
Total TOP 10	**56,264**	**89**
World Total	**63,013**	**100**

Figure 13 Top 10 of newly installed wind power capacity in 2015 [25]

Wind turbines can be used either individually or gathered in groups forming wind farms. As such wind turbines can be used for stand-alone applications or off-grid applications or integrated to the electricity grid. Wind turbine cost per kW produced has come down appreciably over the past decade. As a result, wind turbines are far more commercially viable in nowadays.

2.5 Remote condition monitoring for wind turbines

Machinery condition monitoring is defined as the process of monitoring a parameter of condition in machinery such that a significant change is indicative of a developing failure. Thanks to condition monitoring it is possible to prevent early breakdown, reduce the number of inspections, improve the capacity factor, build wind farms in remote places and improve maintenance scheduling [26].

There are two main types of condition monitoring concepts. These are a) online which involves continuous monitoring of the nacelle components concerned and b) offline which involves only periodic monitoring. However, it should be noted here that in certain cases on-line continuous monitoring can be carried out at intervals because in certain cases there is no need to monitor certain subcomponents continuously. Therefore, a more appropriate definition for online condition monitoring could be when the sensors used for monitoring a specific component are permanently installed for this purpose.

Online condition monitoring involves the continuous or scheduled acquisition of data while offline condition monitoring involves data acquisition during a specific period during which a component is under evaluation. Although offline condition monitoring is not ideal, it can be sufficient for the evaluation of onshore wind turbines. However, this is not the case for offshore wind farms where accessibility is not straightforward and in certain cases adverse weather conditions may postpone the visit of maintenance engineers to carry out scheduled inspection on the turbines for extended periods of time which can range from a few days up to a few weeks. Consequently, although offline monitoring is standard practice on commercial wind

turbines, modern designs need to consider online condition monitoring systems which offer several advantages over offline systems.

The main advantages of online condition monitoring systems are the fact that they offer the possibility of early warning thus limiting the likelihood of unpredicted failures and downtime. Furthermore, they enable better planning of maintenance schedules and under certain conditions they can be used to identify the exact problem remotely allowing the right service at the right time, minimizing unnecessary replacements and related costs [26].

There are different methods on which monitoring systems are based. They are accounted below.

2.5.1 Vibration analysis

Currently the most extensive technology applied for condition monitoring, especially for rotating equipment. In the case of wind turbines, it has been applied for gearbox, generator bearing and main bearing CM. Generally, a baseline sample of vibration levels is collected for a healthy wind turbine, from which operating vibrations are compared. An "out of range" vibration will signify a fault, which can be further diagnosed by analysing the frequency of the vibration [27].

2.5.2 Acoustic emission

AE is related to vibration monitoring but with a different principle because in the acoustic monitoring case, the acoustic sensors "listen" to the component instead of registering its local motion. AE sensors detect the stress waves that are generated during crack initiation and propagation within materials. AE has been shown to detect some faults earlier than vibration analysis. AE has been applied successfully to gearboxes, bearings and blades. The AE

technique does not require trending like the vibration method. Although at the moment AE has found limited use so far in the wind energy industry largely due to the lack of sufficient experience with the application of this technique for WT gearbox monitoring this will change in the near future. The first significant step towards this direction was made during the NIMO project [28].

2.5.3 Oil analysis

Oil analysis is mainly carried out offline by taking oil samples for laboratory evaluation. However, for safeguarding the oil quality, application of on-line sensors is increasing since various oil analysis sensors are nowadays available at an acceptable price including wear debris detectors and moisture sensors which measure the presence of water in the lubricant oil of the WT gearbox. Characterisation of parts is often only performed in case of abnormalities. Practically all utility scale WTs employ oil temperature sensors nowadays to avoid overheating of the lubricating oil which may result in combustion and subsequently loss of a WT due to fire [29].

2.5.4 Thermography

Thermography is often used for monitoring electrical and electronic components; in particular it could be applied to monitor failure prone power electronics. Currently, this technique is only applied off-line, but the development of on-line monitoring techniques will likely induce a larger uptake in this technology for turbine monitoring [30].

2.5.5 Strain measurement

Strain measurement of turbine blades is generally performed with strain gauges, however the development of a cost effective optical fibre strain measurement device will likely increase the use of strain measurements for turbine monitoring [31].

2.5.6 Ultrasonic

Widely used for the analysis of turbine towers and blades, ultrasonic techniques can evaluate the structural integrity of the turbine by detailing the size and location of defects within the material [32].

2.5.7 Eddy current inspection

Eddy current sensors are a well-established technology that is commonly used within NDT technology. By utilising either a permanent or oscillating magnetic field, the passing of conducting material induces eddy currents into the material. This in turn generates an opposing magnetic field, which leads to a change in voltage within the sensing coil. Eddy current inspection can be applied for the detection of fatigue cracks on the WT tower. However, encircling coils have been lately applied for detection of debris in the lubricant as mentioned earlier in this section. Any metallic debris ferrous or non-ferrous passing through the encircling coil will change its impedance response. Depending on the amount and type of change in the impedance response of the encircling coil the nature of the particle, ferrous or non-ferrous that caused the variation in the electromagnetic field within the sensor can be ascertained together with its dimensional range [33].

2.5.8 Radiography

Taking X-rays of blades and towers is very rarely undertaken in the wind industry, although it can provide useful information regarding the structural condition of the turbine. Portable radiography based systems will reduce the cost of this technique which may increase its use within industry [34].

2.5.9 Shock pulse method

Only occasionally used within industry, the shock pulse method detects shock waves when a rolling element in a bearing comes into contact with a damaged area of the raceway or debris [35].

2.5.10 Electrical effects

Motor Current Signature Analysis or MCSA is used to detect unusual phenomena in electrical components [36].

2.5.11 Process parameters

The evaluation of process parameters is a very common practice in order to evaluate the overall operation condition of wind turbines. The control system of the turbine becomes more sophisticated and the diagnostic capabilities improve [30].

2.5.12 Performance monitoring

For security and improved performance purposes, the relationship between wind speed, power, blade angle and rotor speed can be used to evaluate the condition of the wind turbine. In the

event of large deviations an alarm is generated [30]. An overview describing the different type of faults associated with the nacelle components is given below.

2.6 Wind turbine faults

Wind turbines as complex systems can develop various types of faults. Some of the key components that can be affected and the types of faults occurring are discussed next.

2.6.1 Gearbox and bearing defects

Gear and bearing faults are both common with bearing failure being the leading factor of turbine gearbox failure. The parts that are more likely to fail are the planet bearings, the intermediate shaft-locating bearings and high-speed locating bearings, while the planet carrier bearings, hollow shaft bearings and non-locating bearings are most unlikely to fail. Misalignment problems are also a relatively common problem in WT gearboxes which can result in poor contact angles between the gear teeth increasing the stresses sustained and causing early fatigue failure. Furthermore, misalignment can contribute to bearing related problems. Currently vibration measurement and spectrum analysis are typical choices for gearbox monitoring and diagnostics. Also, manual-based oil analysis can be used to assess the condition of the bearings based on particle counting [37].

2.6.2 Generator faults

Generator bearing faults and stator insulation breakdown (which form up the generator) are the main causes of generator failures. Faults in induction generators produce one or more of the following symptoms: unbalanced air-gap voltages and line currents, increased torque pulsation, decreased average torque, increased losses and reduction in efficiency, disturbances in the

current, voltage and flux waveforms. Motor current signature analysis (MCSA) has been investigated for turn-to-turn faults based on generator current spectrum analysis [38].

2.6.3 Power electronics and electric controls

Electronic controls account for only about 1% of the cost of a wind turbine, but it is cause of large amount of failures. Thermography is often applied for monitoring and failure identification of electronic and electric components. Hot spots, due to degeneration of components or bad contact can be identified in a simple and fast manner. The technique is only applied for off line usage and interpretation of the results is always visual. At this moment the technique is not interesting for on-line condition monitoring [39].

2.6.4 Yaw system faults

The change in degrees of yaw gives the degree of fault like 5° (within normal operating range), 10° (unusual wind changes), and 20° (significant loads on wings). The analysis of the yaw error simulations showed that the level at the 1P-frequency of the electrical power is altered by the amount of yaw error which makes it possible to distinguish between rotor blade pitch errors and rotor yaw errors, since only the latter has influence on the 1P-level frequency [40].

2.6.5 Pitch mechanism faults

Problems in the pitch bearing are currently of concern to WT manufacturers and operators. However, due to the very limited motion of the pitch mechanism (approximately 90°) conventional vibration analysis is not applicable. AE is also unlikely to prove successful due to the amount of the limiting motion in detecting faults in pitch bearing. Measurements related to the motor of the pitch mechanism may provide more useful information regarding the overall condition. Nonetheless, simulations have shown that pitch error is detectable by the 1P-

amplitude of the acceleration in the X and Z direction, where a difference of 3–4 dB between pitch error increments of 0.5° is observed [39].

2.6.6 Blade defects

Blades can suffer from various structural defects including delamination, fatigue cracking and erosion. Blades are exposed to extremely complex dynamic loads which are stochastic in nature. Although wind turbine blades are normally inspected using visual, ultrasonic and thermographic inspection, some wind turbine manufacturers have recently begun using accelerometers and acoustic emission sensors to remotely monitor their condition.

2.6.7 Tower defects

Towers are discussed earlier can develop fatigue cracks or suffer from corrosion effects. They are normally inspected visually, ultrasonically or with magnetic flux leakage or eddy current testing. The collapse of towers is not common, but it does happen occasionally resulting in the complete loss of the affected turbine in all cases.

2.7 Summary

Wind turbines are complex systems consisting of a variety of critical components, therefore effective remote condition monitoring can prevent unexpected breakdowns and help plan maintenance efficiently. There are two main types of condition monitoring concepts, online and offline. Online RCM involves continuous monitoring of the nacelle components concerned whilst offline involves only periodic monitoring.

There are different methods on which monitoring systems are based but currently the most extensive technology applied for condition monitoring of gearboxes in particular is based on vibration analysis. Acoustic emission is an alternative technique to vibration monitoring based

on different principles since it employs acoustic sensors to capture the noise generated by different components instead of detecting their vibrational response. Power electronic components cause a large number of failures, but so far the application of RCM technologies has been limited. Although offline monitoring is used as a common practice on certain commercial wind turbines, modern designs employ online condition monitoring systems which offer several advantages over offline systems.

CHAPTER 3

WIND TURBINE POWER ELECTRONICS

3.1 Fundamentals of power electronics

Power electronics are employed in wind turbine in order to enable power processing. All modern wind turbines, regardless whether geared or direct-drive employ power converters. Electronic circuits are employed to control the power converter in order to change the input voltage or current magnitude and/or frequency so as to be appropriate for different loads. In a power electronic system, the flow of electric energy is controlled based on the load demand [41]. The key purposes in modern power electronic systems are to transport the power with maximum efficiency, lowest cost and weight in an integrated circuit. Power electronics have generally a significant role in a wide range of industries apart from the wind energy sector when power processing is required including IT, telecommunications, motor drives, automotive and alternative energy systems [41].

Power electronic devices can be divided into a power and an electronic circuit. The power circuit converts the input and delivers it to the output. The electronic circuit will controls the converter by measuring the input and output voltage and current and also the signals for the power circuit [41]. That means that the controller compares the output voltage or current with the reference and then generates the signals at low voltage and low power. Therefore, it is possible to turn off and turn on the power switches in the converter to cut the high voltage or high current in order to generate the same singles and same voltage or current waveform in very high voltage and high-power systems. Hence, through power processing means a mapping from low voltage into high voltage can be achieved. By using signal processing, it is possible to sensitise any voltage or current waveform, enabling generation of the same signals in high voltage or high current. Figure 14 shows a simplified block diagram of a power electronic system.

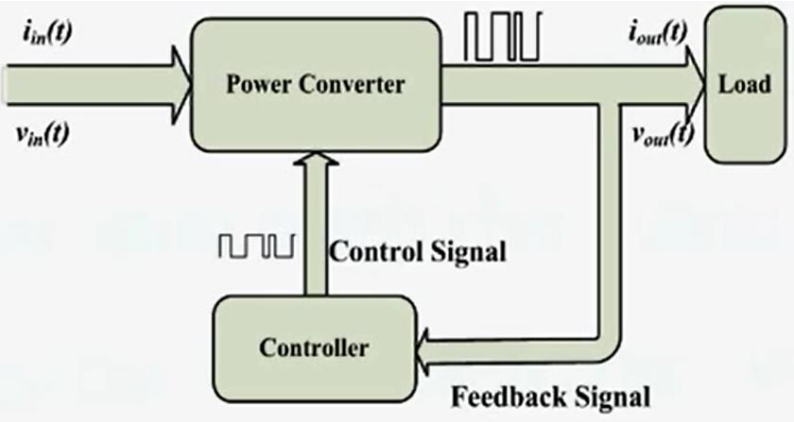

Figure 14 Simplified Block diagram for a power electronic system [38].

A power electronic system may process input power and deliver it to a load based on these following converters: DC-DC, AC-DC, DC-AC, AC-AC. Figure 15 below shows different types of power converters.

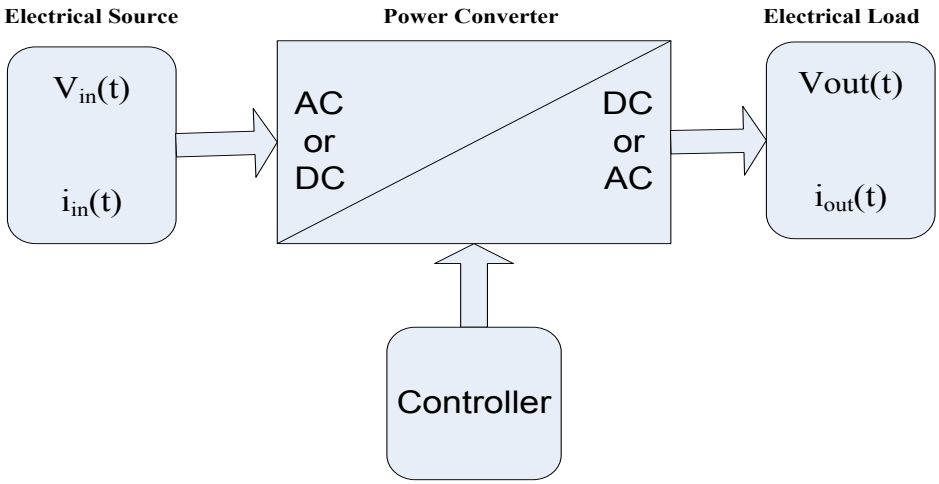

Figure 15 The different types of power converters and their input and output. The controller unit is also shown.

Different applications have different load requirements and hence need special considerations in topology and control circuits. For example, in DC power supply, an output DC voltage may be regulated while in a DC motor drive the output DC voltage must be adjustable. In an AC power system, an output frequency may be constant while in an AC motor drive both frequency and magnitude must be adjustable [41].

The controller is an important part of the system to control and regulate output voltage and current and also to protect the system under harsh operational events, such as in cases involving spikes in current, over-voltages and/or overheating. Therefore, the power converter controller can measure the output voltage or output current. In addition, it can also compare these with the reference signal. The reference signal can also be in the form of current or voltage. The reference signal can then be used to generate the control signals. The simplified schematic diagram in figure 16 shows the principles of operation of power converters.

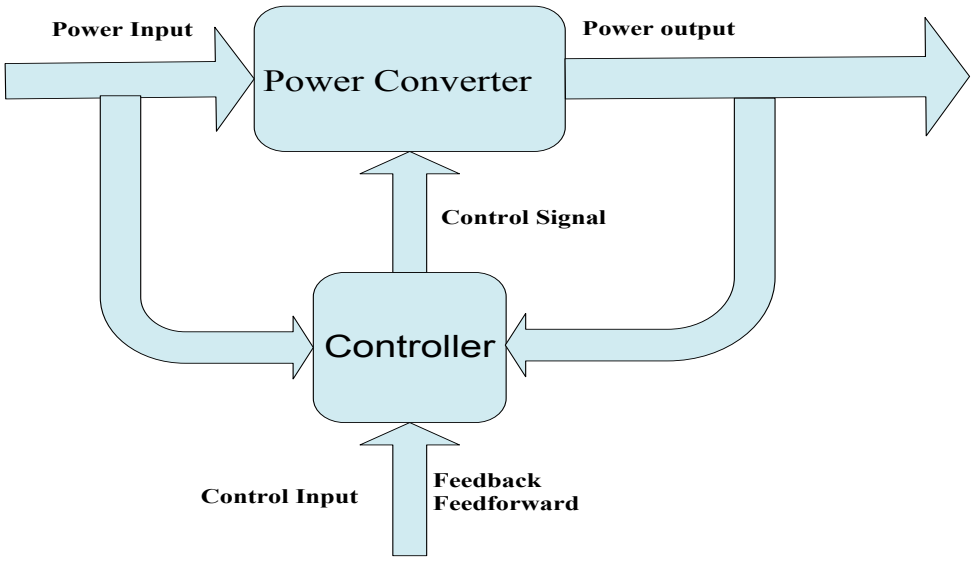

Figure 16 Schematic diagram showing the overall operation of a power converter system

In power electronic systems, line and Electromagnetic Interference (EMI) filters are important components of the system. This means, that filters on the input and/or output side are required, depending on the type of the application. Sometimes there is no need to have an output filter, such as AC motor drives. However, for some applications, especially for power generation applications output filters are required. Input filters are necessary because it is important to be able to control low and high frequency noises. Figure 17 shows the location of the filter in the overall power converter architecture.

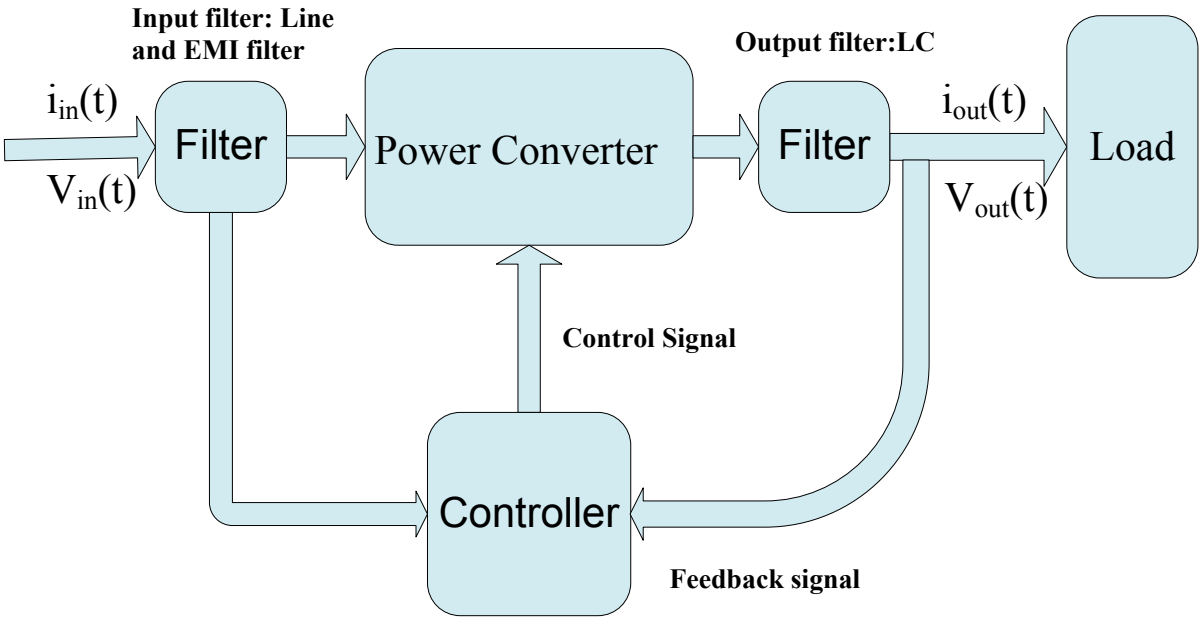

Figure 17 Location of filter in the power converter system architecture.

In modern power converters, thanks to the advances in semiconductor switches, they can be classified accordingly as low or high frequency switching devices. Low frequency power converters are naturally commutated. The power switches are turned on and off at the grid frequency of 50 or 60 Hz. High frequency converter operation is based on the use of hard or soft switching. In such power electronic devices, controllable switches in the converters are turned on and off at frequencies higher than the frequency of the grid (i.e. >50-60Hz).

3.2 Power converter packaging

There are two different packaging types for power devices, as shown in figure 18. The press-pack technology has been proposed for medium voltage (MV) converters in multi-MW wind turbines. This type of packaging is more reliable due to the absence of bond wires and double-sided cooling, but is more expensive mainly due to the difficulty in packaging and complex assembly process that it involves. The power module type is still the most common packaging applied in modern wind turbines. The semiconductor chips are electrically connected by bond

wires and soldered to an insulating ceramic subtract (also called direct bonded copper substrate, DBC) [42].

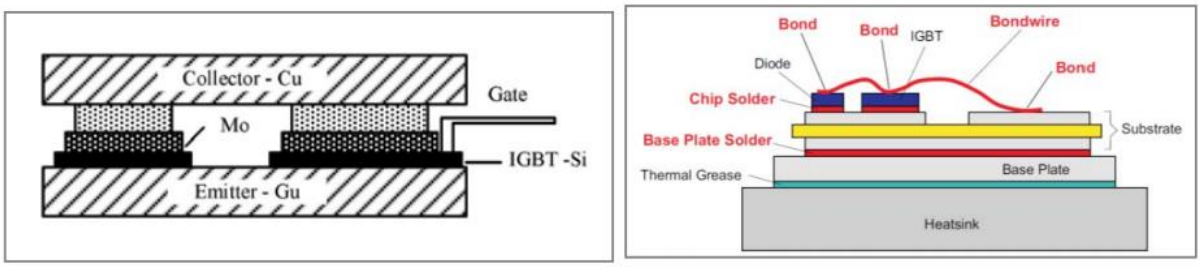

Figure 18 Packaging technologies for power devices (left: press-pack technology, right: power module) **[42]**

3.2 DC link capacitor

There are two types of DC link capacitor for converters, including aluminium electrolytic capacitor and metallized polypropylene film capacitor [43]. Electrolytic capacitor has high power density and a lower price, but is less reliable. Temperature-related effects are the main aging acceleration mechanism.

Metallised polypropylene film capacitors have higher tolerance to higher voltages and currents. Moreover, many have inherent self-healing capability, thus achieving a higher reliability and longer lifespan. However, film capacitors in general have a lower power density. The main aging accelerator in this case is the peak current.

3.3 Power converter system failures

Failure of electrical systems in wind turbines have been a subject of concern for manufacturer and operators alike. The EU FP7 RELIAWIND project investigated the cause of failures and downtime in wind turbines and which are the key components that are more likely to be affected [44]. According to the findings of the RELIAWIND consortium, electrical faults account for an average of 32% of all the wind turbine failures [45] [46]. The graph in Figure 19 shows the

percentage contribution to the overall downtime caused by failure of various components for the wind turbines considered during RELIAWIND.

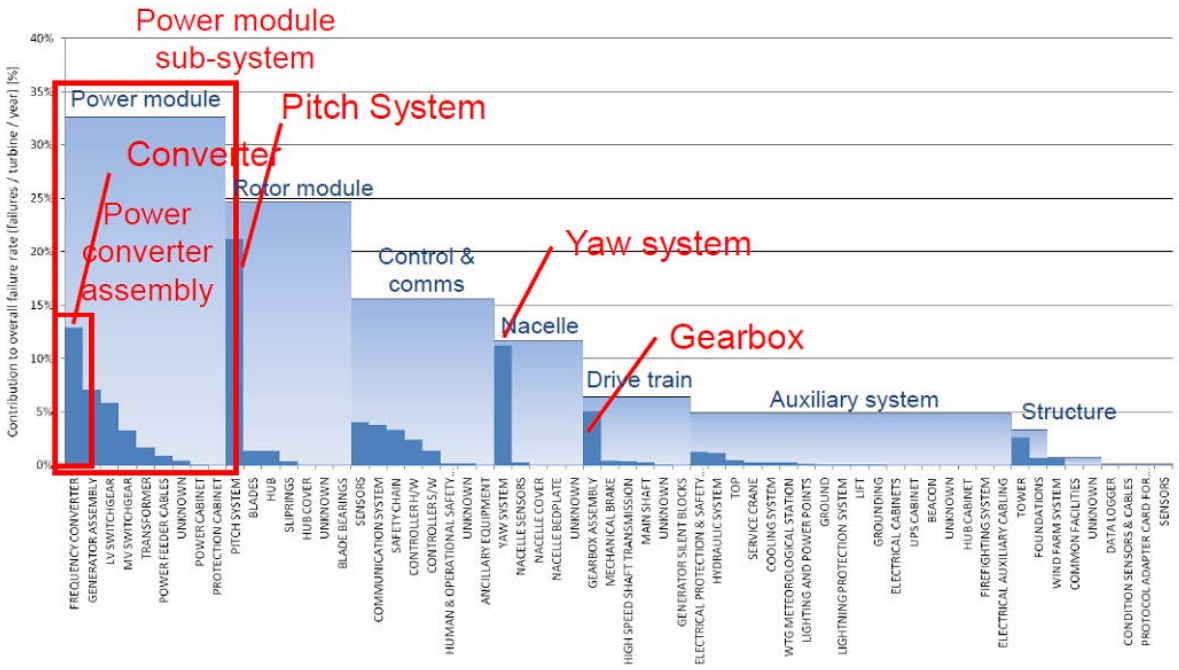

Figure 19 Graph showing the percentage contribution to overall failure rate for 350 wind turbines considered in RELIAWIND [47]

The electrical system failures of the wind turbine are categorised as shown in Figure 20 [48] . It is obvious that it is important for the future development of wind turbines and the economic viability of offshore wind farms to address the reduced reliability levels of these components [46].

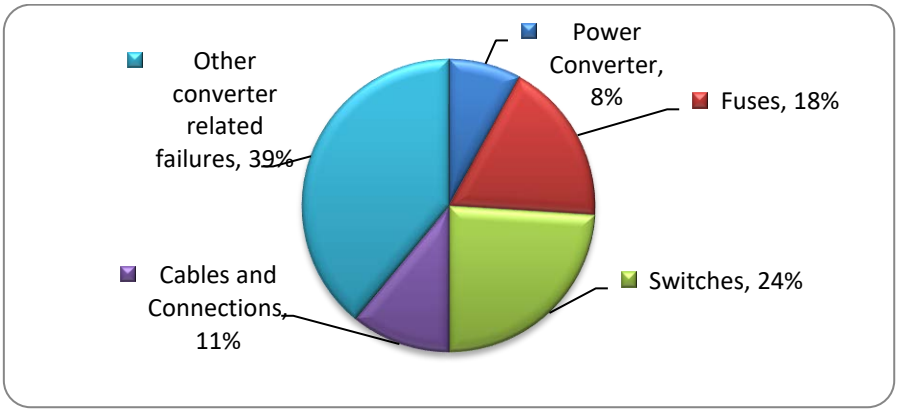

Figure 20 Electrical faults categorised [48]

An attempt to address these technical challenges is through the optimisation of the reliability of the electrical systems of wind turbines, investigating a redundancy model for the power converter system. For this redundancy model a case study of a recently commissioned (mid-2013) offshore wind farm (the London Array) is used, in order to identify how the redundancy model affects the reliability of the wind turbines, the overall availability levels of the OWF, the cumulative energy output and the Levelised Production Cost (LPC) of energy [48] [46].

Several studies have confirmed that the higher failure rates exhibited by the electrical components of the wind turbines are directly related to the operating conditions of the power converter system or indirectly related to malfunctions of the converter components, for example malfunctions in the IGBT switches and the converter control unit resulting in fuse and cable connections failures [49].

These studies suggest that the load conditions of full output current at low output current frequencies cause thermal fatigue of the IGBT switches and the converter control unit, resulting in the power converter failing [49]. It has also been reported in offshore wind farms that there is a close correlation between lightning strikes and converter failures. Furthermore, evidence of salt accumulation and related corrosion in the converter enclosures have been reported [50]. This indicates that in the offshore environment reduced reliability of the power converter can be expected as compared to onshore applications although some studies indicate similar trends for onshore and offshore wind turbines.

3.4 Doubly fed Electric machines

One of the most widely adopted doubly-fed electric machines used in the wind turbines are the doubly-fed induction generators. Doubly-fed induction generators play a major role in production of electricity [51] [52]. The main reason for the adoption of DFIGs into wind power

converters is to produce a three – phase voltage with constant stator frequency. Therefore, the frequency of stator remains equal to network frequency of the AC power grid which the generator is connected to [53].

One of the main advantages of DFIGs is their stationary and rotating windings which enable the power to be transferred between the shaft and the electrical system from both windings. The winding of the stator is connected to the three-phase grid which is fed from the grid through a rotating or static frequency converter.

One of the most important advantages of doubly-fed induction generators is the ability to connect to the AC power network directly while remaining synchronised with at all times. Besides DFIGs are able to operate at a variable rotor speed while both the frequency of the generated voltages and amplitude remain constant. DFIGs are capable of generating electrical power at lower wind speeds and can control the power factor while keeping the power electronic devices in the wind turbine at a reasonable size [51]. The schematic diagram in figure 21 shows the main features of a doubly fed induction wind generator system.

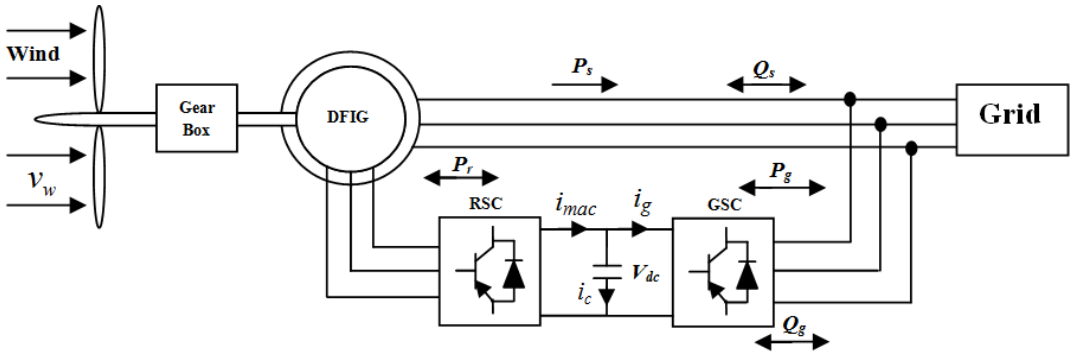

Figure 21 Doubly fed induction wind generator system [53].

In addition, DFIGs help optimise the amount of power generated as a function of the wind available up to the nominal output power of the wind turbine generator. On the other hand, the virtual elimination of unexpected fluctuations in the rotor torque and generator output power is one of the unique capabilities of DFIGs [54].

The interface between the generator control and the IGBT power modules is obtained by using the driver boards. As shown in the schematic diagram of figure 22, a number of half-bridges are connected in parallel in order to allow for the required operating currents.

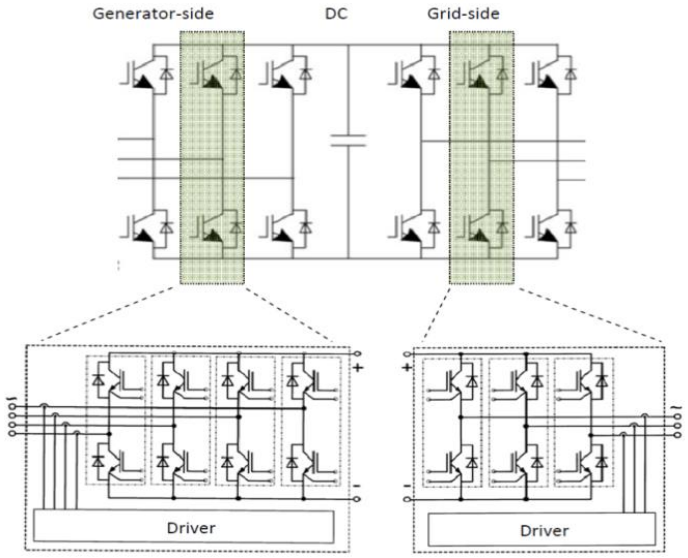

Figure 22 Back-to-back converter of a DFIG turbine with paralleled half-bridges in each phase module to provide required current capacity [23].

3.6 Insulated gate bipolar transistor (IGBT)

The cutting-edge progress achieved in switching device technology is playing a major role in the improvement of high power converters for wind turbines with advanced efficiency and great consistency [55]. The most important and main choice amongst all are IGBT modules which based on industrial experience have multiple known and beneficial advantages. IGBTs are very suitable for power electronics applications, especially for Pulse Width Modulation (PWM) [56]. PWM is a method to control the width of the pulse, formally the pulse duration, based on modulator signal information.

IGBTs are extensively used in wind turbine power converters but unfortunately are prone to failure resulting in unnecessary downtime for the wind turbine operators. IGBT faults can develop due to various reasons including short-circuiting, overvoltage, high temperature

fatigue, dynamic failure, etc. Therefore, in the condition monitoring of power converters in wind turbines these parameters must be taken into consideration [55] [57].

3.7 IGBT failure modes in wind turbine applications

As discussed earlier the failure of IGBTs could lead to an overall system failure, causing the wind turbine to be non-operational for a significant amount of time until the fault has been rectified. The following diagram in figure 23 summarises the most common failure modes of IGBTs in industrial use [58]. Figure 24 also shows the failed wind turbine IGBT module.

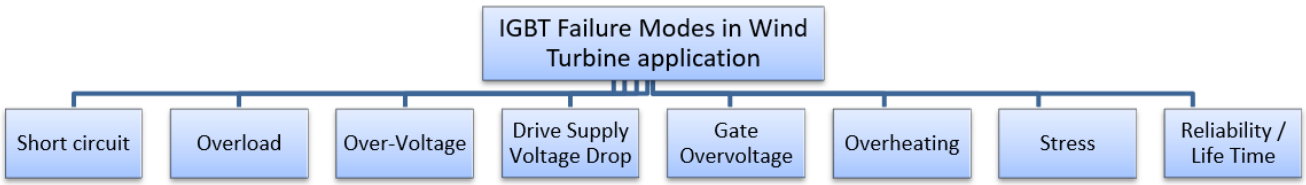

Figure 23 main IGBT failure modes

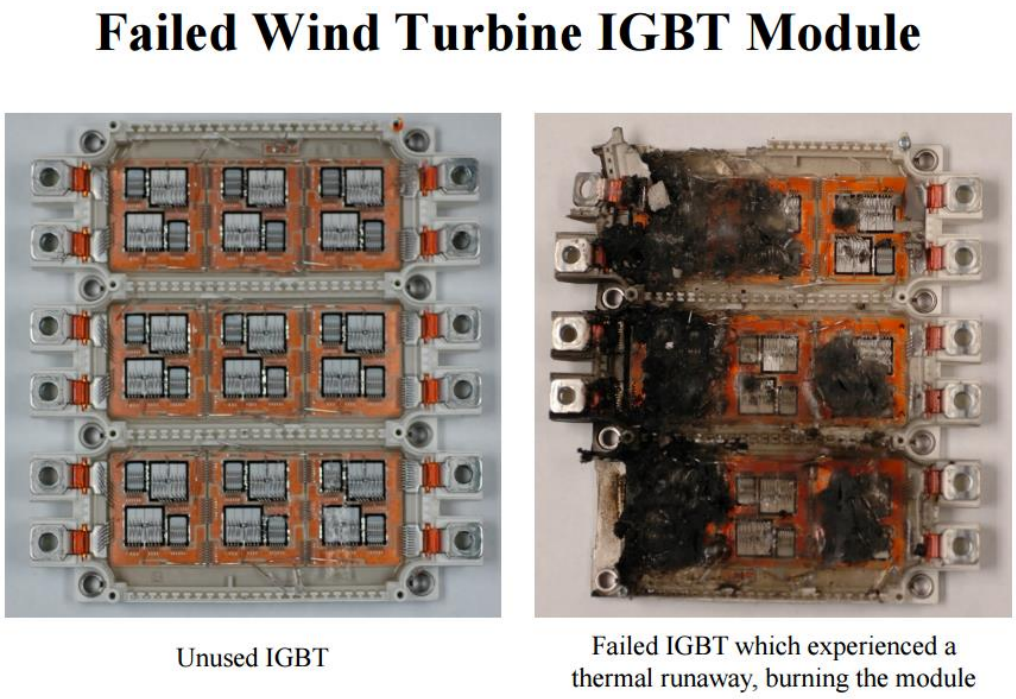

Figure 24 failed wind turbine IGBT module [59]

Short circuit: One of the most intense stress factors on the IGBTs is short-circuit switching, since a large current is flowing through the device while supporting the whole bus voltage. As a result, short-circuiting of the IGBT during long time usage, leads to its gradual degradation. The challenge is to delay the failure of the device. Therefore, detection of faults must be achieved as early as possible [60]. There are four types of short circuits:

- Arm short circuit: often caused by short circuit destruction of one element leading to a device failure mode which is known as “outside SCSOA”. In order to prevent this, the waveform (locus) and device ruggedness should match during an arm short circuit.
- Series arm short circuit: mostly caused by:
    - Gate or logic circuit malfunction,
    - Noise causing outside SCSOA failure mode to occur. Consequently, the circuit must be checked for malfunctioning coupled with the steps taken above in arm short circuit abnormalities.
    - dv/dt, insufficient gate reverse bias, gate wiring too long, dead time too short and date/time setting error would all cause the device to overheat and malfunctioning and/or incapability of wind turbine to continue operation.
- Output short circuit and Ground short: usually known to occur due to miss wiring, abnormal wire contacts and abnormal wire contact causing outside SCSOA mode to arise. The most common checkpoints to carry out upon the failure occurrence are: checking the conditions of the overall system / wiring condition at the time of failure and ensuring the device ruggedness and protection circuit match during the operation process of the wind turbine.
- Overload: often caused by logic circuit malfunction and overcurrent protection circuit setting error that leads to overheating. In order to prevent this, the logic circuit, overload

and gate voltage match are to be checked. Also; in some cases, if necessary adjust the overcurrent protection level.

- Over-voltage: there are two known common types of over-voltage.
    - Excessive input voltage: often caused by insufficient over Voltage protection leading to protection device over Voltage failure mode that could be prevented by adjusting the over Voltage protection level.
    - Excessive spike voltage, mostly caused due to: Switching turn – off, high dj/dt resulting, transient on state (short off pulse reverse recovery) that lead to the occurrence of outside Reverse Bias Safe Operating Area (RBSOA) failure and/or protection device overvoltage mode which could be avoided by checking the turn-off operation (loci), RBSOA match, calibrating the over current protection level, checking the logic circuit and gate signals interruptions which leads to noise interference.
    - Overload: often caused by logic circuit malfunction and overcurrent protection circuit

It is important to know the thermal behaviour of the IGBT module in various load conditions to ensure safe operation at all times. There is a specified maximum temperature for an IGBT chip that cannot be exceeded without changes in the functionality of the device. The thermal dimensioning made in the design phase of a frequency converter should leave some safety margin in the heat transfer capacity because of variations in the thermal parameters of the power modules. The device must also be capable of temporary overloading in normal use. In practice, the safety margin is provided by oversizing the heat sink and cooling capacity, which increases the manufacturing costs of the device.

IGBTs device overload can be caused by excessive current or by excessive voltage. In both cases, possible destruction of the component is caused by (local) overheating of the silicon. Destruction of the elements can be prevented by appropriately limiting the duration of the overload. Surge current is the measure used to deduce current overload capacity. Surge current refers to the maximum, instantaneous input current drawn by an electrical device when first turned on. Surge current is usually about 10 times greater than the rated current.

- Drive supply voltage drop: often caused by one and/or combination of multiple causes mentioned below:
  - DC-DC converter malfunction,
  - Drive Voltage rise is too slow
  - Disconnected wire

In all of the cases above overheating of the IGBT occurs.

Gate over voltage is often caused by static electricity spike voltage which is led by the excessive length of gate wiring. This failure mode is often referred to as avalanche over voltage. The common checkpoints at this stage would be inspection and ensuring the operating conditions and / or anti – static protection coupled with gate voltage.

One the most common failures of IGBT in the wind turbine industry in often stated as overheating which is mainly caused by one and/or multiple factors as shown below:

- Overheating: mainly caused by loose terminal screws or cooling fan shutdown/malfunction.
- Thermal Stress: Vanessa Smet et al. (2011) [61] identify the effects of power cycling and the value of high temperature in IGBT modes. Initially, there are two original thermal stresses in power electronics arising from power and thermal cycling. Simply,

the thermal stress of power cycling arises due to loss variations in the power devices when using IGBTs subject to different loads caused by mission profiles. The thermal cycling basically is generated by the changes of thermal environment around the IGBTs [62].

Reliability / operational lifetime. As the operational condition exceeds the design parameters of the device, it takes less time for the IGBT to reach its maximum operational lifetime resulting eventually to its failure.

3.8 Lifetime Prediction for IGBTs using the Rainflow Counting Algorithm

The cycle counting method has been applied in order to reduce and simplify a complex loading history into a series of measurements which could be compared to the existing constant amplitude test data at a later stage [63]. Many approaches have been employed in order to count the cycles, based on the hysteresis loop characteristic of the stress – temperature as shown in the schematic diagram of figure 25.

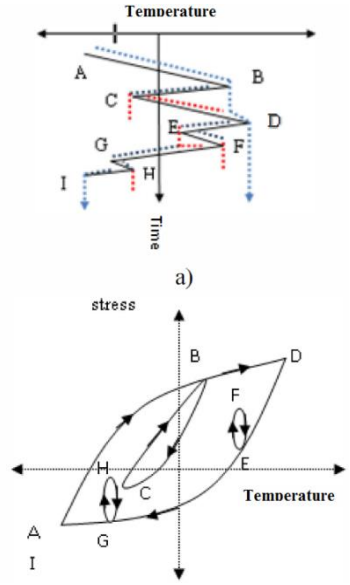

Figure 25 A temperature-time sequence and stress-temperature hysteresis plots [60].

In order to count the cycles for life estimation purposes in figure 25 shown above, which made from hysteresis loops characteristic of the irregular stress against time profile, many methods are available such as half-cycle peak through counting, maximum edge peak through counting, rising edge peak through counting and rainflow algorithm. [64]. The rainflow algorithm is a counting method which has gained popularity due to its ability to provide average value, with yet as little relative error as possible [65]. The rainflow counting algorithm is a method, which is normally used for decreasing the spectrum of varying stress and modifying it into sets of reversals that are simple to comprehend, by using fatigue and failure data [66]. Through the application of the rainflow counting algorithm the complicated history of data acquired by the condition monitoring system can be narrowed down into a number of events that can then be compared with the present constant amplitude test data [67]. However the rainflow counting method is a good way of separating small, uninteresting oscillations from the large important oscillations, without affecting turning points caused by the smoothing effect of a filter or interrupting a large range before it is actually completed [68].

In order to be able to predict the lifetime of an IGBT in a power converter application such as a wind turbine a sequence of logical steps should be outlined as shown in the following diagram in figure 26.

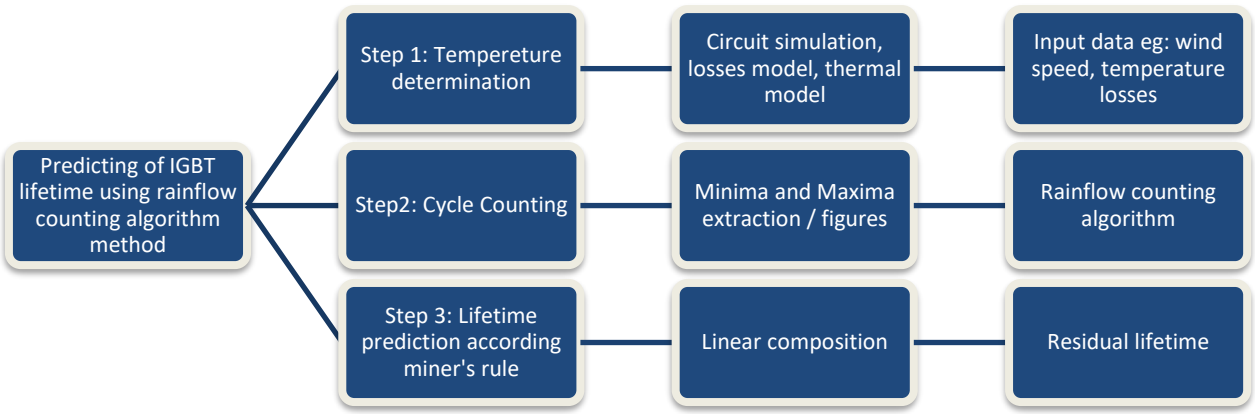

Figure 26 Diagram showing the steps required in estimating the remaining IGBT lifetime.

Step 1: During the operation of the wind turbine the thermal stress is applied to the device operating under cyclic conditions. In order to predict the lifetime in a power converter it is essential to determine the losses / virtual junction temperature of the semiconductor devices as a function of time. This needs to be done with respect to a typical operation that could be derived by either calculating or direct measurement, which could require mathematical models for both the losses and thermal transmission in the device. The inputs could be based on the operation conditions of the converter by means of a circuit simulation or simply the analytical equation from a wind turbine approximated data [69].

Step 2: The cycle counting is used at this stage in order to indicate the temperature cycles of the IGBT in the sequence format along with the frequency of occurrence during the operation of the wind turbine. At this stage a time-based junction temperature sequence of the IGBT of step 1 is input. Next, using the rainflow counting algorithm the portfolio of cycles is created [70].

Step 3: Lifetime prediction according Miner's – rule: at this stage the lifetime consumption based on each cycle could be calculated with regards to the lifetime curves provided by the device manufacturers. At last; the lifetime is derived based on linear composition according Miner's rule [71]. Using Miner's rule which is a linear model for different mathematical load leading to different fatigue by comparing the temperature cycles extracted from step 2 to the lifetime curves and consequently; all-over lifetime consumption.

3.9 Summary

Power electronics are employed in industrial wind turbines in order to enable power processing. All modern wind turbines, regardless whether geared or direct-drive employ power converters. IGBTs are very suitable for power electronics applications, especially for Pulse Width Modulation (PWM). PWM is a method to control the width of the pulse with respect to the pulse duration, based on modulator signal information. IGBT malfunction can lead to overall system failure, causing the wind turbine to become inoperative. Many factors can contribute towards the failure of IGBTs but in all cases overheating of the IGBT will occur. Consequently, the rainflow counting algorithm can be employed in order to identify incipient failure in IGBTS by evaluating the extent that they have been stressed during operation.

CHAPTER 4

WIND TURBINE GEARBOX AND FAILURE MODES

4.1 Wind turbine gearboxes

Wind turbine gearboxes are important sub-systems for the operation of all the wind turbines that are not based in direct-drive designs [72]. The gearbox is responsible for translating the slow input rotational speed of the rotor to a high speed rotational output in the generator. Most gearboxes are based on three-stage designs incorporating a slow, intermediate and high-speed section [73]. The gearbox comprises of the various shafts, the planetary gears and bearings, the intermediate and high-speed gears and bearings [74]. The input rotational motion is transmitted from the rotor to the gearbox through the main shaft. Subsequently the rotational speed is increased by a corresponding factor at each of the stages. Smaller industrial wind turbines capable of producing power up to a few hundreds of kW have input rotational speeds which are in the range of 25-26 revolutions per minute (RPM) [75]. The input rotational speed is subsequently increased through the gearbox to a maximum output speed of 1500-1600 (RPM). Larger machines, in order to avoid increasing too much the stresses sustained by the blades operate at lower rotational speed although the tip of the blades is travelling at speeds that are much higher than those in smaller turbines. For example, 1.5 MW wind turbines have an input rotational speed of 16 RPM and an output rotational speed of 1100 RPM [76]. Larger machines such as the 9.5 MW V-164 have input rotational speeds as low as 8 RPM. More specifically, the V-164 incorporates an intermediate gearbox which means the output rotational speed is kept relatively low at around 400 RPM. The gearbox of the wind turbine apart from increasing the rotational speed transmitted to the generator, it also reduces the rotor torque by an equivalent factor [76]. Figure 27 shows gearbox of a wind turbine.

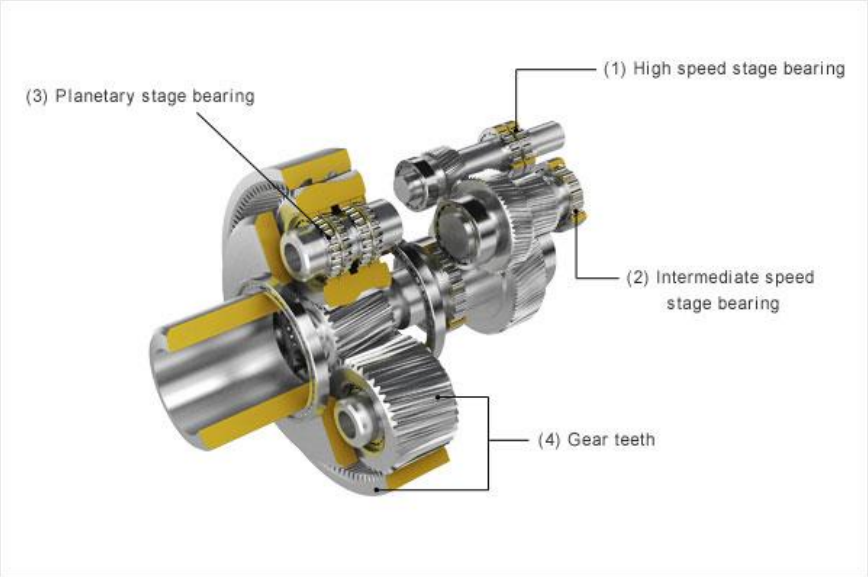

Figure 27 gearbox of the wind turbine [77]

Gearbox subcomponents are normally manufactured from high Cr steels which have been further surface treated to ensure an optimum combination of hardness and toughness [78]. Due to the extreme adverse operational conditions of gearbox components high quality lubrication is of utmost importance in ensuring a prolonged operational lifetime. Unfortunately, variability in lubrication quality is an issue, which has plagued the wind energy industry since its inception. This has been predominantly attributed to the effects caused by high variable loads due to wind speed variations and turbulence [79]. Therefore, gears, bearings and shafts within a wind turbine gearbox are prone to suffer from a variety of defects. These defects need to be detected in time in order to avoid failure of the gearbox, which can be catastrophic in nature depending on the sub-component or sub-components that have been affected. As such, the gearbox has been one of the primary sub-systems of a wind turbine whose operation has been deemed necessary to monitor using RCM techniques [80].

Initially, wind turbine gearboxes were solely monitored for overheating events and therefore incorporated only temperature sensors. These temperature sensors were responsible for

monitoring the temperature of the lubricant. Hence, in an event of the fixed predefined temperature threshold being exceeded the wind turbine would generate an alert leading to its shutdown. Without the use of a temperature sensor the lubricant would continue to overheat, reaching to a critical temperature at which it could combust and resulting into a fire in the nacelle. Practically all modern industrial wind turbines are monitored using accelerometers. The accelerometers are installed at threaded locations opened on the gearbox casing. Normally, 7-8 accelerometers are used for monitoring the entire gearbox although different numbers of sensors can be used depending on the requirements of the manufacturer and operator. The vibration measurements can be trended and through spectral analysis the components that have been affected from damage can be identified [81]. The major issue is the fact that wind turbine gearboxes operate continuously under variable loading conditions. As a result, data trending and assessing the precise severity of the damage become extremely challenging. Therefore, it is not uncommon for existing commercial systems to generate false positive alarms, where there are no actual faults present. Due to this uncertainty in the measurements, more severe defects can be underestimated, leading to unpredicted failures becoming possible. Alternatively, acoustic emission (AE) techniques can be employed for monitoring the rotating parts of the gearbox. Despite the fact that AE offers much higher sensitivity in comparison with accelerometers, its use in the field has not been standard so far and the cases that this technique has been employed are very few, predominantly in the form of pilot trials.

4.2 Materials for wind turbine gearboxes

Wind turbine gearbox gears and bearings are manufactured from surface treated ferrous alloys. Gears and bearings are typically manufactured from grades 2 or heat treated and subsequently quenched steel grades. Typical steel grades used in manufacturing of wind turbine gearbox

gears and bearings include nickel-chromium-molybdenum low-alloy steels such as SAE4320, SAE4820, SAE9310, 18CrNiMo7-6, 3CrMo, 3CrMoV and 3NiCrMo [82].

Surface treatment techniques such as carburising and nitriding have been widely applied to gears and bearings in order to increase wear resistance. The combination of carburising and nitriding has been recently investigated and has been found to have considerable advantages over individual surface treatment methods based solely on carburising or nitriding [83]. Figure 28 shows the wind turbine materials usage.

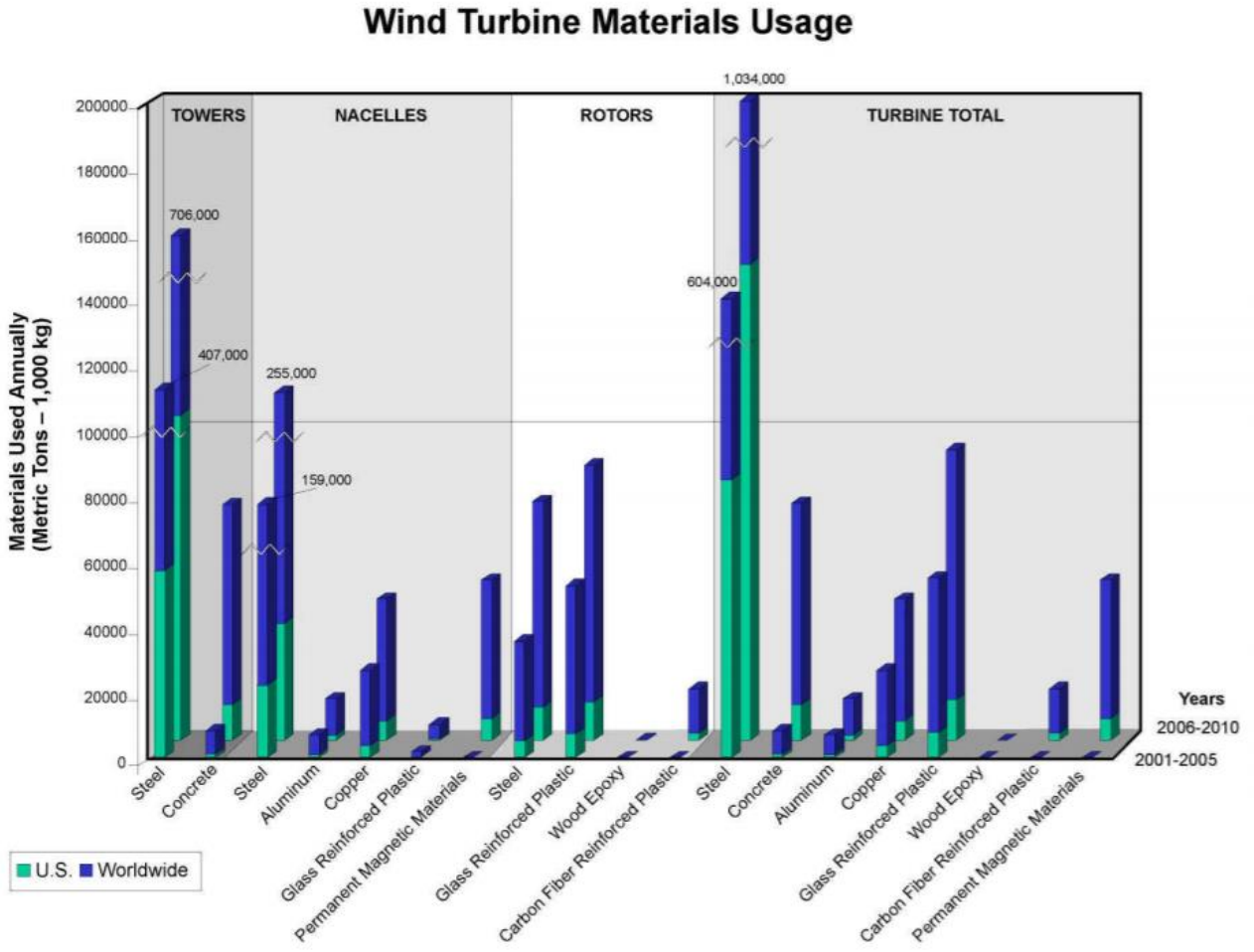

Figure 28 wind turbine materials usage [84]

4.3 Wind turbine gearbox faults

The majority of gearboxes are based on planetary design due to the compact size of this configuration. They also allow the input load to be shared among the different planet gears and bearings reducing structural degradation. Parallel, helical or spur gears may be used for the different stages of the gearbox [85]. Unfortunately, the majority of gearboxes despite the fact that they have been designed for a minimum lifetime of twenty years, rarely achieve to reach it. Most require replacement of repair within the first six or seven years of operation [86]. In offshore wind farms structural degradation occurs even quicker so certain older gearbox designs have been reported to have been replaced as early as within a few months after being commissioned. This is one of the reasons for which direct drive wind turbine models have seen a higher penetration in the construction of new offshore projects in comparison with onshore ones where performance although not yet at required level is not as bad [87]. In order to identify the defects, present in a wind turbine gearbox, its kinematics need to be known. Therefore, the Gear Mesh Frequency (GMF) and bearing models should be known in order to extrapolate from the RCM measurements which component has actually been affected [88]. This will enable more effective and prompt maintenance actions to be performed. The GMF frequency can be calculated using the following equation [89]:

$$\mathrm{GMF} = \text{shaft synchronous speed (revolutions per minute)} \times \mathrm{N} \qquad (4\text{-}1)$$

Where N is the number of teeth of the gear.

The gear ratio on the other hand is given by:

$$\frac{\omega_C}{\omega_S} = \frac{N_S}{N_R + N_S} \qquad (4\text{-}2)$$

Where ω_C and ω_S are the angular velocities and NS and NR are the numbers of gear teeth respectively. So, the GMF can be calculated as follows.

$$\mathrm{GMF} = \omega_C \times (N_R + N_S). \qquad (4\text{-}3)$$

Finally, the torque applied on a gear would be related to the ratio of the transmitted power, P, and the angular velocity, ω which is equal to 2πN. Therefore, the applied torque on a gear will be:

$$T = \frac{P}{\omega} \tag{4-4}$$

In addition, the Hertzian compression stress between a pair of spur gear teeth in contact and the maximum bending stress will be given respectively by the following equation.

$$\sigma_C = \sqrt{\frac{F_t}{bd_1}\frac{E}{\pi(1-\nu^2)}\frac{u+1}{u}\frac{1}{\sin\alpha\cos\alpha}} \tag{4-5}$$

Where F_t is the force between the gear teeth at right angles to the line joining the gear centres, b is the gear face width, d_1 is the pinion pitch diameter, u is the gear ratio (greater than unity) and α is the angle at which the force acts between the gears, usually 20-25°.

$$\sigma_B = \frac{F_t h}{\frac{1}{6}bt^2}K_S \tag{4-6}$$

Where *h* is the maximum height of single tooth contact above the critical root section, *t* is the tooth thickness at the critical root section and K_S is a factor to allow for stress concentration at the root.

Gearbox defects include faults in shafts, bearings and gears. For example, shafts can experience misalignment causing excessive stresses to be applied to gears and bearings. In addition, albeit more rarely, they can develop fatigue cracks which if they remain undetected can result into fracture. Bearing and gear faults include surface wear-related defects such as micro- and macro-pitting, false brinelling, white etching, fretting corrosion, fatigue cracking, rolling contact fatigue cracking, excessive plastic deformation and even thermos-mechanically induced cracking [90].

Figure 29 shows the side view of the broken tooth retrieved from the gearbox of an industrial wind turbine and figure 30 also shows the broken teeth related to unanticipated wear of bearing/pinion.

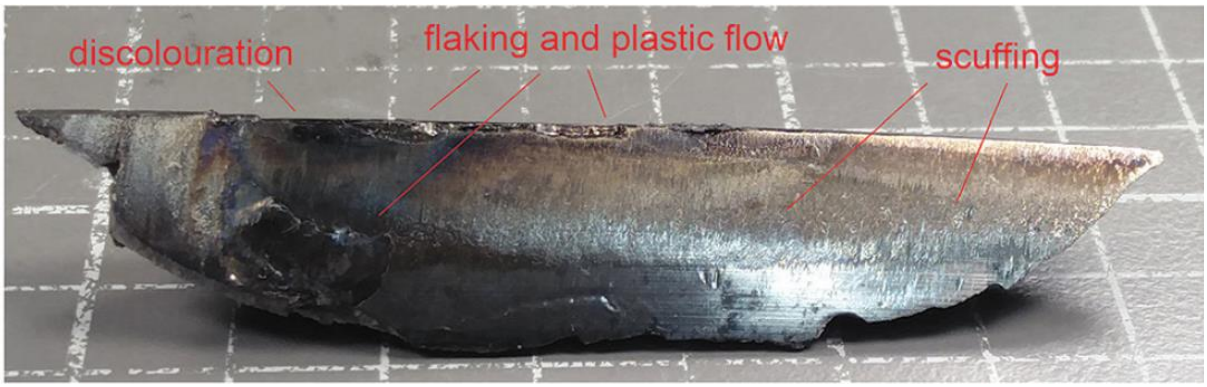

Figure 29 Side view of the broken tooth retrieved from the gearbox of an industrial wind turbine [91].

Figure 30 broken teeth related to unanticipated wear of bearing/pinion [92].

In general, lubrication issues are a major factor of the time and way that damage will initiate and subsequently propagate in such components. Inconsistencies in lubrication can reduce the lifetime of wind turbine gearboxes by up to 80% [80].

Therefore, it is imperative for the wear resistance of rolling materials and components to have optimum lubrication conditions during operation. Unfortunately, in the case of wind turbines, the very high amplitude and sudden fluctuations in the applied stress levels can cause the oil film to be squashed out of the interface between two rolling elements. As a result, dry contact becomes possible.

During such events damage can initiate and subsequently propagate. Also, the mechanisms of structural degradation can be influenced accordingly with the lubricant causing hydraulic opening of surface breaking cracks, helping them propagate further.

4.4 Onshore vs. offshore operational environment

Onshore wind farms availability, although not yet optimal has achieved levels as high as 98%. Unfortunately, this is not the case for offshore wind farms where availability has been found to rarely exceed 85% and in several cases, can be far lower than this [93]. One of the main reasons for the lower availability of offshore wind farms has been attributed to the poor performance of gearboxes. This is due to the fact that commercial gearbox designs have been unable to cope with the loading conditions prevailing in offshore locations, thus, sustaining considerable structural integrity degradation from the start of their operation [94]. Figure 31 show the availability for different offshore wind farms.

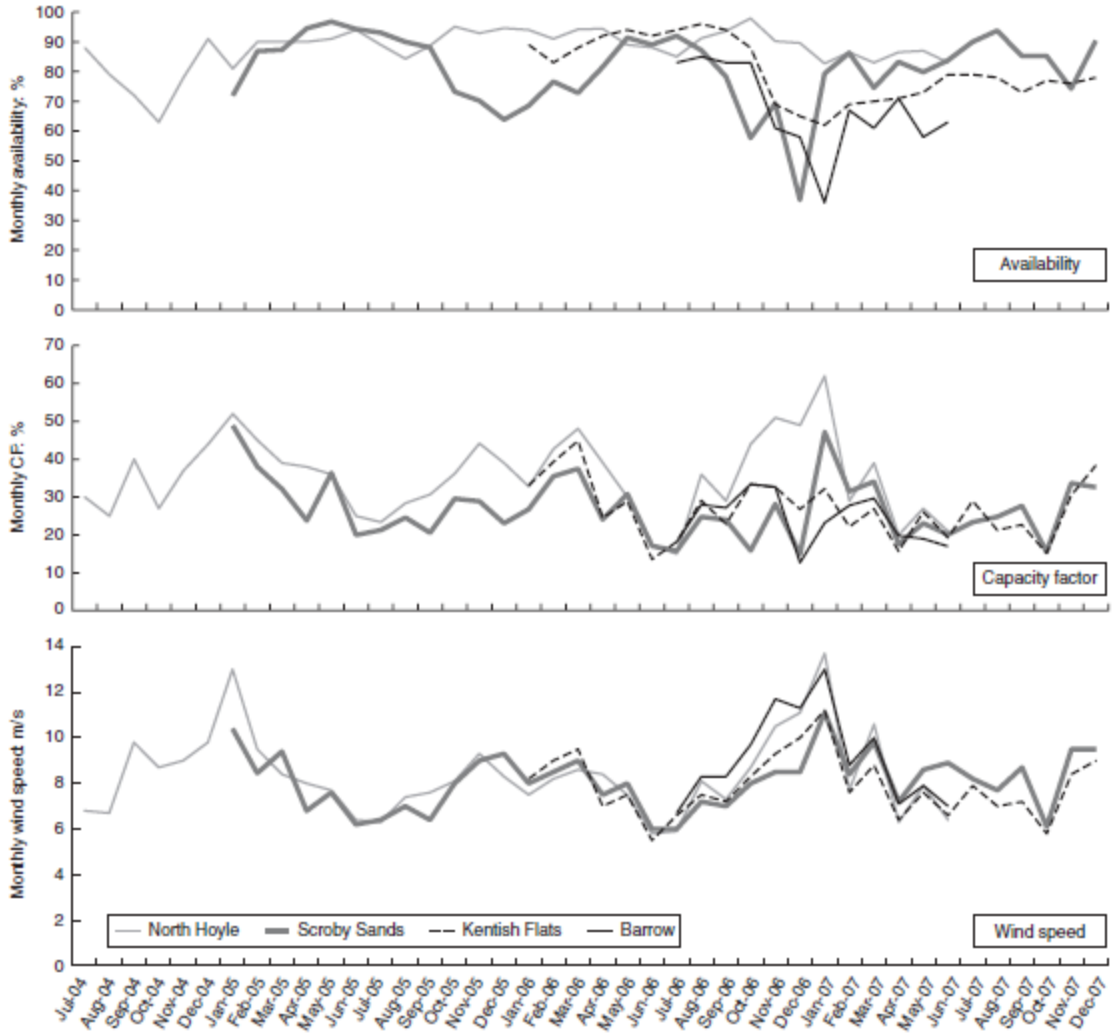

Figure 31 Availability at four different offshore wind farms between July 2004 to December 2007 [95]

Figure 32 shows the annual availability of several offshore wind farms in comparison to normal average availability of onshore wind farms.

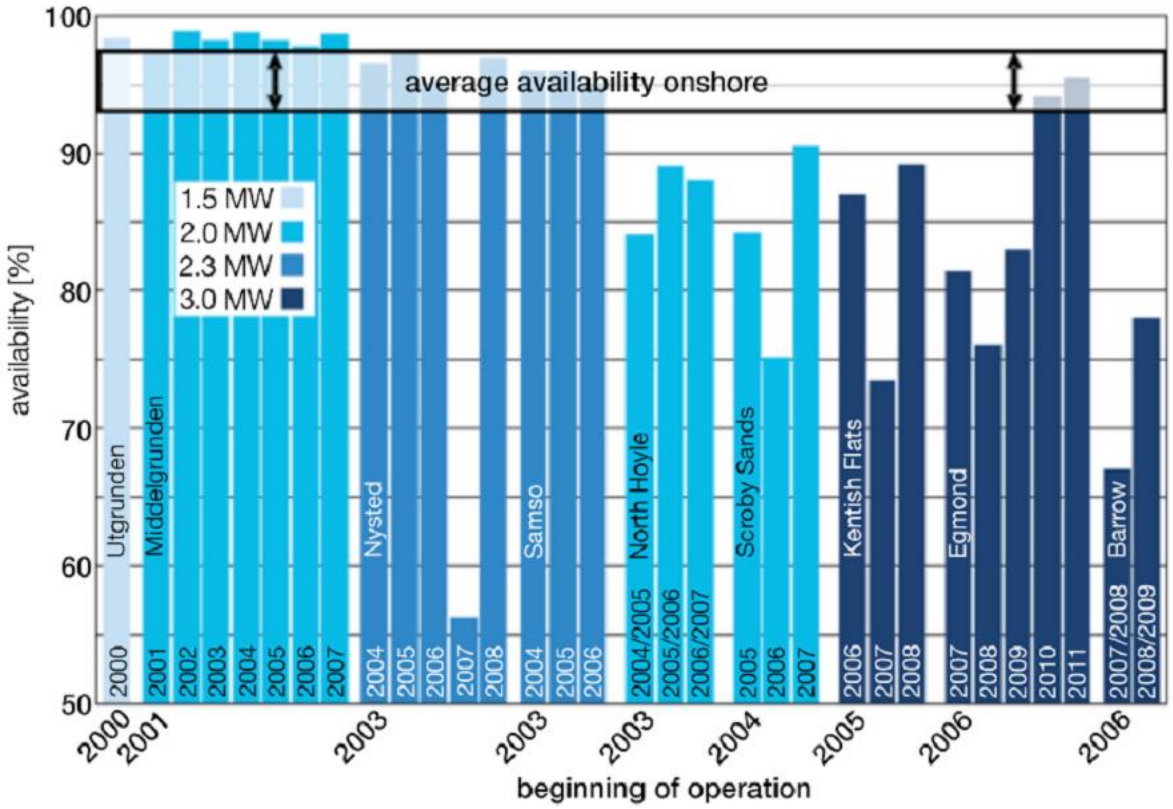

Figure 32 Annual availability of selected offshore wind farms compared to the average availability of onshore wind farms [92]

Wear once it initiates will result in debris travelling through the different parts of the gearbox with the lubricant. The asperities of the debris when caught between the surfaces of two rolling elements can cause excessively high contact stresses resulting in further damage. Therefore, efficient lubricant filtering becomes quite important. However, even if the debris particles are largely removed through the use of efficient filters, the high-amplitude and sudden changes in loading conditions, can cause momentarily misalignments of the gearbox shafts. These misalignments will result in the contact angles of gear teeth as well as bearing to shift. Consequently, a dramatic increase in the contact stress levels will occur further promoting early structural degradation.

Figure 33 shows the number of failures associated with planetary bearing faults at the Horns Rev 1 wind farm reported by Vattenfall.

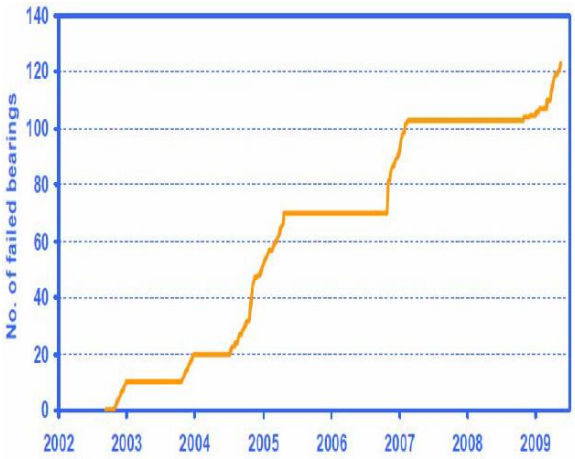

Figure 33 Planetary bearing failures at Horns Rev 1 offshore wind farm reported by Vattenfall [96]

4.5 Operational characteristics of wind turbines and their effect on gearbox

Pumps and compressors are typical conventional rotating machines which are designed to operate at known loads. Their operational parameters are set to be constant throughout their in-service lifetime. This makes prediction of structural degradation more straightforward.

Although operational loads can be adjusted at times, this will not fluctuate unpredictably. Unfortunately, this does not apply to industrial wind turbine gearboxes which operate under constantly varying load conditions regardless of the output they generate. This by default increases the complexity of predicting structural degradation of rotating components installed in the gearbox [97].

The lubrication quality as mentioned earlier is critical for ensuring a prolonged operational lifetime and avoiding structural degradation early in service. In theory, unless moisture has penetrated in the lubricant or other detrimental mechanisms such as excessive overheating have affected its quality, the lubrication quality should degrade gradually and at a predictable rate. The lubricant condition can be checked by retrieving oil samples at pre-determined intervals [97].

With the occurrence of gradual wear, debris particles will progressively accumulate in the lubricant. From the retrieved oil samples, it is possible to evaluate the overall particle population present as well as their average size and type (ferrous or non-ferrous). Larger particles not captured in oil filters will gradually be milled to smaller sizes every time they move through the contact surfaces of two rolling elements, whilst heavier particles may not be captured at all in the oil sample retrieved simply because they may sink to a lower level from where the sample was taken. Therefore, oil samples retrieved manually may not provide the entire picture of what is actually happening in terms of wear progression at different parts of the gearbox. Nonetheless, the information provided by the evaluation of oil samples will be useful in determining future maintenance [98].

Misalignment effects combined with poor or inconsistent lubrication quality can rapidly result in excessive fatigue due to the high contact stresses arising. Although, in theory Paris-Erdogan law and the Palmgren-Miner linear damage model can be used to predict the remaining lifetime, the results will most likely be highly inaccurate due to the high level of inaccuracy involved. It is obviously even more challenging to try and predict the remaining lifetime of individual gearbox components based on vibrational analysis or AE signal evaluation. Therefore, these RCM approaches are more useful for diagnostic purposes rather than prognosis [99].

It is important to take into account the large number of variables that are present in estimating the remaining lifetime of gearbox components. Therefore, it is in considering remaining lifetime it may be best to consider a range of acceptable fatigue damage conditions that can potentially be extrapolated from the RCM data as discussed in the following chapter. In terms of gearbox reliability there are several possible patterns of failure. Certain components in conventional rotating machinery are expected to follow a normal bathtub curve. However, in

modern maintenance theory different components can exhibit different probability of failure patterns so the bathtub pattern may not be necessarily applicable in all cases. The normal bathtub curve (Pattern I) predicts an initial stage with increased number of failures known as infant mortality. Probability of failure gradually stabilises with time and becomes random. Towards the end of life of the component failure rate increases again due to wear and fatigue (wear out period). Pattern II assumes an increasing probability of failure during the break-in period which subsequently stabilises after some time. Pattern III involves a relatively stable initial probability of failure which gradually increases with time. Pattern IV involves a random failure rate throughout the in-service lifetime of the component the level of which will depend on the quality and operational conditions. Pattern V based on fatigue degradation assumes a linearly increasing probability of failure. Finally, Pattern VI involves higher infant mortality rate where initial operation has inherently a higher probability of failure due to unknowns in the design and the quality of the product followed by a relatively lower and stable probability of failure at later stages as various issues are gradually addressed [91]. Figure 34 shows the different patterns of reliability that different components can exhibit.

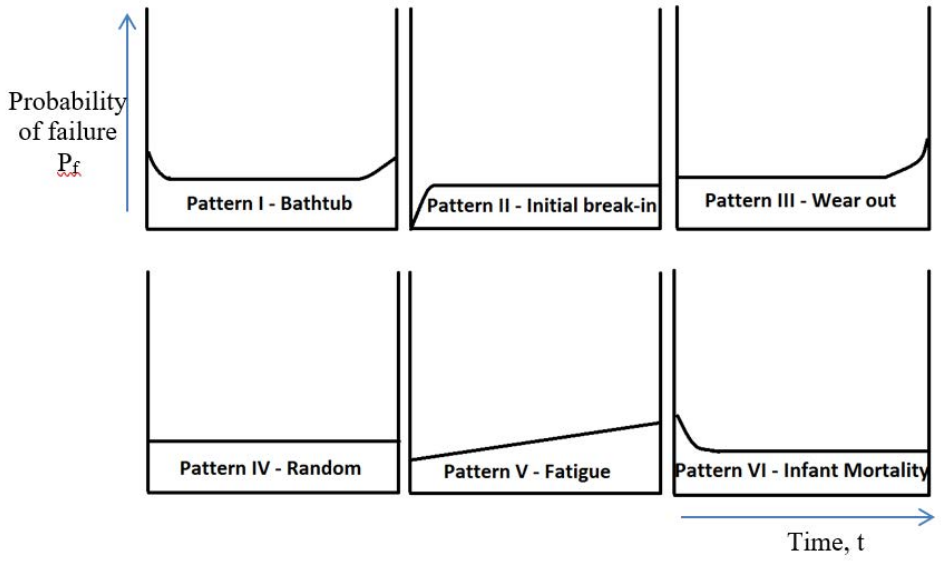

Figure 34 Patterns of reliability in modern maintenance theory

It has been generally considered that wind turbines exhibit a bathtub pattern with respect to their reliability. This has also been the traditional approach to failure for most complex machinery and systems over the last half a century or so. However, from available data, particularly those concerning wind turbines installed offshore, it can be deduced that the reliability curve will follow different patterns in comparison with the one predicted by the bathtub curve. Considering the available failure data that have been reported from various studies including the RELIAWIND project for various wind farms including onshore and offshore ones, it can be safely concluded that failures have occurred almost across the entire board much more rapidly than anticipated by design standards [72] [100]. Since the loading conditions offshore are normally much more severe than onshore, damage propagation has been seen to cause problems much earlier in comparison with what has been observed onshore.

It is important to take into account that practically all studies concerned with the collection of wind turbine failure data have been mixing together different types and makes of wind turbines and types of faults. This can lead to erroneous conclusions particularly since wind turbines have been constantly evolving, whilst at the same time their size and complexity have also been increasing. The technological developments at subcomponent level, together with the progress in the overall wind turbine design, further complicates the correct and meaningful analysis of the available failure data as well as the conclusions drawn from the results obtained.

It appears that so far only limited effort has been expended on establishing a valid relationship between failures and environmental factors prevailing at local level such as average wind speed, turbulence, terrain morphology, icing conditions, maximum wind speed, time operating at maximum power output, etc. However, these parameters are only a small fraction of the large

number of various parameters that need to be quantified in order to fully evaluate the actual condition and risk of failure of the individual gearbox components in industrial wind turbines.

4.6 Summary

Wind turbine gearboxes are important sub-systems for the operation of all the wind turbines that are not based on direct-drive designs. The gearbox is responsible for translating the slow input rotational speed of the rotor to a high speed rotational output in the generator.

Unfortunately, the majority of gearboxes despite the fact that they have been designed for a minimum lifetime of twenty years, rarely manage to reach this. Most require replacement of repair within the first six or seven years of operation. In general, lubrication quality fluctuation issues are a major factor influencing the time and way that damage will initiate and subsequently propagate in such components. Inconsistencies in lubrication can reduce the lifetime of wind turbine gearboxes by more than 80%.

Offshore wind farms have generally availability which is lower than onshore wind turbines. One of the main reasons for the lower availability of offshore wind farms has been attributed to the poor performance of gearboxes. This is due to the fact that commercial gearbox designs have been unable to cope with the loading conditions prevailing in offshore locations.

CHAPTER 5

WIND TURBINE GEARBOX AND POWER ELECTRONICS REMOTE CONDITION MONITORING

5.1 Remote condition monitoring for wind turbine gearboxes

As already discussed earlier in this study, gearboxes can suffer from various defects which if remain undetected can lead to final catastrophic failure. Therefore, it is imperative that gearboxes are monitored for evolving damage while the wind turbine is in service. Since wind turbines are located in remote areas and the gearbox is installed in the nacelle, accessibility is always an issue. Therefore, any evaluation of the actual condition of the gearboxes and the subcomponents it consists of is only realistically feasible using Remote Condition Monitoring (RCM) techniques. Early wind turbine designs did not use any type of sensors for RCM. However, after the occurrence of a number of wind turbines lost to fires caused by lubricant combustion due to overheating bearings, the use of temperature sensors became the default. It was also subsequently realised that damage in gearboxes propagates faster than originally anticipated by designers who had predicted a twenty-year minimum lifetime. As a result, RCM based on vibration analysis became commonplace in all industrial wind turbine models. Acoustic emission has only so far been used to a limited extent but can also be applied for monitoring damage evolution at its early stages. Real-time oil sampling using online sensors is also possible for the presence of moisture and the amount of debris present including the characteristics of the particles detected, i.e. whether they are ferrous or non-ferrous. RCM is supplemented by manual inspection techniques that are scheduled to take place at specific intervals by the personnel attending the wind farm on a regular basis.

5.2 Temperature sensors

Temperature sensors are widely used in industrial wind turbines to monitor the temperature of the lubricant. The sensors can trigger an alarm when a preset threshold is exceeded alerting the wind farm supervisor to proceed with an emergency shut down. The wind turbine controller

can also automatically shut-down the wind turbine to avoid further overheating without the intervention of the wind farm supervisor. However, in case of erroneous alarms the personnel attending the wind farm can override the controller and restart the wind turbine. Although temperature sensors are reliable and inexpensive, they will only generate an alarm when the damage has already progressed significantly. At this point the only option available to the wind farm operator is to proceed with emergency maintenance. This will lead to unpredicted loss of production and associated losses until the problem has been fixed. Moreover, in the event of a malfunctioning temperature sensor, overheating can still occur potentially resulting in a fire to break out as a result. Figure shows some industrial temperature sensors.

Figure 35 industrial temperature sensors **[101]**

5.3 Oil analysis

Although oil analysis is predominantly carried out offline by retrieving oil samples at pre-scheduled intervals (normally every 6 to 12 months), modern sensors enable the online RCM of the oil condition. The oil condition and the amount of particles present in a sample or the population of particles flowing with time through an oil sensor can be used to detect early

degradation and wear of the gearbox components. Moreover, depending on whether ferrous or non-ferrous particles are involved and their size it is possible to identify the component affected and the severity of wear. However, some error is introduced in the assessment due to the gradual milling of the particles as they pass through contact surfaces and get squashed as well as the removal of some particles through the filters installed in the lubricant system.

5.4 Accelerometers and vibration analysis

RCM of gearboxes has mainly focused on vibration trending. The analysis of the acquired vibration signals is performed using various algorithms including moving RMS, moving Kurtosis, moving Crest Factor, Fast Fourier Transform (FFT), power cepstral analysis and spectral kurtosis.

Vibration data are acquired using several accelerometers, normally 7-8, which are installed at appropriate locations on the gearbox casing. A large number of vibration systems are commercially available. Some of these systems are capable of automatic analysis without requiring human intervention unless further in-depth evaluation is required. Unfortunately, such expert systems require large datasets in order to be accurate. Therefore, the normal condition should be defined and trended for each gearbox type and wind turbine type. Then any variations caused in the data trending can be recognised as particular faults evolving with time. However, the major challenge at the moment, which renders this process inaccurate are the variable loading and lubrication conditions, causing large excurses in the vibration signals even when no apparent damage is present. It has not been uncommon for gearboxes to have been trended over a long period of time, consistently showing increasing amplitudes in the captured vibration data suggesting that there is a severe fault which is rapidly growing present. Unfortunately, in several cases the gearboxes have been subsequently opened and found to be

in good condition. Therefore, false alarms is an additional issue for existing wind turbine gearbox RCM technology.

In addition, for each measurement location per component, three directional vibration readings are required. Six such readings are required for averaging in order to build the reference signature per direction and per location. This form of analysis in many cases can involve large errors in the diagnosis since structural vibration and background noise could alter the vibration profile and thus lead to a wrong evaluation of the actual condition of the machinery being inspected. Moreover, in most cases bearing faults remain difficult to diagnose and require further and more complex analysis which in many cases may not achieve the desirable result.

In order to ascertain which component(s) within the gearbox have been affected, spectral analysis needs to be carried out. However, the kinematics of the gearbox need to also be known. This may not always be possible depending on the confidentiality agreements signed between the wind turbine manufacturer and operator.

5.5 Acoustic emission

Acoustic emission (AE) is an extremely sensitive technique which can be used for the early detection of wear in rotating components of the wind turbine gearbox. The AE technique is different from vibration analysis, as it detects the noise produced by the rotating components of the gearbox. In the case of vibration analysis, the vibrational response of the structure and its changes are evaluated instead. Therefore, more severe defects are required in order to cause detectable changes in the vibrational response of the gearbox in comparison with changes in the noise produced. Hence, AE offers a valuable tool which is capable of detecting damage much early than vibration analysis. Also, the operational range of AE is normally above

100kHz, whilst accelerometers used in vibration measurements of wind turbine gearboxes tend to operate between 0.1 Hz and 18 kHz.

Since AE listens for noise, the transmission path is far less attenuative. Therefore, the AE sensors can be at a distance from the actual source of the signal. This means that for monitoring an industrial wind turbine gearbox, two to three AE sensors would suffice. In the case of vibration at least seven accelerometers would be required. Taking into account that the cost of AE sensors and accelerometers is comparable, the reduction in the number of sensors coupled with the increased sensitivity can result in significant savings to the operator without compromising accuracy.

For AE data, the same signal analysis principles as those employed for vibration data can be used. Again, the kinematics of the gearbox need to be known in order to identify accurately which component has been affected. AE can stand alone as an RCM technique but can also be used to complement the vibration measurements, helping establish a more cost-effective maintenance plan which can be based on condition-based approaches rather than corrective. In the future, it will become realistically feasible to move towards true predictive maintenance approaches. Unfortunately, at this particular moment, considering the complexity of the issue of predicting the remaining lifetime of a wind turbine gearbox, although effective diagnosis is achievable, effective prognosis still remains largely elusive.

5.6 Remote condition monitoring of power electronics

RCM of wind turbine power electronic converters is not widely used yet. The RCM technology still faces a lot of challenges in terms of data acquisition approaches, types of sensors used, number of sensors required, establishing Key Parameter Indicators (KPIs), KPI trending, KPI analysis approches, data handling and storage, understanding the relationship between the physical and mechanical properties of the various materials that the various parts (e.g. IGBTs, connectors, stators, etc.) of the power converter are manufactured from and what their failure mechanisms are.

In wind turbines, semiconductor devices, particularly the IGBT, and capacitors have been identified as the key sources of faults and failure of the power electronics. Hence, the majority of the limited RCM effort expended for evaluating online power converters in wind turbines that has focused on these two component types. IGBTs can deteriorate with time due to various reasons, including exposure to high temperatures, thermomechanical stresses due to thermal variations, accummulation of salt in the connectors, excessive humidity, etc. Therefore, one of the key challenges that need to be addressed in order to render power converter effective is the identification of KPIs that are directly related to the actual degradation. Unfortunately, several KPIs of interest, such as the chip junction temperature, cannot be easily measured during normal operation [36-37].

For assessing the condition of power electronics remotely, a wide range of sensors thus needs to be employed. These include current and voltage sensors, temperature sensors, accelerometers, and humidity sensors. The sampling rate used for each of these sensors, including the time of acquisition should be carefully selected. For example current intensity and voltage would need to be continuously monitored otherwise significant events could be

missed. On the other hand temperature and moisture will not change very rapidly, hence, data acquisition rates as low as 1 Hz or even less would be acceptable. Vibration analysis should need to be carried out at regular intervals which are indicative of the operational condition of the wind turbine with respect to wind speed and output. The other difficulty that needs to be addressed is the fact that the sensors should be embedded within the power converter for smooth operation and the generation of useful data.

Previous researchers has focused so far predominantly in on-state voltage or resistance based measurements for the detection of bond wire lift-off, thermal resistance and temperature-based analysis, switch time-based RCM for the power device and its gate driver, gate-signal-based RCM for gate degradation, in-situ or sensor-based RCM which is also the interest of the present study as discussed in the following chapters, system identification-based RCM.The advantages and disadvantages of each of the aforementioned techniques are summarised in Table 1 [102].

Table 1 Advantages and disadvantages of the different approaches for RCM of the wind turbine Power Electronics

CM Method	**Advantages**	**Disadvantages**
Vce, Ron	High relevance for detection of degradation	Difficult to measure small variations of Vce signal
Rth (thermal resistance)	Identifying solder fatigue	Difficult to measure Tj
Gate voltage waveform	Identifying electrical faults	High real-time requirement
Prolonged switch-time	Identifying gate drive failures	Hard to measure ns-range switching times
Embedded sensors	Reliable and accurate	DBC modification is necessary; expensive CM
System-level identification	No additional hardware required	Difficult to correlated faults with system symptoms; complicated algorithms neede

System Level Identification means relationship between component-level faults and system-level faults should be recognised. Wind turbine its subsystems include many components, and thus the system- or subsystem-level fault detection and current isolation complicated. Fault isolation also requires more systematic analysis. Relationship between component-level faults and system-level faults need to be established efficiently.

5.7 Summary

RCM for wind turbine convertes is admittedly in an embryonic stage of research. It is necessary to first of all understand the different failure modes and mechanisms involved before RCM can become effective and the appropriate types of sensors and data acquisition rates are employed. However, as already discussed in previous chapters, power converters are currently responsible for a significant percentage of faults and cumulatively contribute significantly to the downtime experienced by modern industrial-scale wind turbines. Therefore, it is of utmost interest to develop and widely implement effective RCM methods and tools for diagnosing and prognosing faults in the power converters of wind turbines. This will support the improvement of the overall wind turbine reliability, resulting in higher availability and hence capacity factor. A higher capacity factor can further strengthn the profitability of wind turbines, further strengthening investments in renewable energy sources and supporting the effective decarbonisation of the global economy at a reduced risk.

CHAPTER 6

EXPERIMENTAL METHODOLOGY: CUSTOM-BUILT POWER CONVERTER TEST RIG

6.1 Design of custom-built power converter test rig

As part of this study, a custom-built power converter test rig was designed and implemented in order to simulate failures of IGBTs. The results obtained could then be compared with the findings arising from the industrial wind turbine power converters monitored using a variety of sensors as well as assess the optimum data acquisition approaches and signal processing methodologies.

A small scale power converter simulating the design of those used in industrial wind turbines was designed and built. The power electronics test rig developed operates at both low voltage and current. Throughout the laboratory experiments carried out the measurements were taken and compared with the real data from the industrial 1.5 MW wind turbines considered in the project. Temperature-related failures were performed by gradually increasing the temperature of the IGBTs and assessing the time to failure. The following schematic diagram in figure 36 illustrates the diagram of the power converter (inverter) which will be completely built at a later stage.

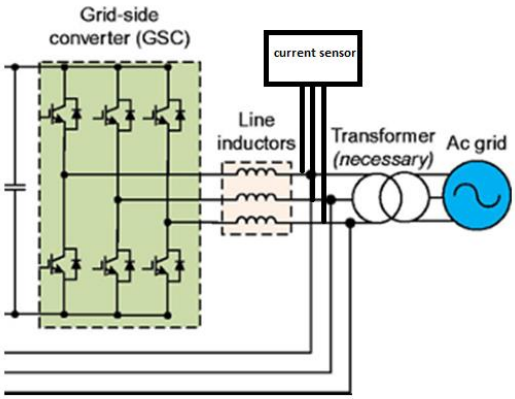

Figure 36 Diagram of power converter **[55]**.

The following schematic diagram figure 37 demonstrates an overview of the power converter system that is to be built with the features of closed loop Current feedback and variable output based on the feedback (load consumption).

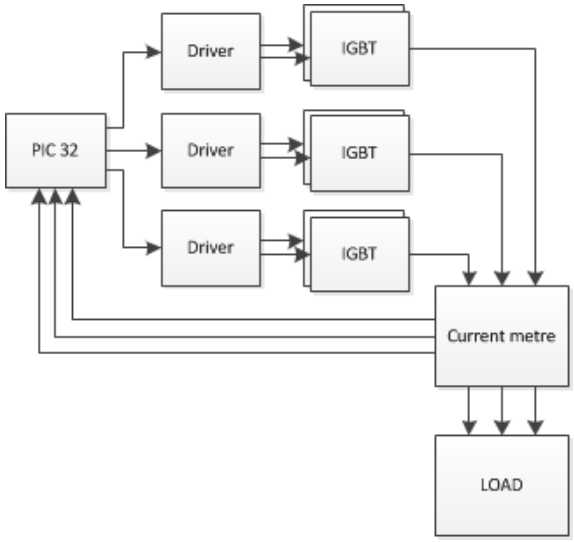

Figure 37 Schematic diagram showing the power converter test rig architecture overview.

6.2 Design of the gate drivers

Control of the IGBTs is achieved by means of signal communication sent to the IGBT by a driver. A high voltage half bridge driver model L6384E has been used in this particular design. This device has been manufactured based on BCD"OFF-LINE" technology, which is of a high voltage and a half bridge driver structure, having the ability to drive N-channel power MOS or IGBT. The floating section, also known as the high side, is intended for feeding almost 600V, which is the equivalent of rail voltage. The following figure 38 demonstrates the block diagram of L6384E.

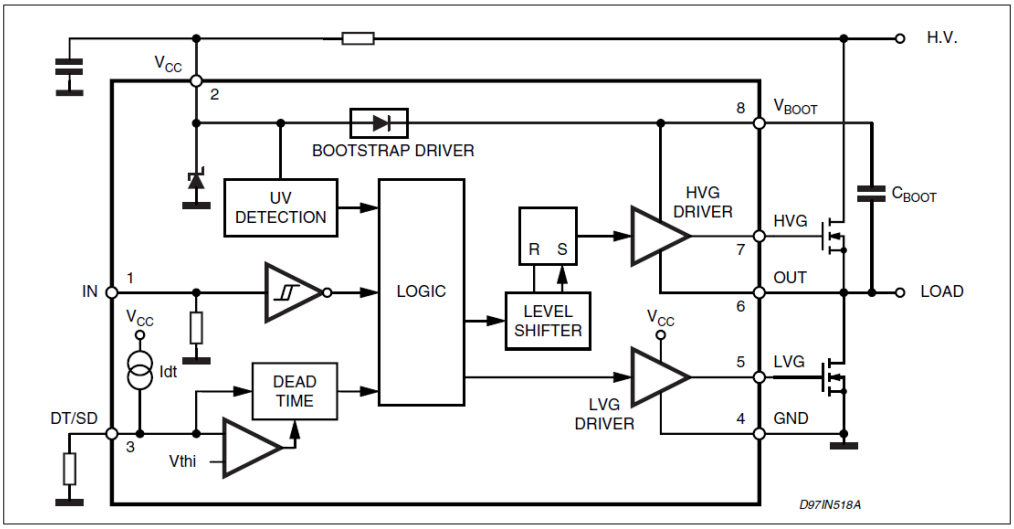

Figure 38 Block diagram of L6384E [103]

6.2.1 Pin connection of L6384E

Figure 39 shows the top view of the L6384E driver used in the test rig design. As shown in the aforementioned figure, there are a total of 8 pins, where pin allocated as 1 is the logic input that is connected to pic 32 in order to transfer the signals to the IGBT. In addition, the input is compatible with the supply input voltage (V_{cc}) at which there is an internal clamp of, in the opposition of phase with low side driver input (LVG) and in phase with high side driver input (HVG). Pins allocated as 2 and 4 are connected to the power supply.

The DT/SD known as high impedance pin, has two primary functionalities. Firstly, it shuts the driver down when the voltage drops lower than V_{dt} [Typ. 0.5V]. Secondly, at a voltage which is higher than V_{dt}, a dead time is set amongst the LVG and HVG.

The LVG and HVG are used in order to send the required signals by the operator to the IGBT. In addition, the high side driver floating reference shown as pin 6 is connected to the load. Finally, pin 8 known as boostrap supply voltage is the high side driver floating supply at which a capacitor is also connected between this pin and high side driver floating reference. This is

often fed by the boostrap driver, which is an internal structure. The internal driver can often be replaced by an external boostrap diode.

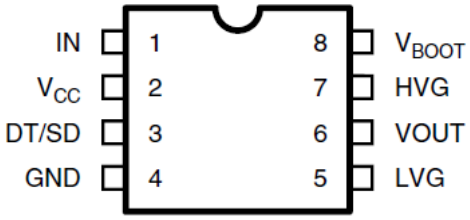

Figure 39 top view of L6384E **[103]**

6.3 Design of the current meter

In order to measure the current over the load for the test rig converter designed and built, a current transducer (CT) LA25-NP has been employed. This CT model has 10 pins for connection of input and output and also 2 pins for connecting the CT to positive and negative voltage. One pin is used for the measurements. The schematic diagram in figure 40 below shows the CT pin connections. There are different ways to connect the input and output pins, but in this study it has been chosen to connect the pins as shown in the figure below.

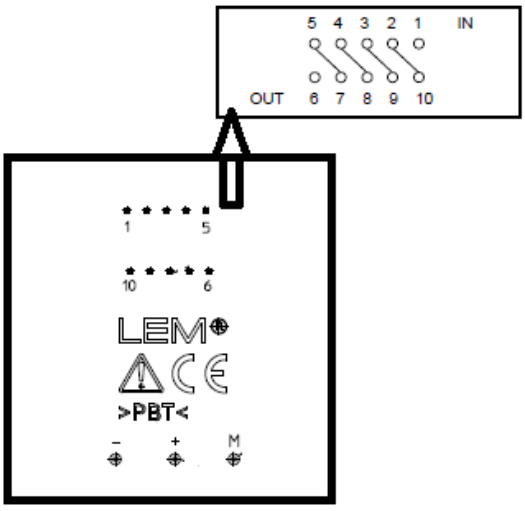

Figure 40 Current transducer (CT) LA25-NP pins.

The measurement provides the current output, but pic32 can only read the voltage. Therefore, the current reading has to be converted to a voltage. In order to convert the current reading to

a voltage, a resistor is used. The resistor is connected to the measurement pin of the CT from one side and to the ground from the other side. The value of the resistor has been recommended by the datasheet of the CT to be between 100 to 320 Ω. A resistor with a resistance of 270 Ω has been used in this particular design. The schematic diagram in figure 41 shown below illustrates this connection.

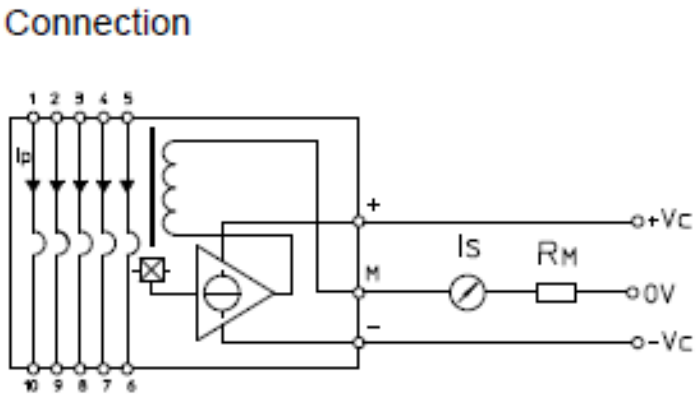

Figure 41 Current transducer connection **[104]**

6.4 Control system

The L6384E is not capable of generating the signal itself. Therefore, the signals need to be generated and sent to the driver. Consequently, a programmed pic32 has been used. Besides, a board is required for the wired connections. A chip KIT uC32 has been determined to be suitable for this task. The uC32 has the advantage of the powerful PIC32MX340F512 microcontroller, which features a 512K flash memory card, 32-bit MIPS processor core operating at 80 Mhz, and 32K of SRAM data memory [105]. uC32 has 42 in/out pins and also provides 12 analogue inputs. The photograph in figure 42 shows the chip KIT uC32.

Figure 42 Chip KIT uC32 **[105]**.

6.5 System design and implementation

A three-phase power converter has been designed which is capable of operating with a total of six IGBTs (that generated AC electricity). However; as designing and building a three phase inverter is a complicated task on its own right and in order to understand the operating procedure of the inverter, a single phase PWM inverter has been designed and built as shown in the following figure 43.

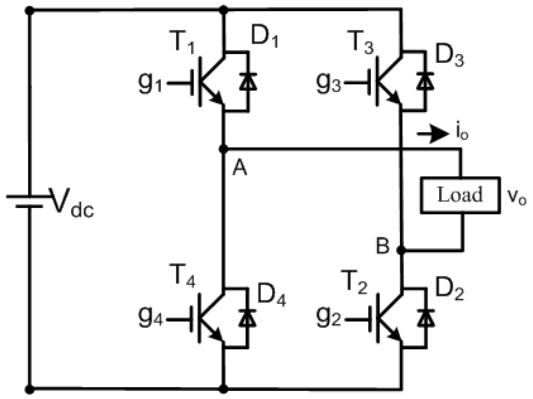

Figure 43 Single phase PWM inverter.

The single-phase inverter holds four IGBTs. At any given time two IGBTs need to be switched on and the other two need to be switched off. This act or processing of operating the switching

device (IGBTs) is carried out by the signals sent by the driver. Constant switching on/off produces sine waves that is used to convert DC to AC.

6.5.1 Generation of sine waves

In order to generate sine waves numerous techniques and methods are available and widely used in various industries. The Sinusoidal Pulse Width Modulation (SPWM) is one of the most effective and popular techniques used in recent years. In this particular technique, digital waveforms are generated at a point, where duty cycle is likely or possible to be modulated in a way that the sine wave is fed and coordinated by the average voltage waveform. The comparison of both the high frequency triangulate wave and the low power sine reference is known to be one of the easiest yet effective methods of producing a SPWM signal. This signal is therefore used to control the switches of the IGBTs.

The driver takes on two tasks upon receiving the SPWM signal. Firstly, the signals are sent to one of the IGBT without changing anything. Secondly, the driver inverts this signal and sends it to the other IGBT. Consequently, at any point given, one IGBT is switched on and another off. Figure 44 shows the generation of the SPWM signal.

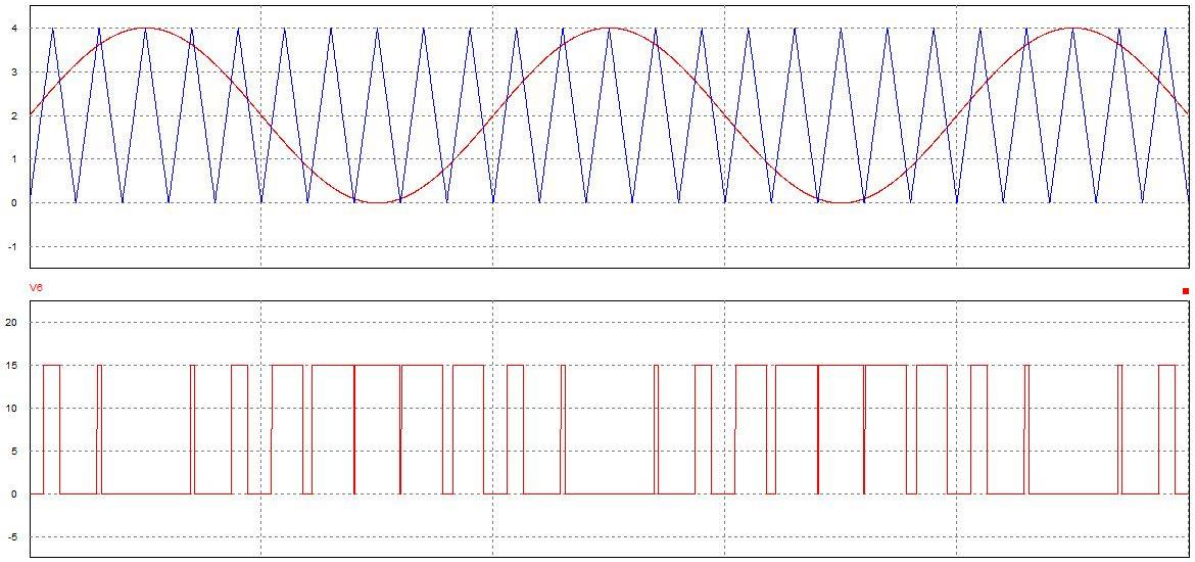

Figure 44 A single phase sine wave inverter

As each driver only controls two IGBTs, three drivers are needed in order to build a three-phase inverter, where six IGBTs are used. In this particular model, three SPWM signals with 120 degree phase difference are required. Consequently; by using inductors as load instead of resistance, these SPWM signals can be smooth and have a shape of similar to sinusoidal or a sine wave. Figures 45 and 46 illustrate the three-phase inverter and overall experimental connection of IGBTs and driver, and other component on the board used for this project respectively.

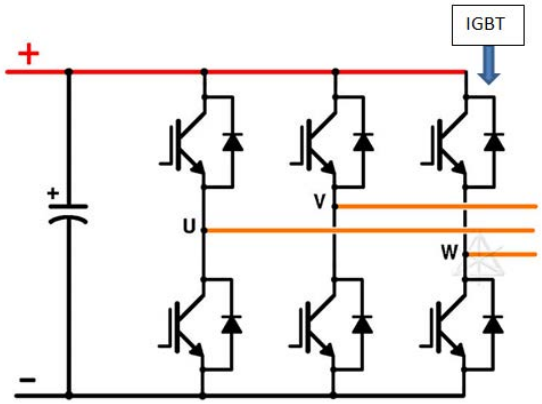

Figure 45 Simplified schematic of the three-phase inverter architecture

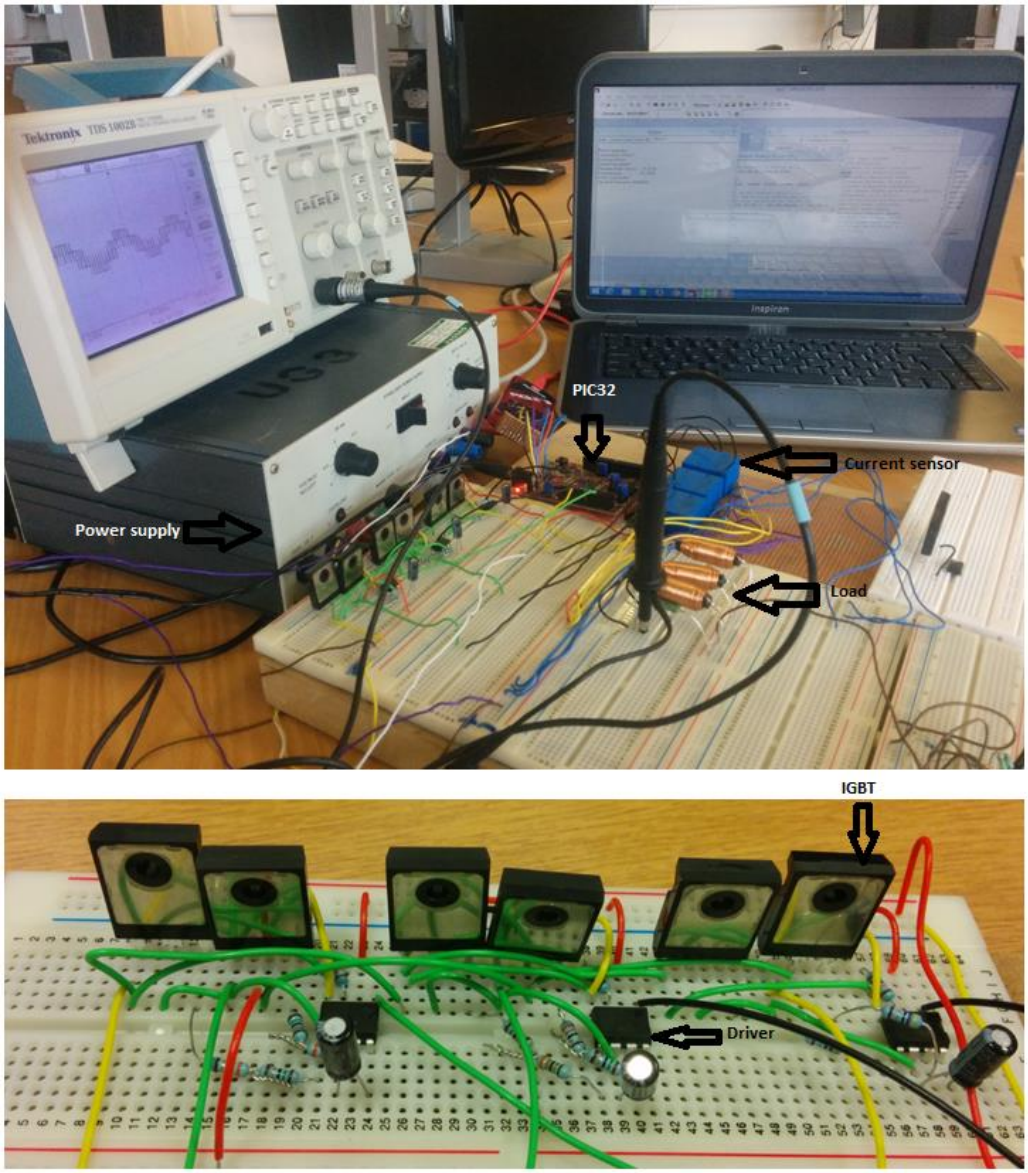

Figure 46 Experimental connection of IGBTs and driver and other component on the board.

The control signals generated by pic32 using comparison between sine and triangular wave that feeds into the driver in order to control the IGBT's switching mode are shown in figure 47. This signal is used for one leg of three-phase inverter and it has triangular wave with frequency of 500Hz and a sine wave of 50Hz. Also as shown in this figure, each unit requires 5 ms and for each sine wave to be completed 4 units of time are required. Therefore, the total time for one sine wave is 20ms which makes the frequency of 1/0.02 or 50 Hz.

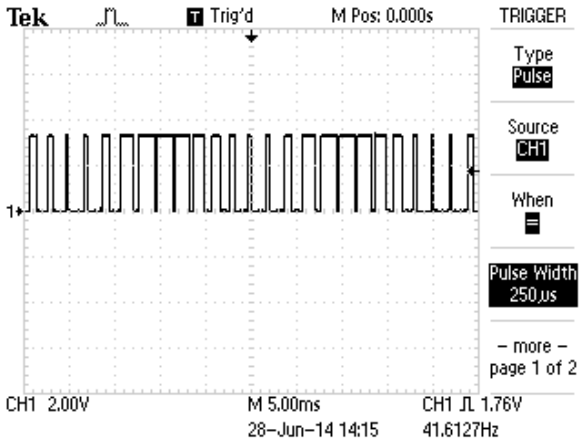

Figure 47 SPWM signals made for leg of inverter using PIC32.

Figure 48 is of a same nature as the above but with two channels shown. The second signal belongs to the other leg of the inverter. By looking at this figure the phase difference between two channels is noticeable. The phase difference is derived to be 240 degrees based on the figure below, with phase one and three shown.

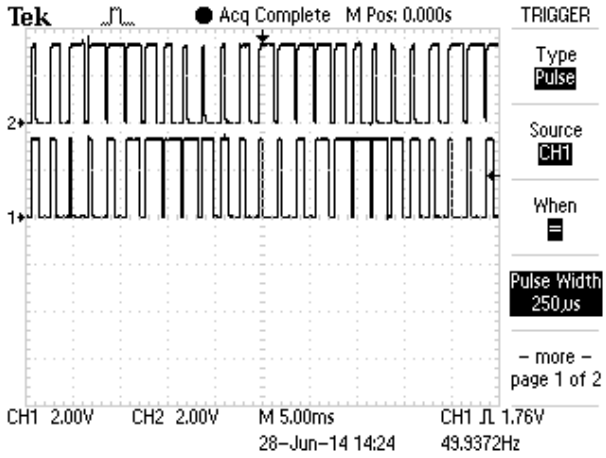

Figure 48 SPWM signals for two legs of inverter with 500 Hz triangular wave frequency.

Figure 49 illustrates the SPWM signals for two channels, where the frequency of the triangular wave has been incraesed from 500 Hz to 1kHz.

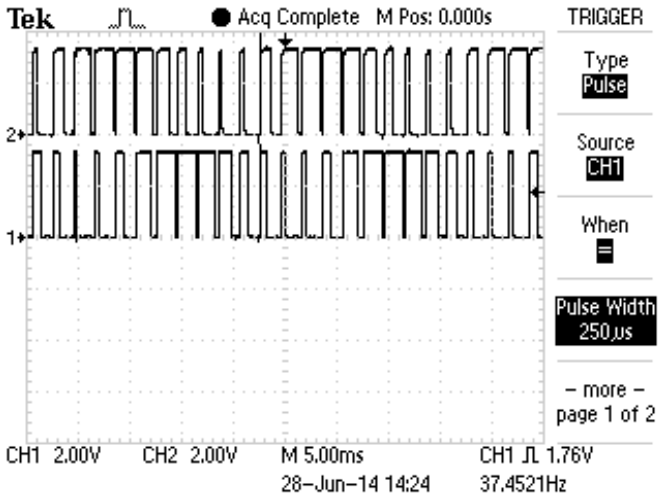

Figure 49 SPWM signals for two leg of inverter with 1 kHz triangular wave frequency.

The following figure 50, shows the subtraction of two waveforms (SPWM). By subtracting this two-phase signals, the difference will show one sine wave. If these 3-phase SPWM signals are connected by means of star connection, each of this phase SPWM signals to the common point will provide one sine wave.

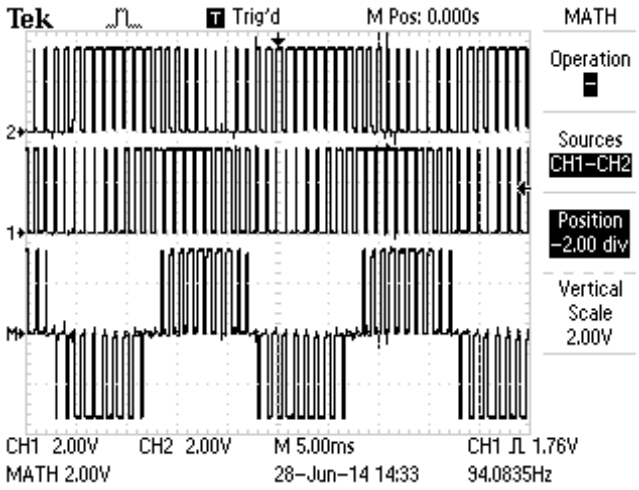

Figure 50 Difference between two phases

6.5.2 Current controller

Current-controlled pulse width modulated (PWM) voltage source inverters are most widely used in high performance AC drive systems, as they provide high dynamic response. The main

objective of the proposed controller is to inject a clean sinusoidal current to the grid, even in the presence of nonlinear/unbalanced loads and/or grid-voltage distortions.

Sometimes the load takes too much current or very small current comparing to the reference current which is set by the user. In order to control the current of load, the voltage needs to be controlled. For example, in figure 51, the load is taking much more current than aimed (reference current). Thus, the current is limited by reducing the size of sine wave which is compared with triangular wave (inside the PIC controller). This leads to less voltage going to the load therefore reducing the current.

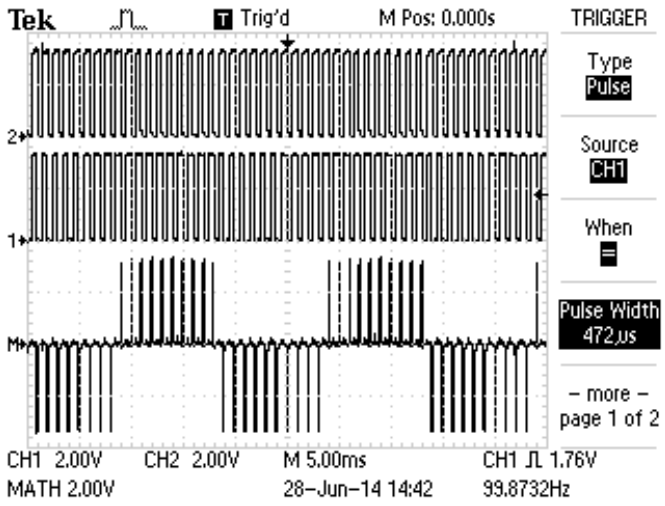

Figure 51 Load taking too much current.

In figure 52, the plot is similar to limiting but this time load is taking too small current and there is a requirement to increase the current, so the size of sine waves is decreased in comparison with triangular wave (inside PIC controller). This leads to more voltage going to the load and therefore more current.

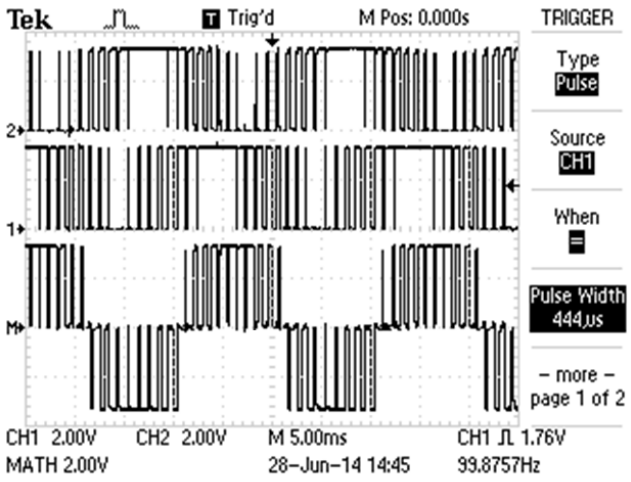

Figure 52 Load is taking too small current.

Providing that the load is taking sufficient current with respect to the defined reference current, and by considering a one-phase to neutral signal for two legs, figure 53 is produced where the phase difference is 120 degrees.

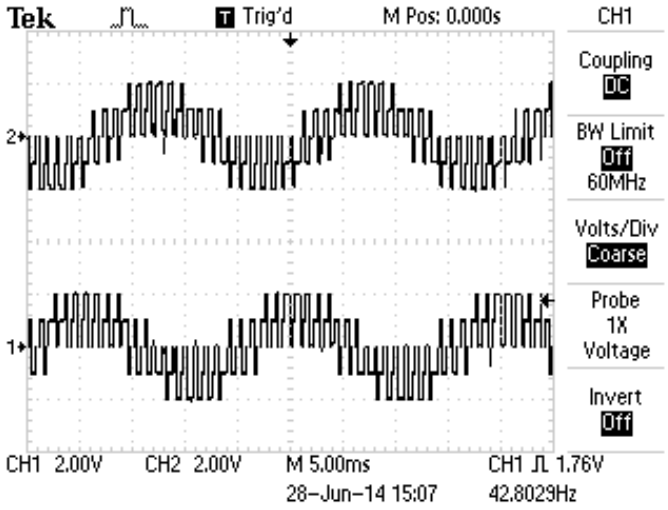

Figure 53 The load is taking enough current with respect to the defined reference current.

Figure 54 also shows a one-phase to neutral signal where the load is taking much more current with respect to the defined reference current. Therefore, by reducing the size of a sine wave in comparison with triangular wave, leads to less voltage going to the load consequently reducing the current.

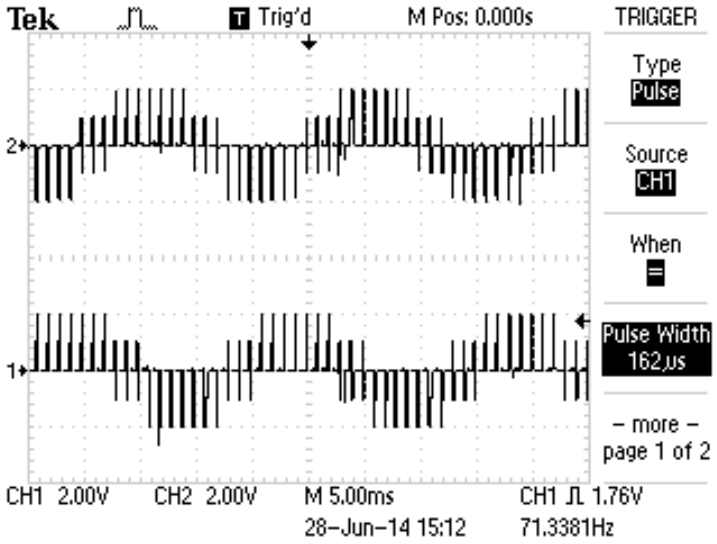

Figure 54 Limiting current.

In figure 55, the plot shown is also similar to the one above with the difference being the increase of the current to obtain to the reference current.

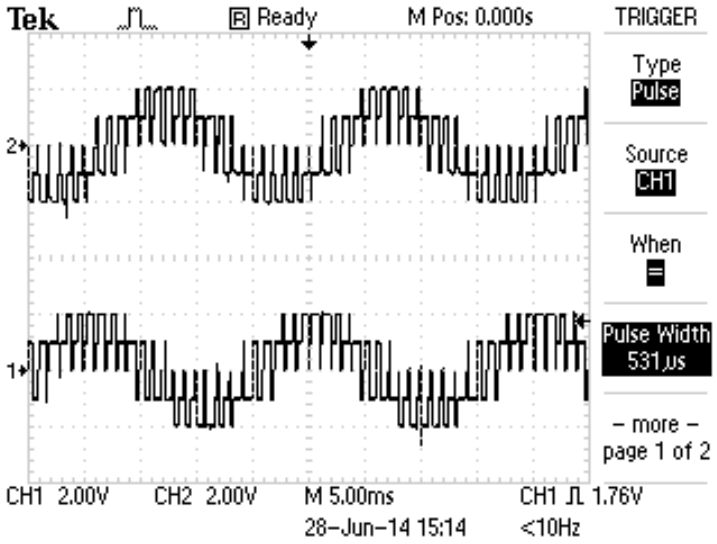

Figure 55 Injecting current.

6.6 System design and implementation of final version of the power converter

In order to use the power converter in the condition of high voltage and high current, the power circuit and electronic board has been designed using the Diptrace software. The design employed is shown in figure 56 below.

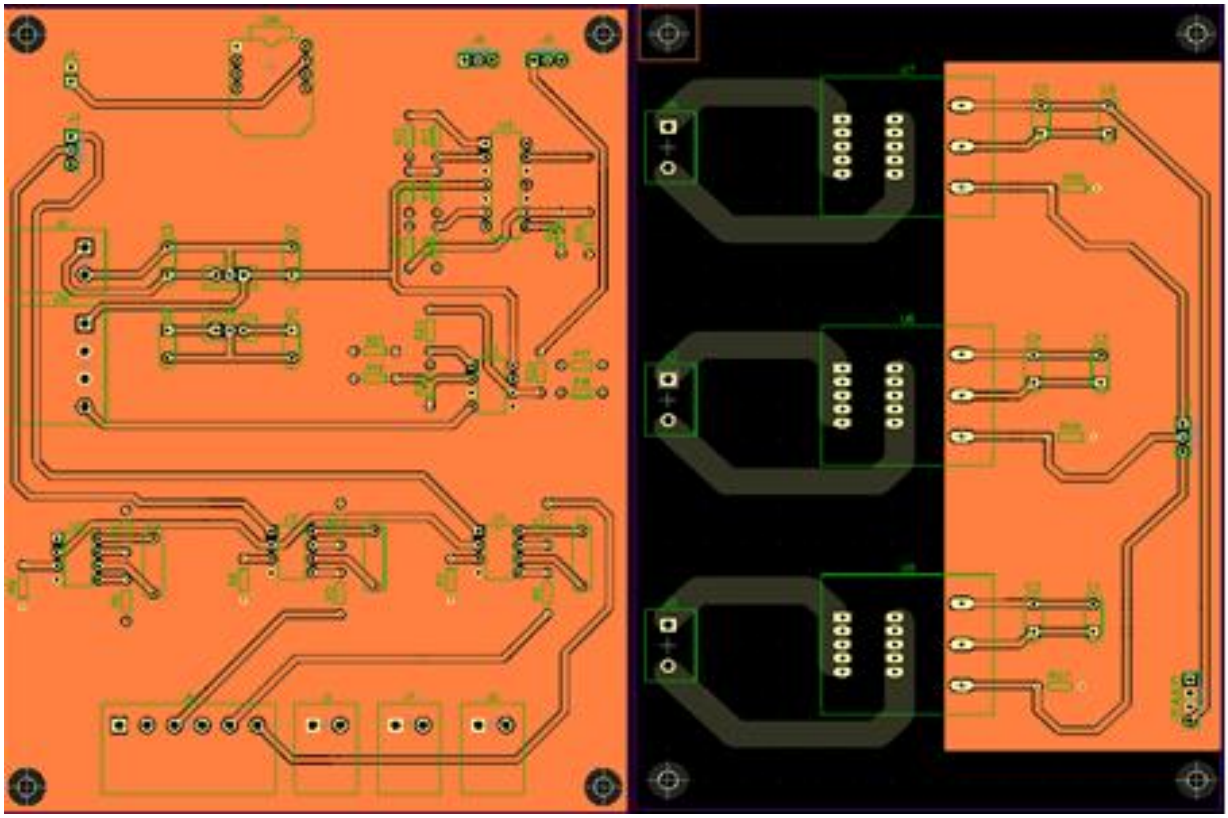

Figure 56 Power circuit and electronic board designed by using the Diptrace software.

Figure 57 shows the final version of the power converter (test rig). As it can be seen all parts of the power converter have been installed on an aluminium plate. This aluminium plate acts as a heat sink. The PCB for the power circuit has been installed separately to the PCB of the electronic circuit so short circuiting can be prevented. There are many terminal connections which are intended to make installation of this part easier.

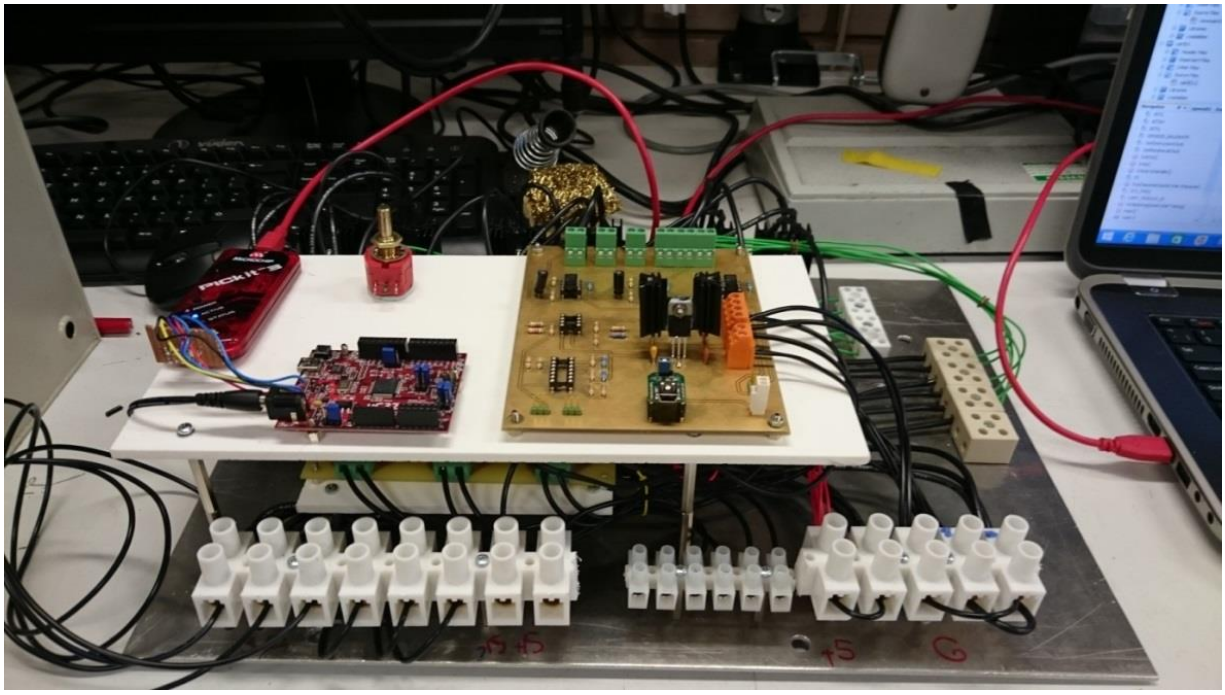

Figure 57 Final version of the power converter (test rig)

In order to test the power converter under different conditions, it is necessary that the power converter is connected to the power load. Therefore, a power load has been designed in this project as shown in the figure 58. By using this power load, we can test the power converter in high current conditions. Therefore, during this study, many tests with different scenarios have been done using this connection.

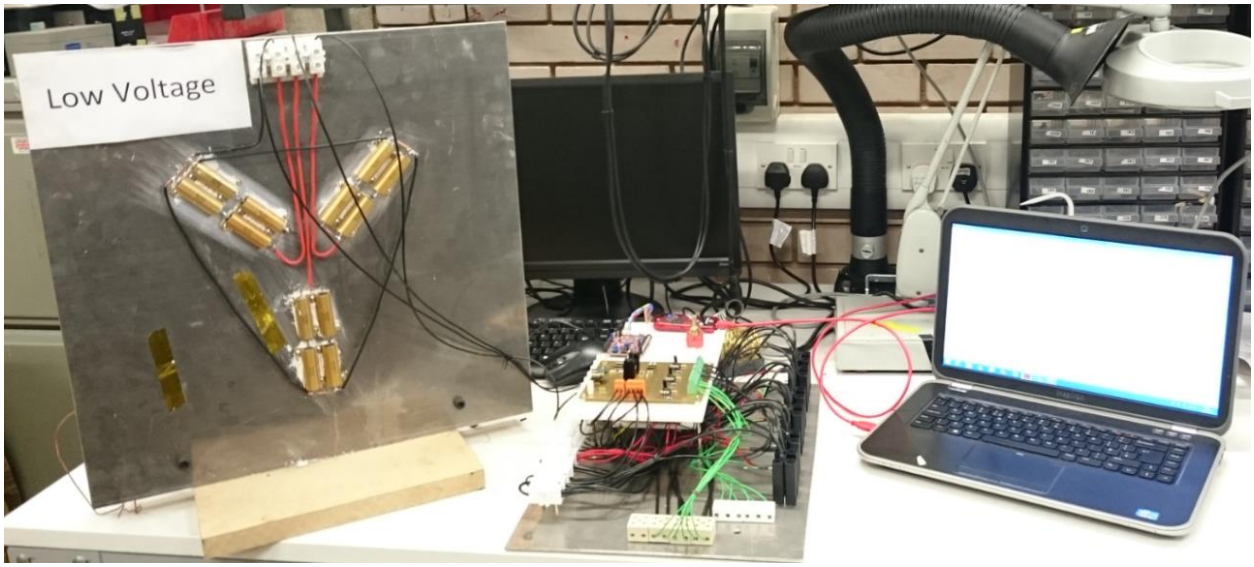

Figure 58 Power converter connected to the power load

In order to test the power converter in the actual operational conditions, it has to be connected to the grid. Therefore, a three-phase transformer has been designed in order to connect the power converter to the grid. The three-phase transformer boosts the voltage of the power converter in order to be the same as the voltage of the grid. Figure 59 shows the power converter connected to the grid by using a three phase Variac Transformer.

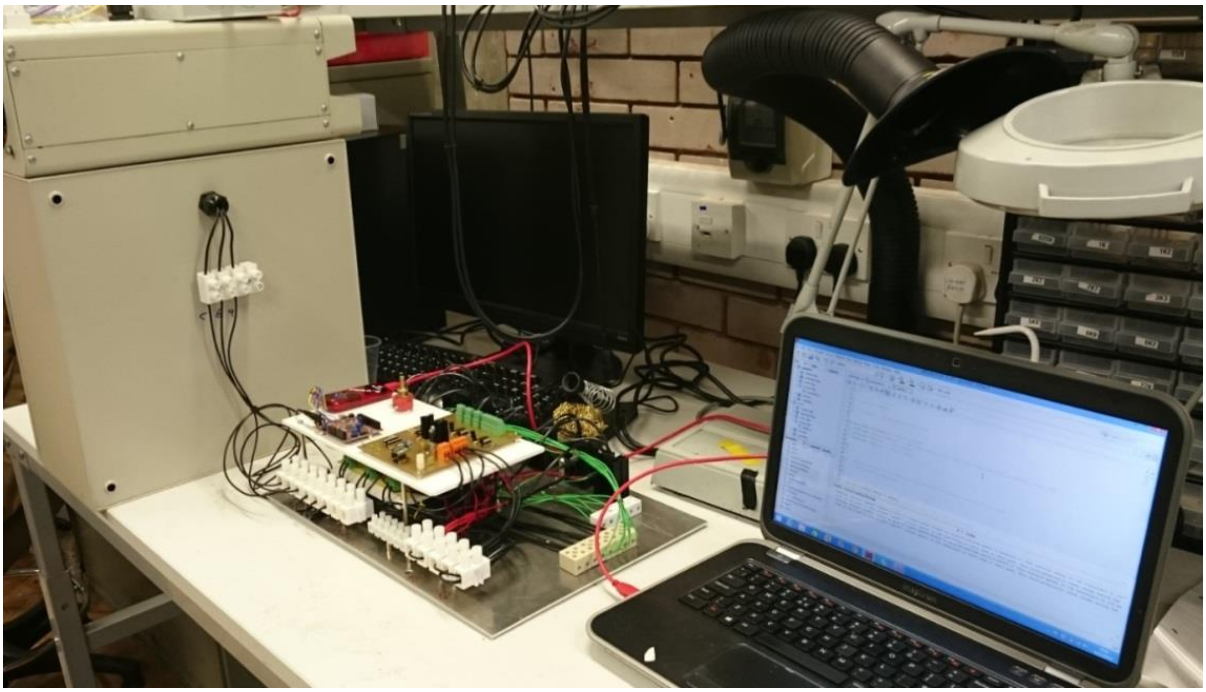

Figure 59 The power converter test rig connected to the grid.

Figure 60 shows three phase Variac Transformer, which has been designed and built for the purpose of this study.

Figure 60 The Variac Transformer used for this study.

In order to prevent short circuiting in the power converter, the power circuit of the power converter has been installed on a separate PCB. The photograph in figure 61 shows the location of the current sensors used for the measurements during testing.

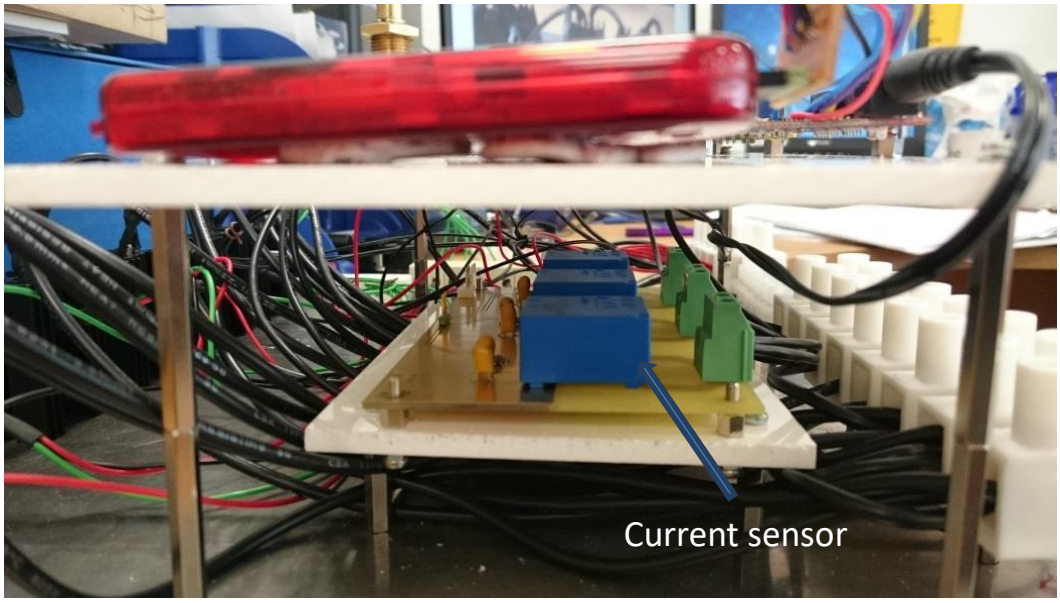

Figure 61 The position of the current sensors on the test rig.

Two different types of heat sinks have been used to build this power converter. Firstly, the heat sink which is connected to the IGBTs and secondly the aluminium plate acting as a heat sink. There, the IGBT heat sinks are connected to the aluminium plate. The temperature sensors have been installed next to the IGBTs, in order to measure the temperature of the IGBTs. Figure 62 shows the location of the temperature sensors installed on the test rig.

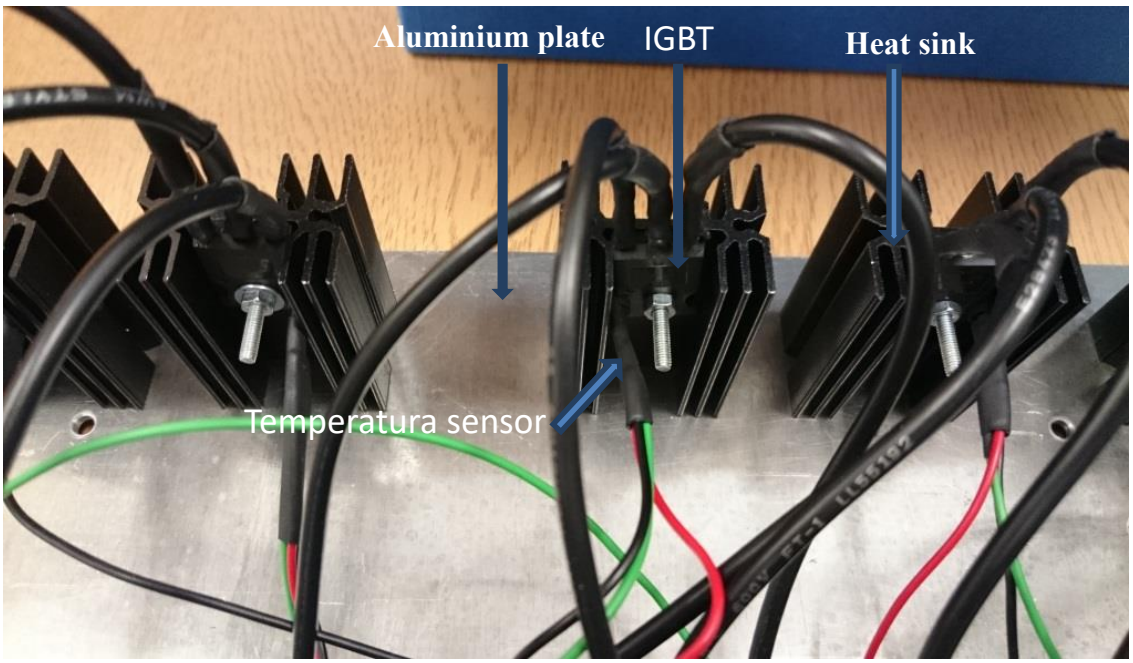

Figure 62 IGBTs and temperature sensor installation.

The plot shown in figure 63 is a typical temperature measurement of one of the IGBTs installed in this power converter.

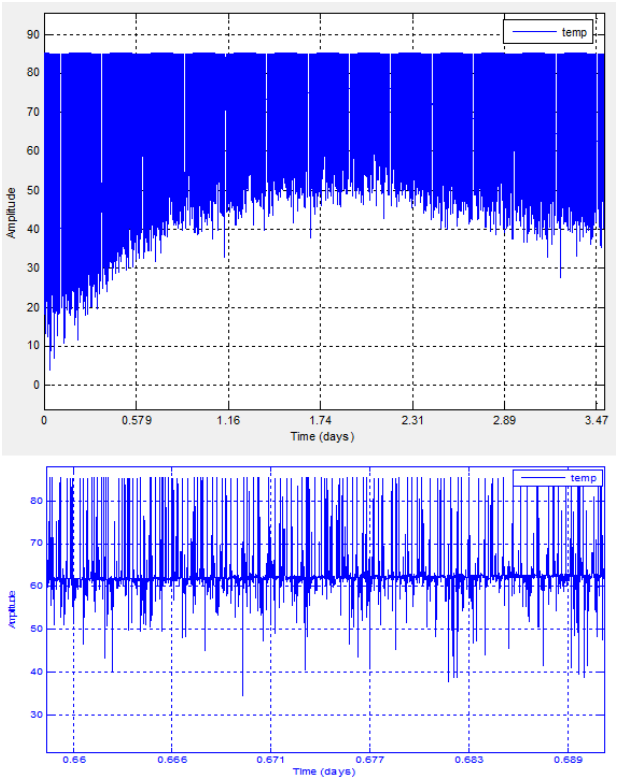

Figure 63 IGBT temperature measurement from the test rig.

As it can be seen in figure 64, there is a lot of noise with the temperature data measurement. Therefore, the filter has been designed in Matlab software in order to remove all noises. So, by doing this it is possible to carry out the analysis of data more effectively and easier. The figure below shows the developed Matlab application created for filtering of signals.

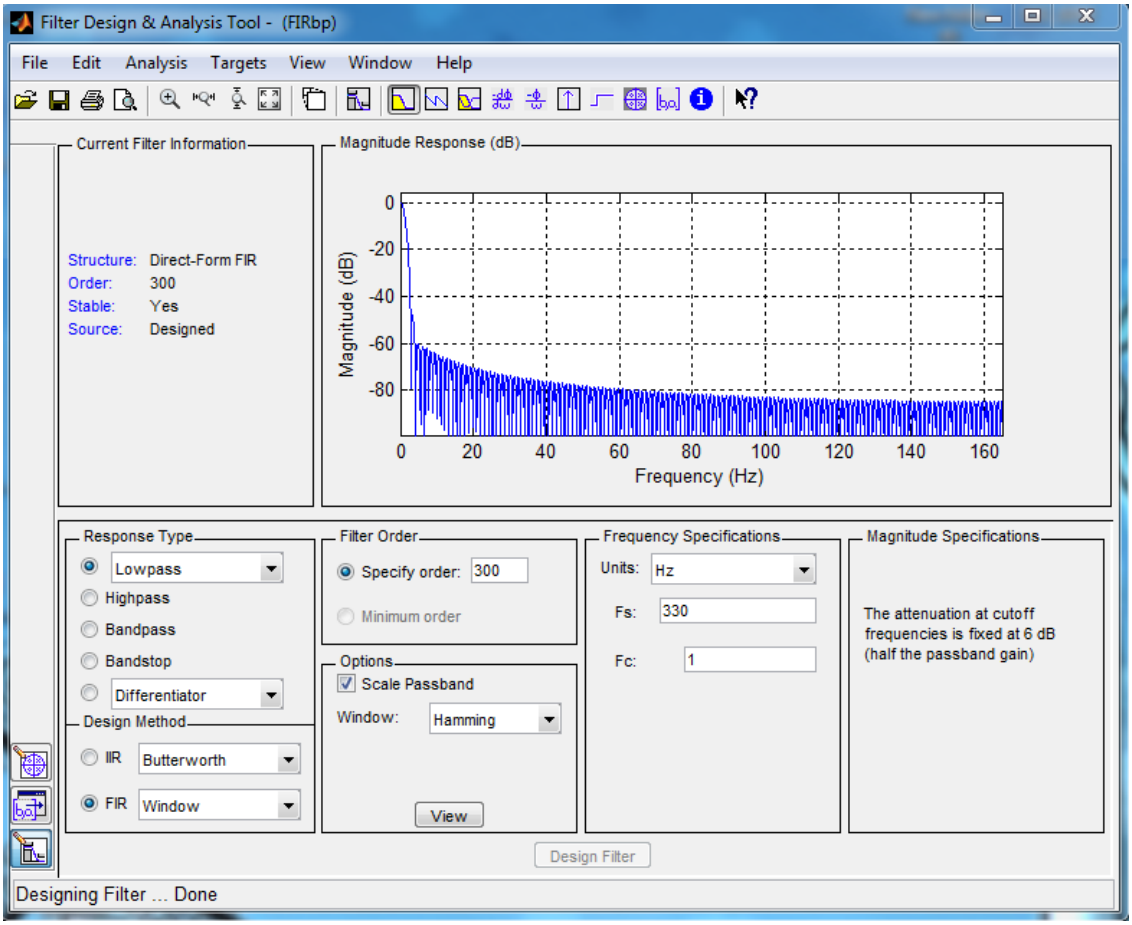

Figure 64 Application written in Matlab software for filtering of signals.

In signal processing, a finite impulse response (FIR) filter is a filter whose impulse response (or response to any finite length input) is of finite duration, because it settles to zero in finite time. This is in contrast to infinite impulse response (IIR) filters, which may have internal feedback and may continue to respond indefinitely (usually decaying)

Figure 65 below shows the temperature data after all the noise has been removed.

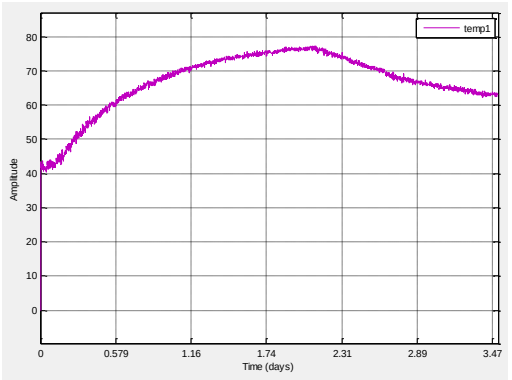

Figure 65 Temperature data after all the noise have been removed.

Figure 66 shows the three-phase current which is generated from the power converter.

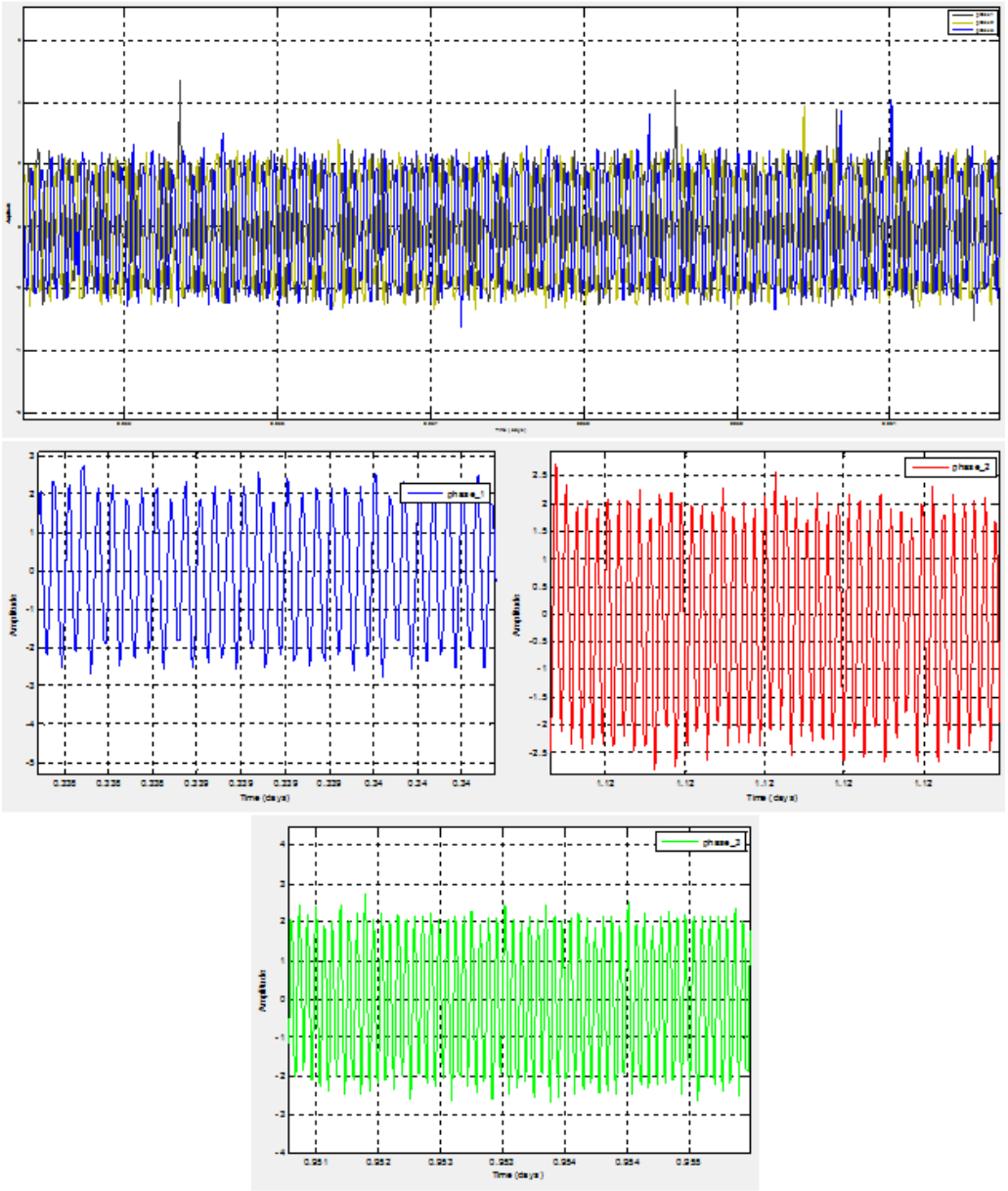

Figure 66 Three phase current generated by the power converter.

6.7 Test rig results analysis

There are a lot of noises with the temperature data measurement. Therefore, to analyses of temperature data, some sort of filter required to remove those noises. MATLAB software is one of powerful software for this job and has been used in this test rig.

Three phase current which is generated by the power converter clearly show that the power converter is working perfectly with 120 degrees phase difference with each phase. Results also show the current controller work perfectly and is able to control output current.

6.8 Summary

As discussed in this chapter, a customised power converter test rig was designed and implemented in order to simulate failures of IGBTs. The results obtained were compared with the data captured from the industrial wind turbine power converters monitored using a variety of sensors as well as assess the optimum data acquisition approaches and signal processing methodologies.

CHAPTER 7

POWER CONVERTER TEST RIG RESULTS

7.1 IGBT fault simulations

Experiments on representative IGBTs, similar to those used in industrial wind turbine power converters, were carried out using the customised test rig described in Chapter 6 of this thesis. The purpose of the experiments performed was to simulate various conditions that can result in different types of IGBT failures. The methods considered in the simulations included IGBT short-circuiting, burned or open circuit and parameter drifting. These were thought to be the key mechanisms that lead to IGBT failure in industrial wind turbine power converters. Failures were detected by monitoring the current output of the IGBTs. The type of failure was determined by visual inspection.

Some of the electrical characteristics of the IGBT were affected by changing the operational temperature of the device. Excessive heat and thermal cycling are well-known mechanisms that can progressively result in IGBT failure. During the experimental simulations carried out using the customised test rig, four different thermal scenarios were considered.

Firstly, by fluctuating the direct current fed to the IGBTs as function of temperature between 100-200°C with the normal heat sink for all of the IGBTs, secondly, adjusting the current so the operational temperature is maintained constantly at 200°C with the small heat sink for all of the IGBTs, thirdly, fluctuating the direct current fed to the IGBTs as function of temperature between 100-200°C with half of the IGBTs connected to a large heat sink and half to the small heat sink, and finally, fluctuating the current rapidly and maintaining the temperature constant at 200°C for all IGBTs.

For Test Conditions 1 and 3 the direct current was increased to 20 A as soon as the temperature reached 100°C. It was then reduced back to 2 A as soon as the temperature reached 200°C. The cycles were repeated until the IGBTs failed.

During the aforementioned simulations several of the IGBTs failed at different numbers of cycles for each of the simulated conditions. Figure 67 shows some of the burned IGBTs retrieved at the end of the simulations.

Figure 67 Failed IGBTs retrieved at the end of simulations.

7.2 Case 1 and 3: fluctuating current as a function of temperature with different heat sinks

The first scenario of simulations named condition 1 involved the fluctuation of current amplitude from 2 A to 20 A as a function of temperature using the normal heat sink. As shown

in figure 68 when the current was increased to 20 A the IGBTs heated up and when the current was reduced to 2 A the IGBTs cooled down. This thermal cycling was repeated as soon as the temperature reached 200°C and 100°C respectively.

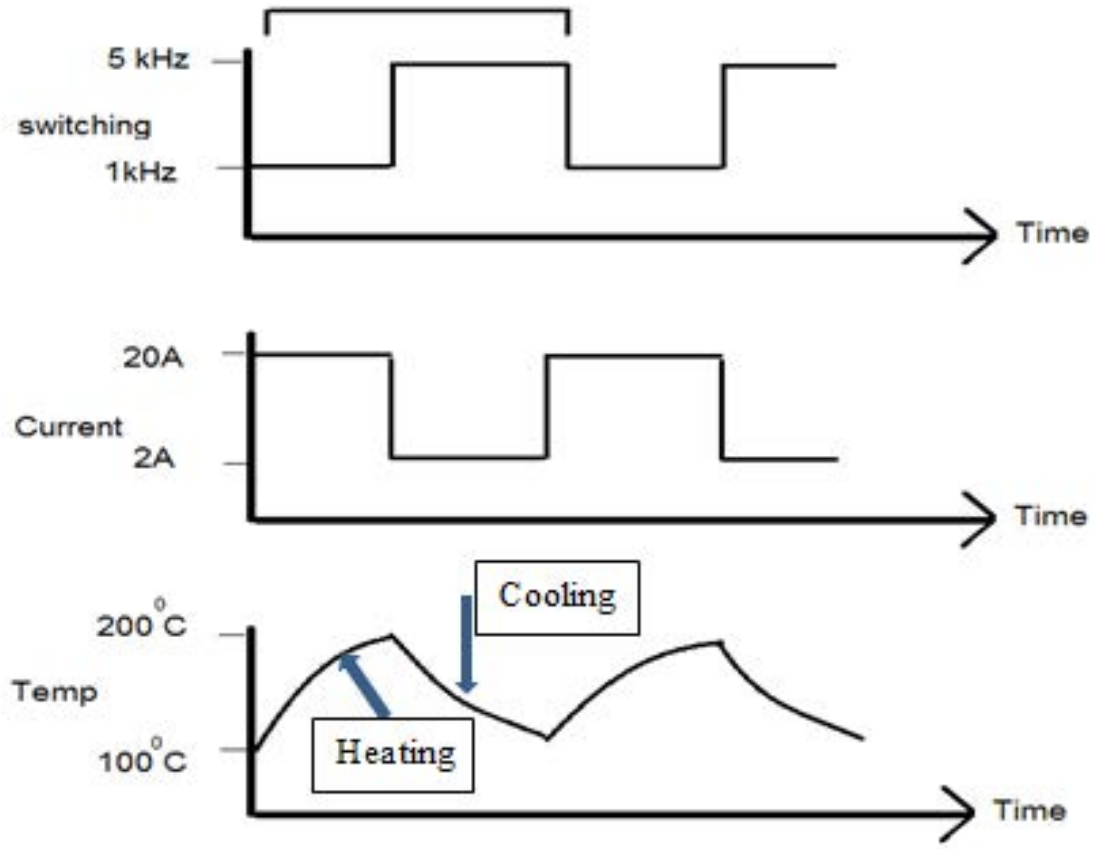

Figure 68 Thermal cycles as a function of temperature.

The thermal cycling was repeated until the IGBTs failed. The number of cycles were recorded for each of the IGBTs up to the point of failure. The results are summarised later on in this chapter. The schematic in figure 69 shows the principle of the thermal cycling process.

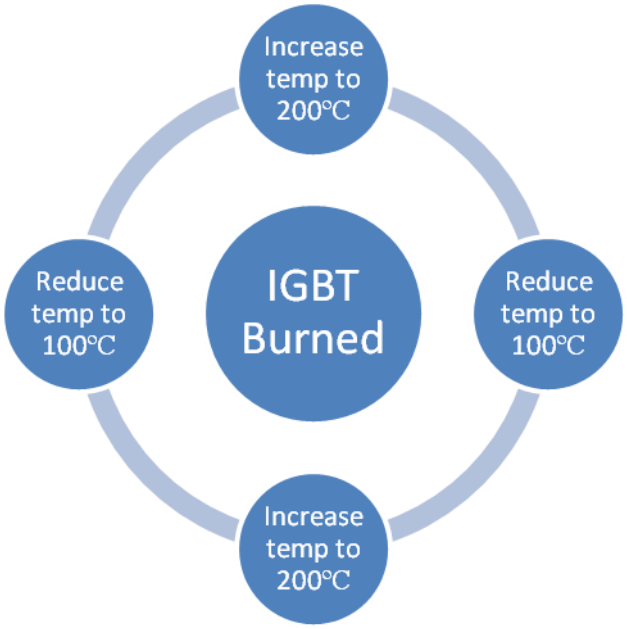

Figure 69 Simulation scenario for Testing Condition1.

During the simulations many IGBTs had burned or sustained other types of damage leading to failure. The plot in figure 70 summarises schematically the different IGBTs that failed together with the exact number of cycles at which failure occurred for Testing Conditions 1 and 3. The type of failure is also shown.

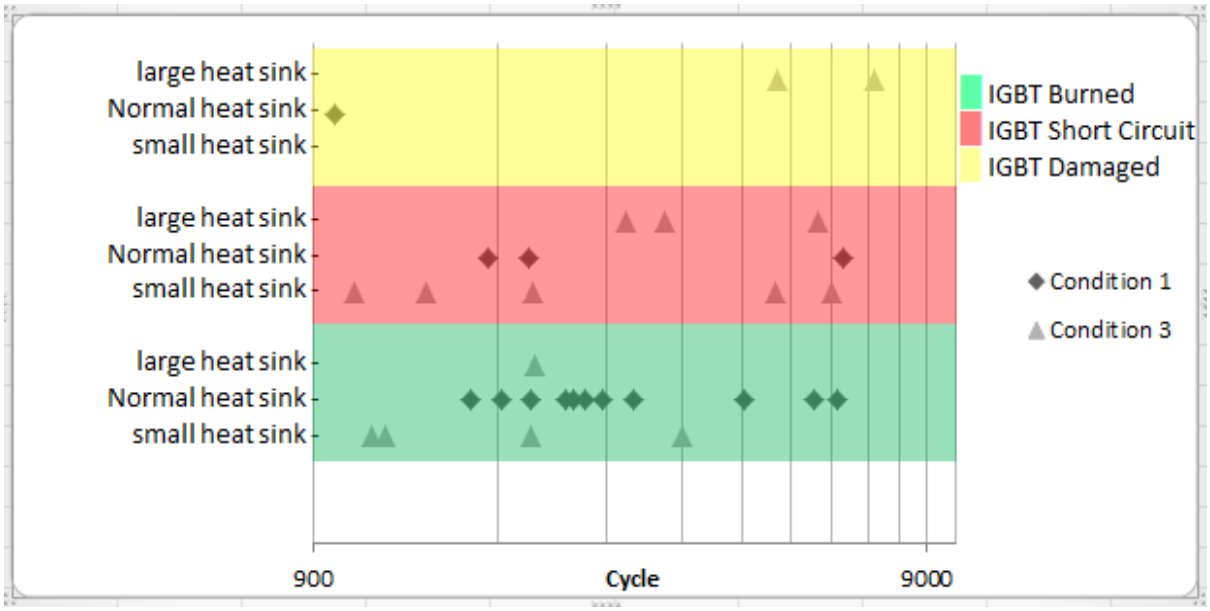

Figure 70 Failed IGBTs for conditions of 1 and 3.

Table 2 summarises the number of IGBTs that failed and the exact number of cycles at which failure took place for Testing Condition 1.

Table 2 Number of IGBT failures and number of cycles for Testing Condition 1

Condition 1		
Failure type	Cycle	Number of IGBTs Failures
IGBT Burned	2999	1
IGBT Burned	1822	1
IGBT Burned	6406	1
IGBT Burned	2391	1
IGBT Burned	2318	1
IGBT Burned	4515	1
IGBT Burned	2035	1
IGBT Burned	5892	1
IGBT Burned	2503	1
IGBT Burned	1622	1
IGBT Burned	2667	1
IGBT Short Circuit	2017	1
IGBT Short Circuit	6574	1
IGBT Short Circuit	1735	1
IGBT Damaged	973	1

Test Condition 3 simulations were based on the same thermal cycling process but using either a small or large heat sink rather than the normal heat sink used in the simulations under Test Condition 1. A large aluminium plate was employed in order to act as a large heat sink to which all individual IGBT heat sinks were connected to. The diagram in figure 71 shows the heat sink architecture for Testing Condition 3. Simulations based on the small heat sink were carried out by removing the aluminium plate and using only the individual IGBT heat sinks.

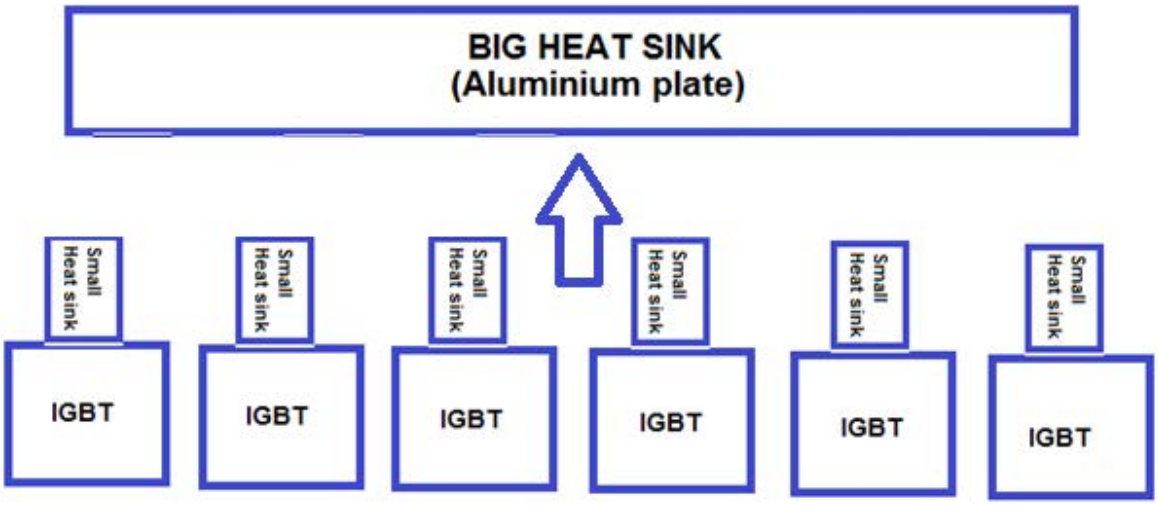

Figure 71 Heat sink architecture for simulations carried out using the large heat sink under Testing Condition 3.

Table 3 summarises the number of IGBTs failures and number of cycles to failure for Testing Condition 3 with the small heat sink and Table 4 shows the number of IGBTs failures and number of cycle for Testing Condition 3 using the large heat sink.

Table 3 Summary of results for Testing Condition 3 using the small heat sink.

Test Condition 3 with the small heat sink		
Failure type	**Cycle**	**Number of IGBTs Failures**
IGBT Short Circuit	5100	1
IGBT Short Circuit	6277	1
IGBT Short Circuit	1372	1
IGBT Short Circuit	1046	1
IGBT Short Circuit	2051	1
IGBT Burned	1123	1
IGBT Burned	1179	1
IGBT Burned	3581	1
IGBT Burned	2038	1

Table 4 Summary of results for Testing Condition 3 with the large heat sink.

Test Condition 3 with the large heat sink		
Failure type	**Cycle**	**Number of IGBTs Failures**
IGBT Damaged	7376	1
IGBT Damaged	5130	1
IGBT Short Circuit	5954	1
IGBT Burned	2060	1
IGBT Short Circuit	2916	1
IGBT Short Circuit	3360	1

From the results obtained it can be clearly seen that failures are largely random. This leads to the conclusion that the failure of IGBTs occur stochastically. This can be the result of several parameters, but it is certainly related to the quality of the materials and the way they degrade from the thermal cycling process. Therefore, estimating the exact remaining lifetime appears to be rather challenging even for a well-coordinated set of known thermal cyclic conditions. The situation would be far more difficult to predict for industrial power converters since operational parameters will change random and without control as in the simulations.

7.3 Case 2 and 4: Prolonged operation at excessive temperature

During simulations under Testing Condition 2 the direct current fed to the IGBTs was increased up to the point that the IGBT temperature reached 200ºC. Then the current was adjusted slightly as required to maintain the temperature at exactly 200ºC. The temperature was kept constant and the time to failure was recorded. The schematic in figure 72 shows the principles of these simulations. Testing Condition 4 was based on the same principles but fluctuating the current rapidly in order to simulate current spiking in the IGBTs. Hence Testing Condition 4 was probably more aggressive in terms of damage potential to the IGBTs.

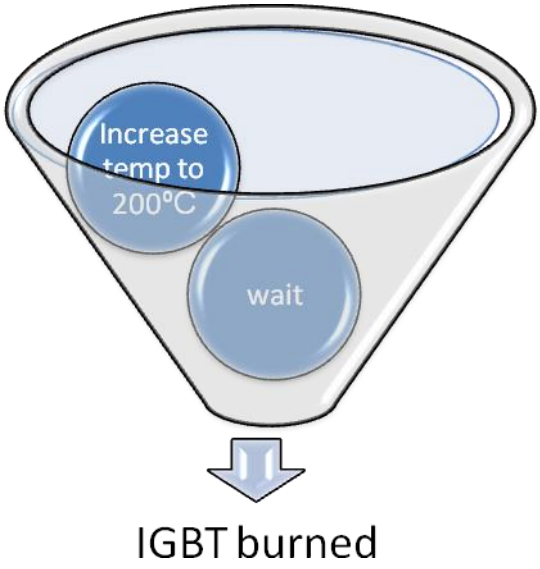

Figure 72 Principles of Testing Condition 2.

Figure 73 summarises the number of IGBT failures and the time to failure for Testing Conditions 2 and 4. Table 5 summarises the number of IGBT failures under Testing Condition 2 and the time that took for the failure to occur.

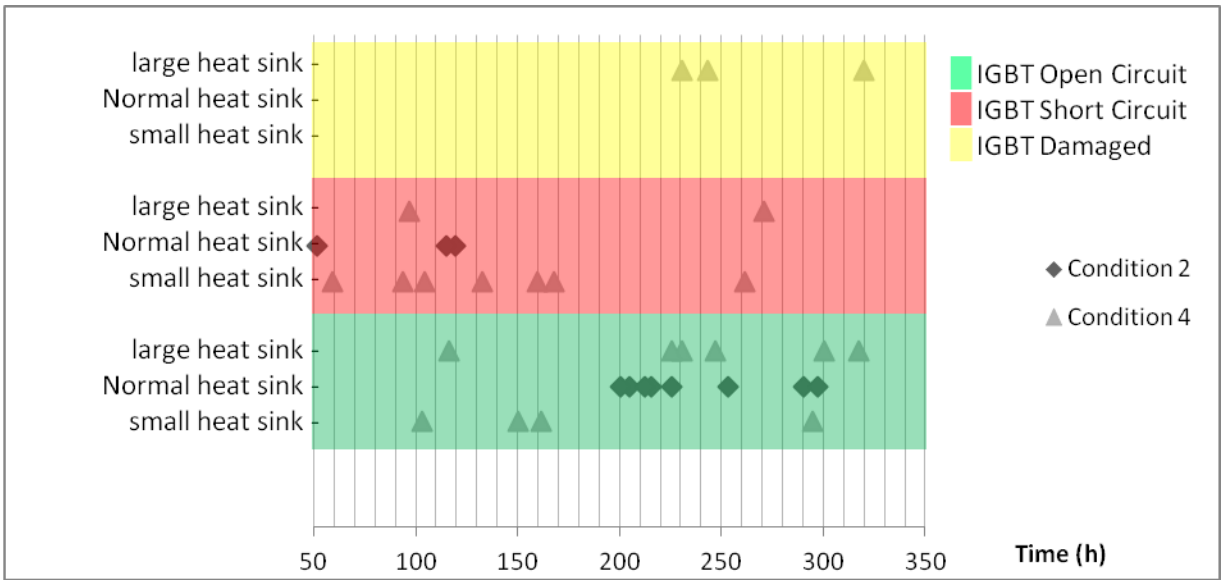

Figure 73 Plot showing the number 73of failed IGBTs for Testing Conditions of 2 and 4 and time to failure for each of them.

Table 5 Number of IGBT failures and time to failure for Testing Condition 2.

Condition 2		
Failure type	**Time (hours)**	**Number of IGBTs Failures**
IGBT Burned	215.79	1
IGBT Burned	225.64	1
IGBT Burned	290.6	1
IGBT Short Circuit	51.72	1
IGBT Short Circuit	119.16	1
IGBT Short Circuit	114.76	1
IGBT Burned	204.81	1
IGBT Burned	212.64	1
IGBT Burned	200.77	1
IGBT Burned	253.34	1
IGBT Burned	297.52	1

Under Testing Condition 4, the direct current fed to the IGBTs was fluctuated rapidly in order to maintain a constant operational temperature of around 200°C. To enable this, test the IGBTs were connected to a large heat sink enabling the rapid loss of heat and hence necessitating the rapid increase and decrease of the current fed to the IGBTs. Figure 74 shows the time difference in terms of cooling and heating of the IGBTs with respect to the size of the heat sinks.

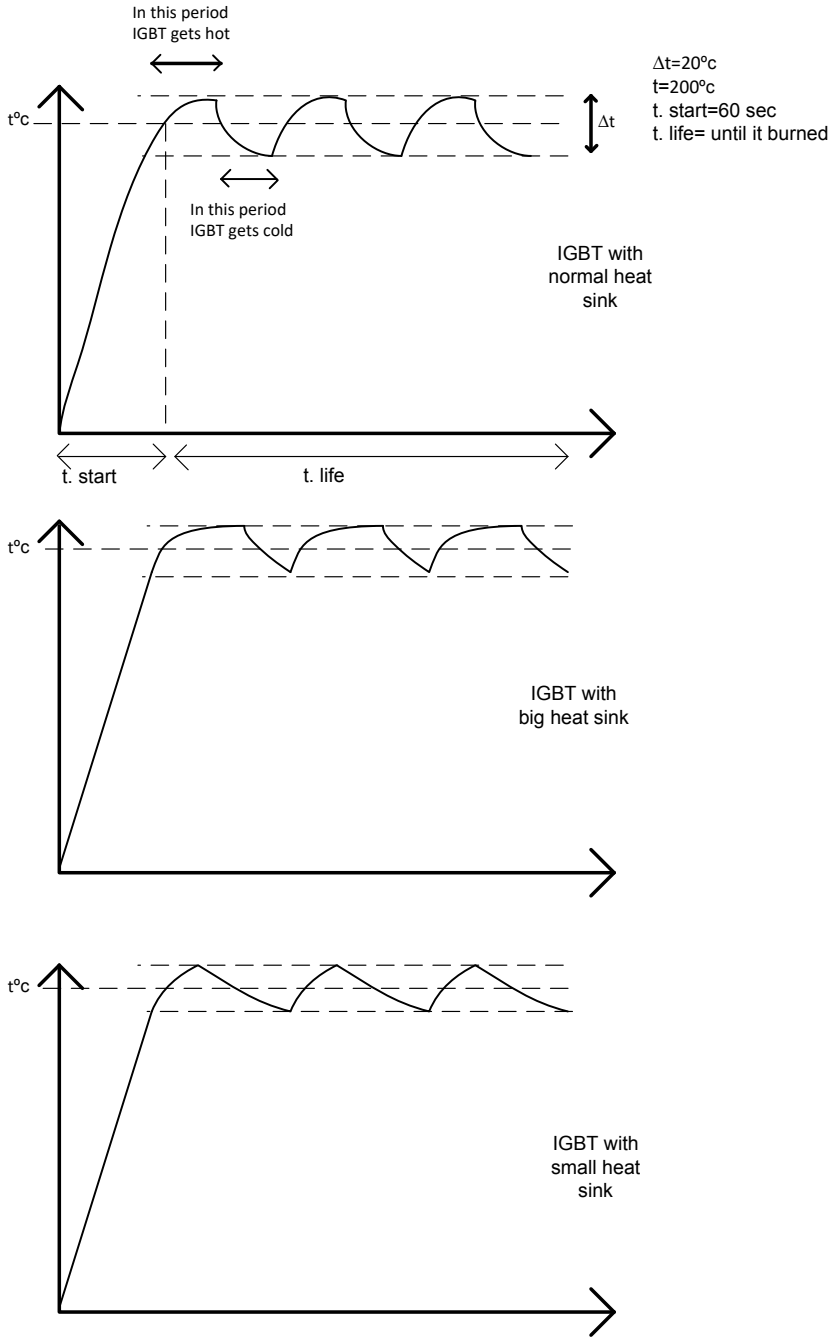

Figure 74 Time difference in terms of cooling and heating of IGBTs as a function of the heat sink size.

Figure 75 shows the principles of the simuations carried out under Testing Condition 4. The amplitude of the current was fluctuated rapidly between 5 A 20 A until the desirable heating and cooling effects were achieved in order to maintain the temperature at the required level.

Table 6 summarises the number of IGBT failures and the time taken for failure to occur under Testing Condition 4.

Figure 75 Principles of Testing Condition 4

Table 6 Summary of results for Testing Condition 4.

Condition 4		
Failure type	**Time (hours)**	**Number of IGBTs Failures**
IGBT Damaged	230.72	1
IGBT Short Circuit	261.35	1
IGBT Burned	161.8	1
IGBT Burned	150.07	1
IGBT Burned	294.56	1
IGBT Short Circuit	167.93	1
IGBT Short Circuit	159.75	1
IGBT Short Circuit	59.15	1
IGBT Short Circuit	93.65	1
IGBT Short Circuit	132.35	1
IGBT Short Circuit	104.44	1
IGBT Burned	102.93	1
IGBT Damaged	243.48	1
IGBT Burned	317.16	1
IGBT Short Circuit	96.98	1
IGBT Burned	230.49	1
IGBT Burned	300.17	1
IGBT Burned	247.26	1
IGBT Burned	225.93	1
IGBT Burned	116.61	1
IGBT Damaged	319.88	1
IGBT Short Circuit	270.74	1

As for the Testing Conditions 1 and 3, similarly for the simulations carried out under Testing Condition 2 and 4 the time to failure appears to be highly random. This again signifies the difficulty in modelling and predicting the remaining lifetime of power converter components. Again, the complexity of the industrial power converters and their operation will be much higher than those exhibited during the simulations carried out. Therefore, more considerable scatter should be expected. It should also not be ignored that in this particular set of experiments all the IGBTs had been obtained under the same batch and same manufacture. This would result in less manufacturing fluctuations and differences in quality control. Therefore, it would be interesting in the future to assess the same simulations for IGBTs from different production batches and manufacturers. It is anticipated that the scatter in the results will be even more significant adding further to the difficulties that need to be overcome in order to predict the remaining lifetime of power converters in industrial wind turbines.

7.4 Summary

Testing Conditions 1 to 4 both show similarities with respect to the time to failure, appearing to be highly random in both testing configurations. This signifies the difficulty in modelling and predicting the remaining lifetime of power converter components. Also it should be taken into account that the complexity of the industrial power converters and their operation will be much higher than those considered during the simulations carried out using the customised test rig developed as part of this study. Therefore, more considerable scatter should be expected. In addition, it should not be ignored that in this particular set of experiments all the IGBTs had been obtained under the same batch and same manufacturer. This would result in less manufacturing fluctuations and differences in quality control.

CHAPTER 8

EXPERIMENTAL METHODOLOGY: GEARBOX TEST RIG

8.1 Gearbox test rig experiments

TWI and Brunel University as part of the REMO FP7 European project designed and developed a customised test rig for simulating different gearbox faults. The faults artificially induced included wear on the gear teeth of the test rig's gearbox, impact on the rotor blades and imbalance. Both vibration and AE measurements were carried out.

The data acquisition of vibration and AE data was carried out using a customised system consisting of an Agilent USB 2531A data acquisition card. AE signals were captured using R50A resonant sensors procured from PAC and vibration using accelerometers procured from Wilcoxon with an effective operational range of 3 Hz -5 kHz due to the magnetic hold-down used to mount it on the test rig. The R50A sensor has an effective operational frequency range of 20 kHz – 700 kHz. Using analogue filters only frequencies above 100 kHz were obtained.

The sampling range was set at 500 kSamples/s for the AE measurements and 20 kSamples/s for the vibration measurements. The acquisition times for vibration measurements were set at 38s and AE measurements was set at 20s. A total of 4 AE sensors and 2 accelerometers were employed. The data were subsequently analysed using an application written in MATLAB software. In this chapter the data processing carried out from different experimental configurations are presented.

The photographs in figure 76 show the experimental setup during tests carried out in collaboration with TWI and Brunel in Granta Park, Cambridge.

Figure 76 Experiments carried out on the test rig developed by TWI and Brunel University. The experiments were carried out at Granta Park, Cambridge.

8.2 Measurements with simulated faults

In order to carry out the analysis of the vibration data acquired and reliably identify different faults simulated in the tests kinematics of the test rig gearbox were required. These were provided by the colleagues from TWI and Brunel University are shown in figure 77 and the shaft rotational speeds and frequencies are summarised in Table 7. As mentioned earlier various faults were simulated including artificially induced gear teeth damage, imbalance, looseness, impact and combinations of the above faults occurring simultaneously. From the analysis shown next it was discovered that dominant and hence more severe faults, tended to mask the presence of other lesser faults present at the same time. The rotational speed during testing was set at 11 RPM from the rotor side.

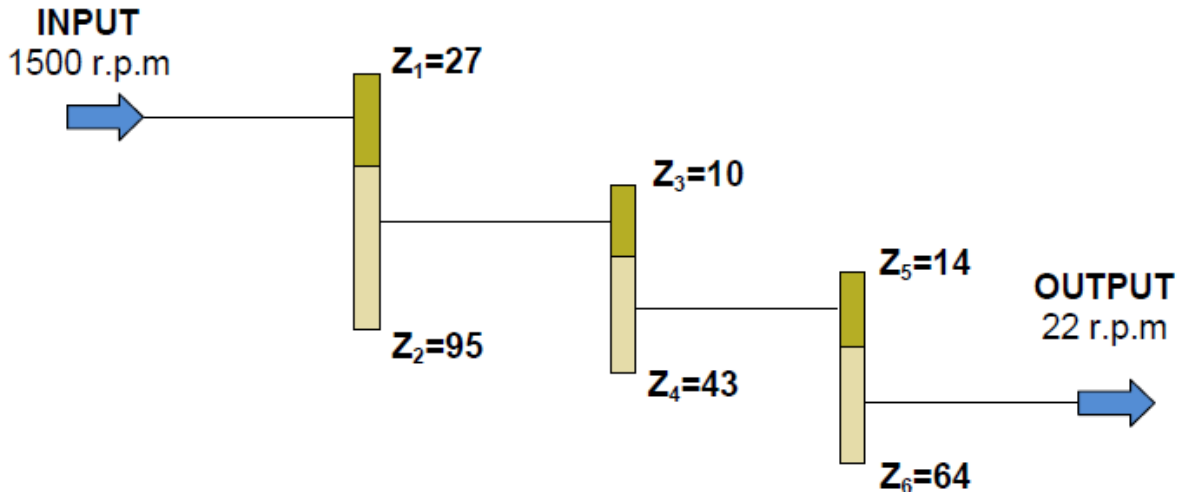

Figure 77 Gearbox test rig kinematics as provided by TWI and Brunel University.

Table 7 Shaft rotational speeds and frequencies provided by TWI and Brunel University.

	Stage 1		Stage 2		Stage 3	
Shaft Rotational Speed (r.p.m)	1500	426.3	426.3	99	99	22
Shaft Rotational frequency (Hz)	25	7.1	7.1	1.6	1.6	0.4

AE signals were amplified using four PAC pre-amplifiers and one KRESTOS four-channel digital amplifier. Accelerometers were powered using a KRESTOS four-channel power supply. Data were logged on using an industrial computer.

Figure 78 shows the power spectrum of the vibration signal obtained with only the gear damage present. The gear damage is evident at 9.7 Hz and a second harmonic is seen at approximately 19.4 Hz. The peak at 21 Hz is the high-speed shaft frequency whilst the peak at 64 Hz is the intermediate GMF.

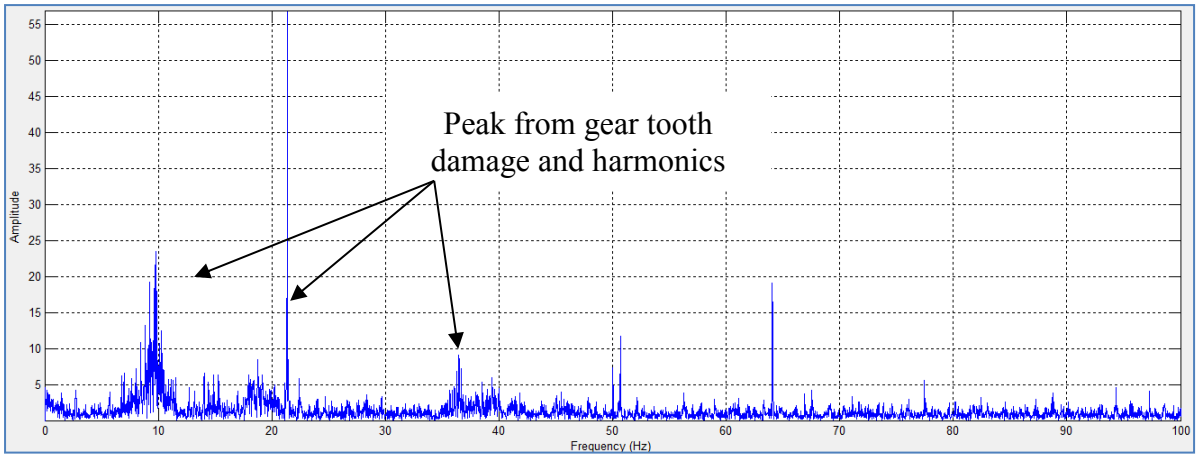

Figure 78 Power spectrum of the vibration measurement gear tooth damage only

The following plot in figure 79 shows the power spectrum for the vibration signal measured with imbalance and gear tooth damage present simultaneously. The peaks from the gear fault have a dominant effect in comparison with imbalance at the rotor side.

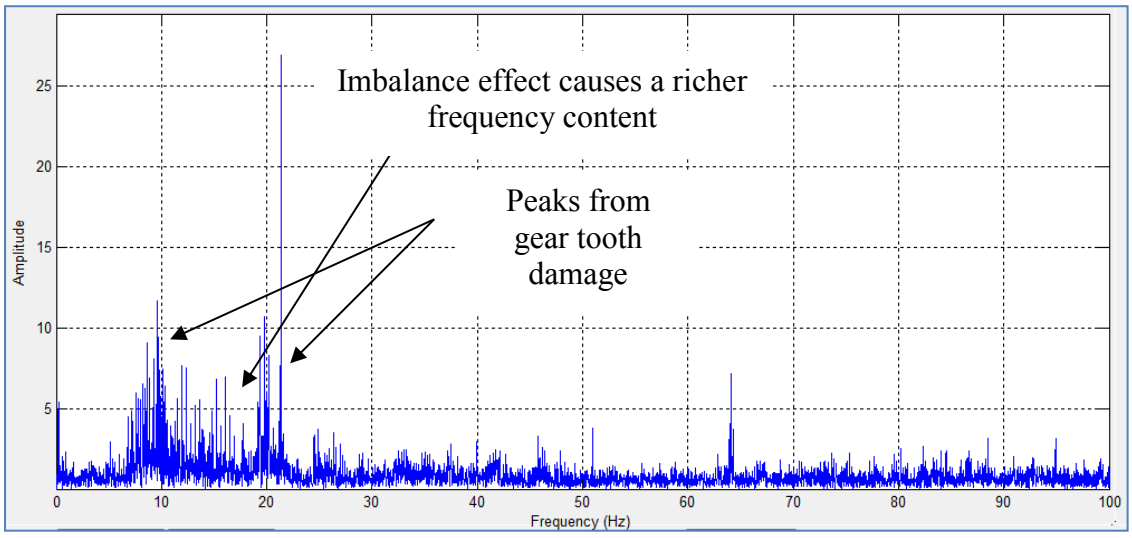

Figure 79 Vibration power spectrum for the measurement with gear tooth damage and imbalance present simultaneously. The peaks associated with the gear tooth dominate in this case.

The top plot (a) in figure 80 shows the raw vibration data for impacts occurring simultaneously with gear tooth damage. The impacts are clearly seen in the raw signal and are manifested more intensively after processing using the moving RMS algorithm at the middle plot(b). The impact incidents produce high energy events dominating the analysis signal. The power spectrum plot is shown in the bottom(c).

Figure 80 (a)

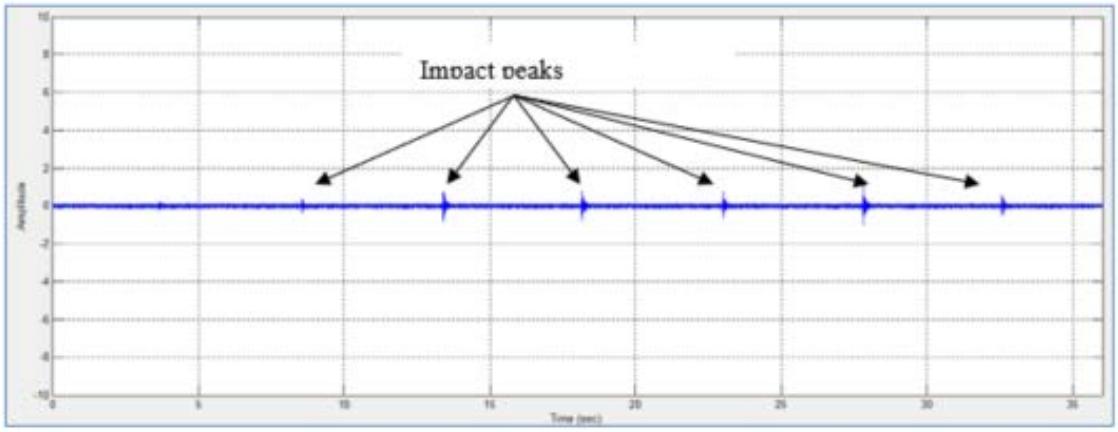

Figure 81 (b)

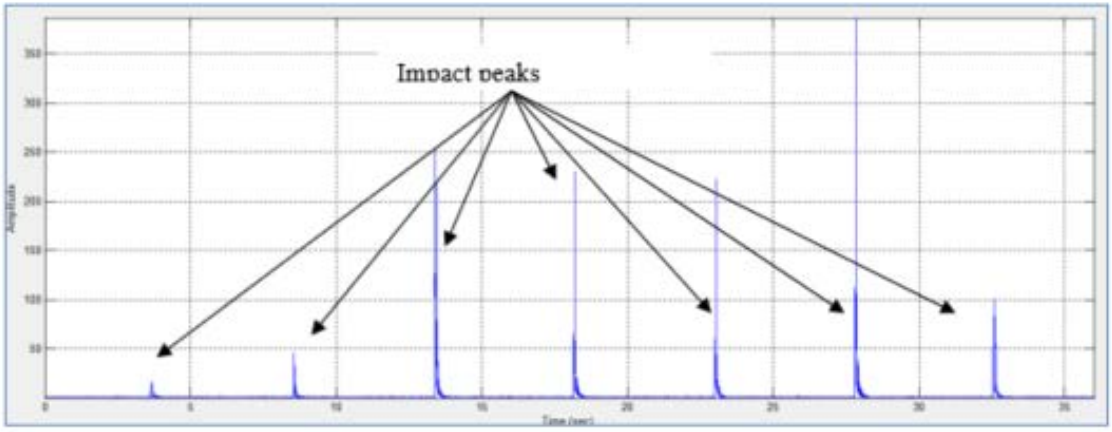

Figure 82 (c)

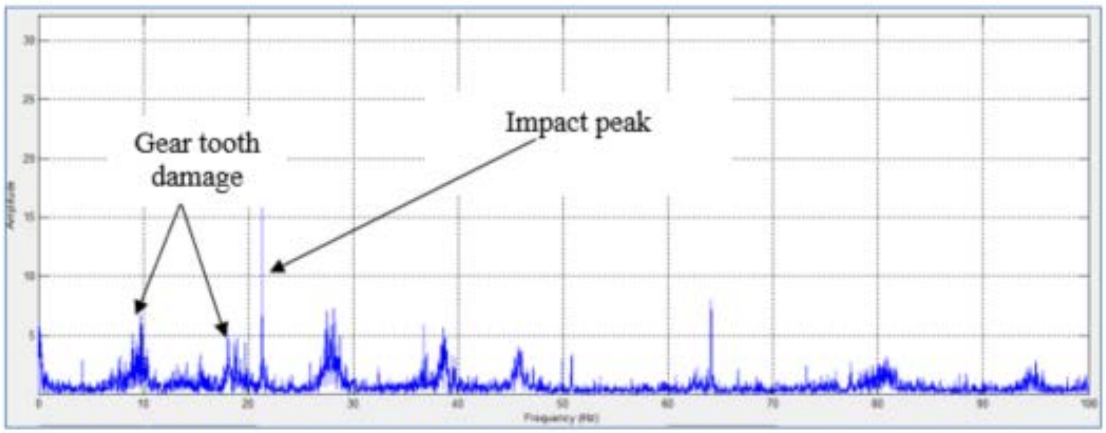

Figure 80 (a) Raw vibration signal for impact and gear tooth damage present simultaneously and (b) signal analysed using moving RMS, (c) power spectrum.

Figure 81 shows the power spectrum for the demodulated AE raw signal captured with gear tooth damage present only. The gear teeth fault peak appears at 43 Hz.

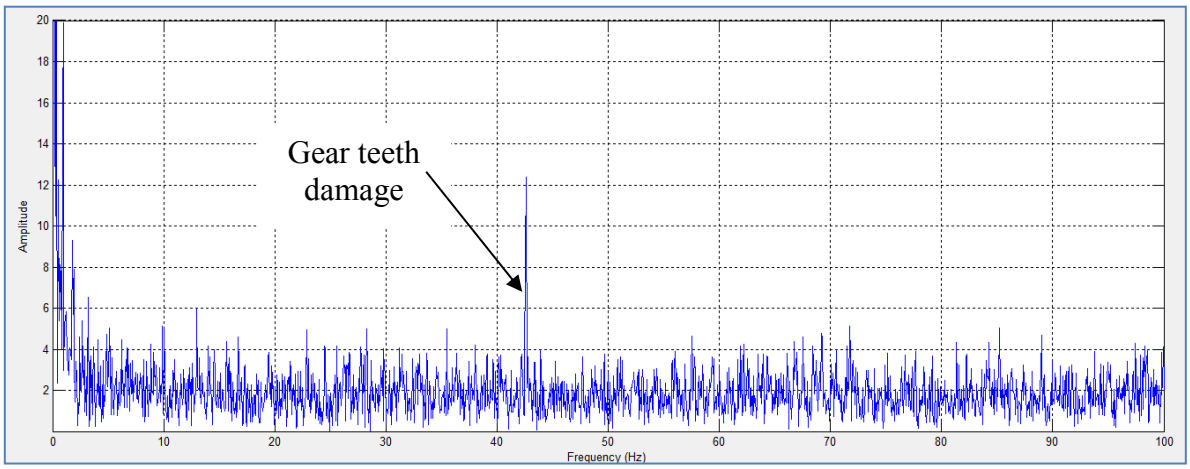

Figure 81 Power spectrum of the AE raw signal with gear teeth damage present. The peak at 43 Hz and subsequent harmonics are seen although only marginally.

Figure 82 shows the power spectrum of the demodulated signal for the AE measured signal for both gear teeth damage and imbalance being present simultaneously. The gear teeth fault related peaks are only evident.

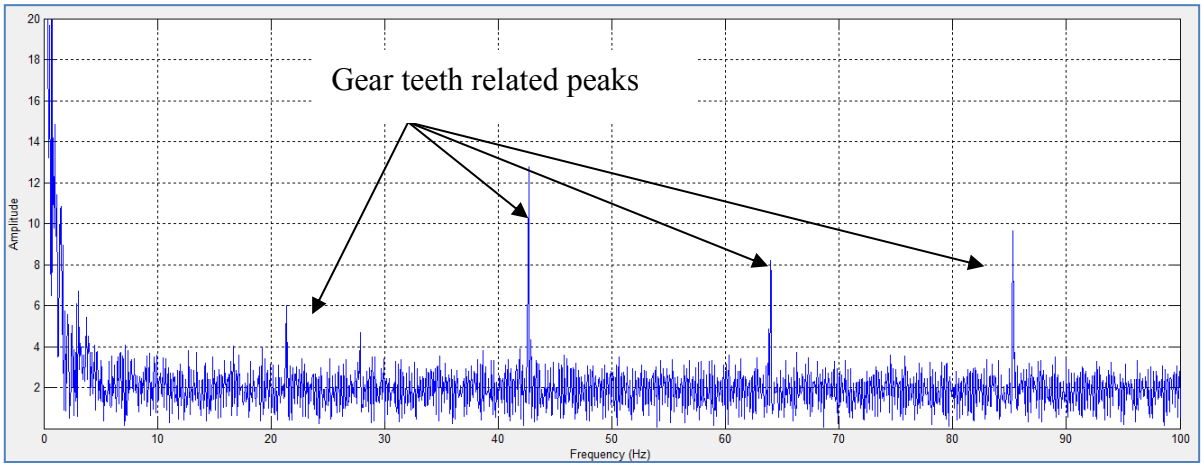

Figure 82 Power spectrum of the demodulated AE signal for gear teeth damage and imbalance occurring simultaneously. Only the gear teeth fault is evident. A suspected imbalance peak is present at approximately 28 Hz.

The top plot in figure 83 shows the raw AE signal captured for impact with gear teeth damage present simultaneously. The impact events are clearly visible in the raw signal. The multiple peaks have arisen from echoes following reflections from the edges of the rotor after each

impact event. The bottom plot moving RMS of the AE signal showing the impact events and associated echoes.

Figure 83(a)

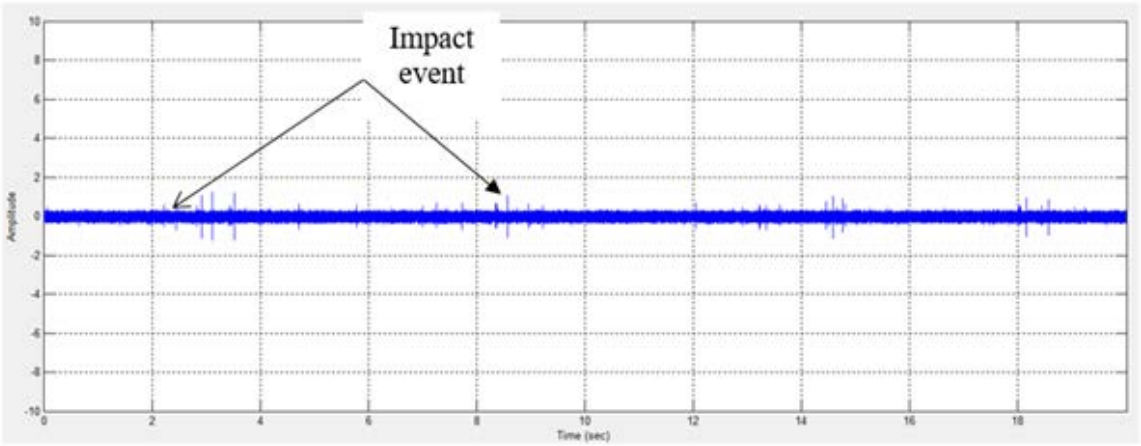

Figure 83(b)

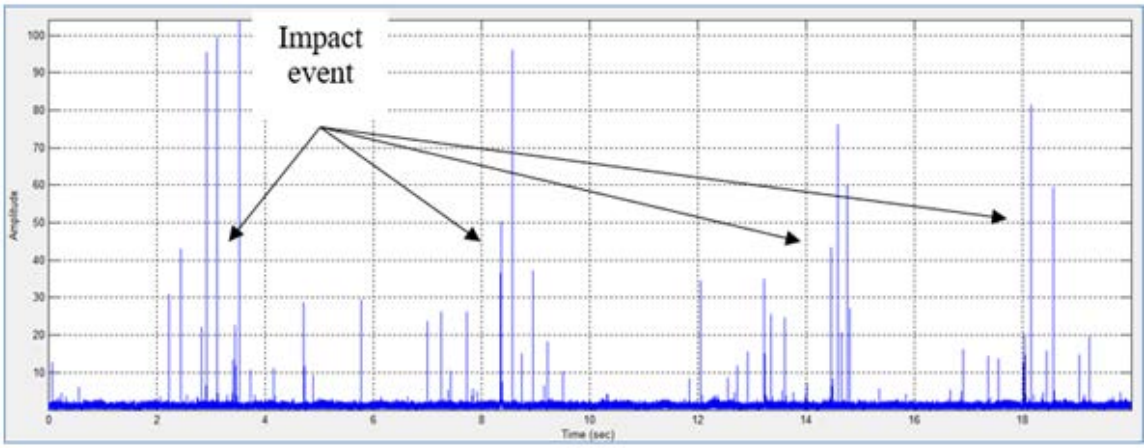

Figure 83 (a) Raw AE signal for impact event occurring simultaneously with gear teeth damage and (b) moving RMS of the AE signal showing the impact events and associated echoes.

Figure 84 shows the power spectrum of the demodulated AE signal. Peaks at 43 Hz and 64 Hz are clearly evident and related to the gear teeth. Other peaks at lower frequencies are also seen possibly arising from the impact events.

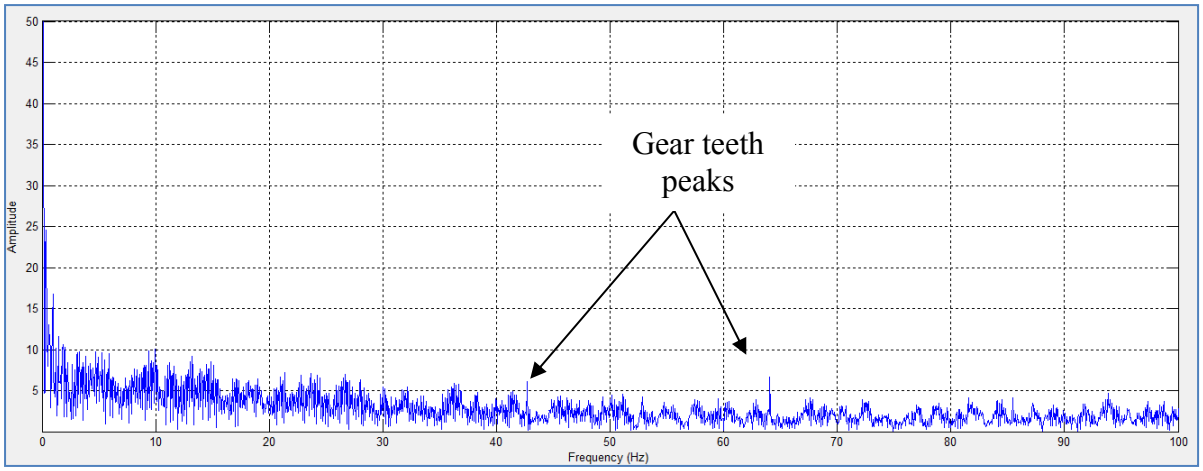

Figure 84 Plot of the power spectrum of the demodulated AE signal showing clearly the presence of the gear teeth defects.

The top plot (a) in figure 85 shows the AE raw signal captured for impact, imbalance and gear tooth damage simultaneously present. The impact events are clearly visible in the raw measurement. The bottom plot (b) shows the processed signal using moving RMS.

Figure 85 (a)

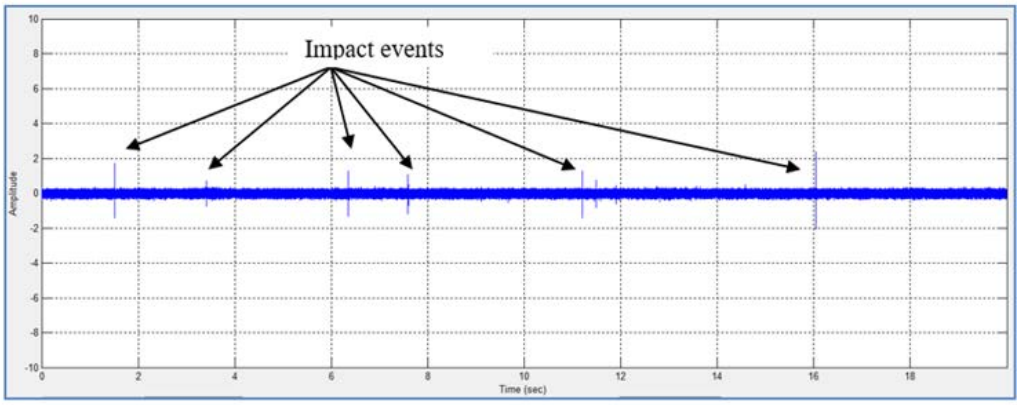

Figure 85 (b)

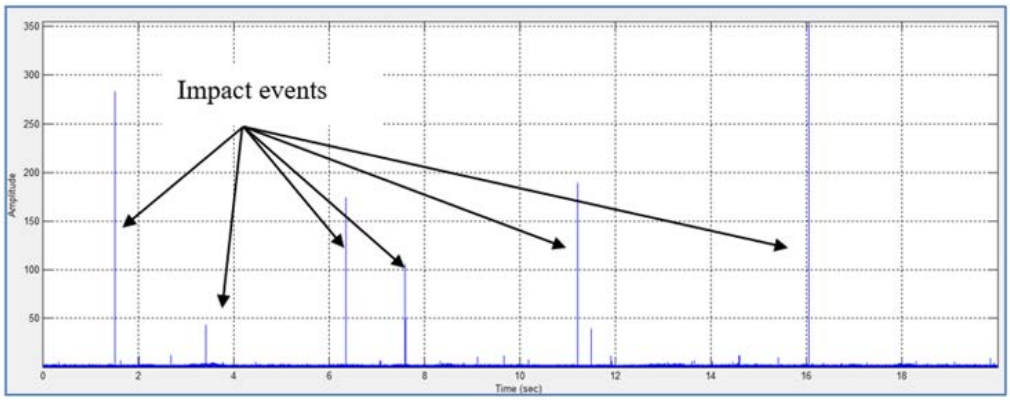

Figure 85 (a) Raw AE signal with impact event peaks clearly visible and (b) moving RMS where impact peaks show up clearly.

Figure 86 shows the power spectrum of the demodulated AE signal. The gear teeth fault is the one that shows more clearly with a clear peak at 43 Hz. Other multiple small peaks are present and are probably associated to the combined effects of the various faults captured in the signal.

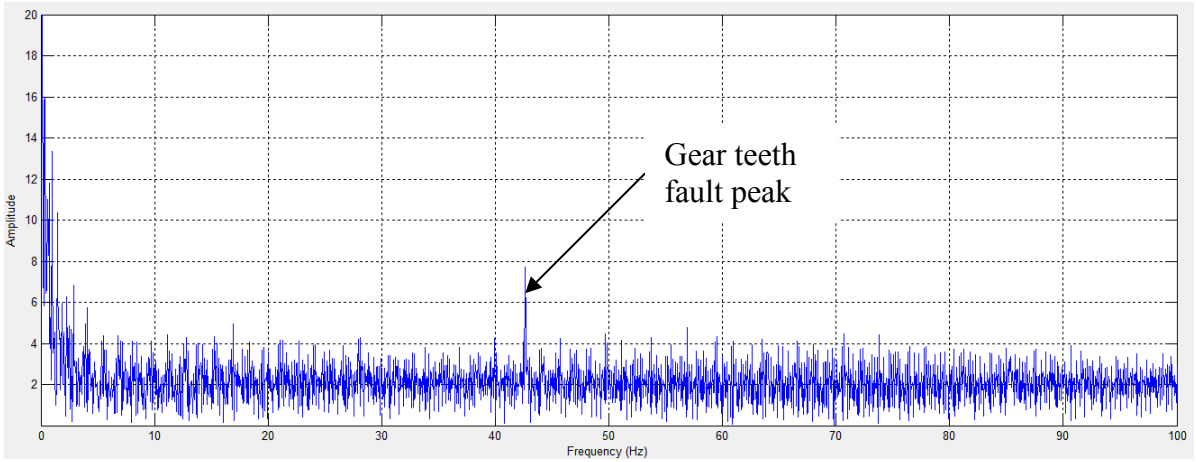

Figure 86 Power spectrum of the demodulated AE signal with the gear teeth fault showing up more evidently.

8.3 Test rig results analysis & Summery

From the results obtained after the test rig measurements were carried out using AE and vibration analysis, it is evident that various faults can be detected and assessed with either technique. However, the dominant effect of certain defects has also been ascertained which should be taken into account when performing measurements on actual industrial wind turbines. From previous experience, it has become obvious that industrial wind turbine gearboxes can suffer from various conditions simultaneously, i.e. damage coexisting in the gears, shafts and bearings. However, in almost all cases it is only one type of fault that results into final failure. The relationship between the various faults is yet to be determined quantitatively. Hence, the assessment of the severity of various gearbox defects, and generally the reliable detection of faults when multiple defects are present, are still challenging due to the masking effects that may influence the vibration and AE measurements. Thus, the subsequent analysis performed can give less accurate output. Moreover, the variable loading factor can further contribute in variations arising in the results arising from the RCM measurements. Although in the particular set of test rig measurements presented in this study the variable loading effects could not be investigated, the effects of the presence of coexisting faults that are different in nature has been evaluated and analysed in sufficient detail.

CHAPTER 9

INDUSTRIAL WIND TURBINE POWER CONVERTER INSTRUMENTATION AND MEASUREMENTS

9.1 Instrumentation of industrial wind turbine power converters

As part of the OPTIMUS FP7 project which also partially funded the present study, the power converters of two ACCIONA industrial 1.5 MW wind turbine power converters were instrumented and remotely monitored using a variety of sensors. The instrumentation was carried out by two of the partners participating in the OPTIMUS consortium and more specifically INGETEAM Service and INDRA. The two ACCIONA 1.5 MW wind turbines instrumented were located in the Vedadillo wind farm in Spain and were operated by ACCIONA Energia. The INGECON-WIND 1500 kW power converters in both wind turbines have been manufactured by INGETEAM.

9.2 Background

The instrumentation of the power converters in both wind turbines was performed and completed in April 2014 by two teams from INGETEAM and INDRA respectively with the support of maintenance personnel from ACCIONA Energia. Data acquired by both RCM systems were later made available by INGETEAM and INDRA to the rest of the partners of the OPTIMUS consortium, including the University of Birmingham. Some of the results obtained are discussed in this chapter.

The INGETEAM power converter installed in the ACCIONA 1.5 MW wind turbines that were instrumented as part of the project is shown in the photograph of figure 87. The cabinet of the inverter is installed at the bottom of the wind turbine tower. It is responsible for performing the functions of control, automation and management of wind turbine power. The inverter consists of five compartments as indicated in figure 87.

Figure 87 The INGECON-WIND 1500 kW power inverter installed in the ACCIONA 1.5 MW wind turbines that were remotely monitored. The photograph is courtesy of INGETEAM.

The cabinet compartments identified as A and B contain the power converter components. These are also known the IGBTs compartment. The setup of compartments A and B is shown in the photograph of Figure 88.

Figure 88 Photograph of compartments A and B. The photograph is courtesy of INDRA.

The cabinet compartments C and D shown in the photograph of figure 89 contain different elements necessary for the proper operation of the inverter. The crowbar overvoltage protection circuit can be seen in the photograph.

Figure 89 Photograph of compartments C and D. The photograph is courtesy of INDRA.

The photograph in figure 90 shows compartment E. This is also known as the Configurable Control Unit (CCU) compartment. The CCU compartment contains the inverter controller.

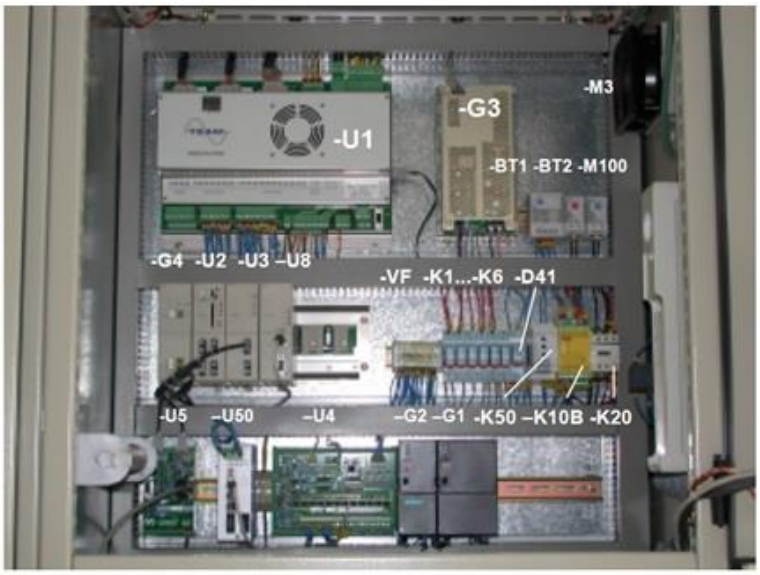

Figure 90 Photograph showing Compartment E of the INGECON power inverter. The photograph is courtesy of INDRA.

The photograph in figure 91 shows Compartment F. It contains protection of the auxiliary supply voltages.

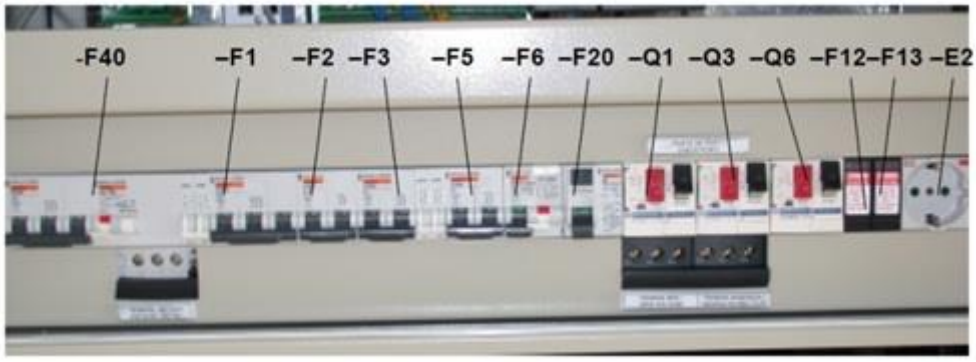

Figure 91 Photograph of compartment F. The photograph is courtesy of INDRA.

The photograph in figure 92 shows compartment G, which is also known as the bar compartment.

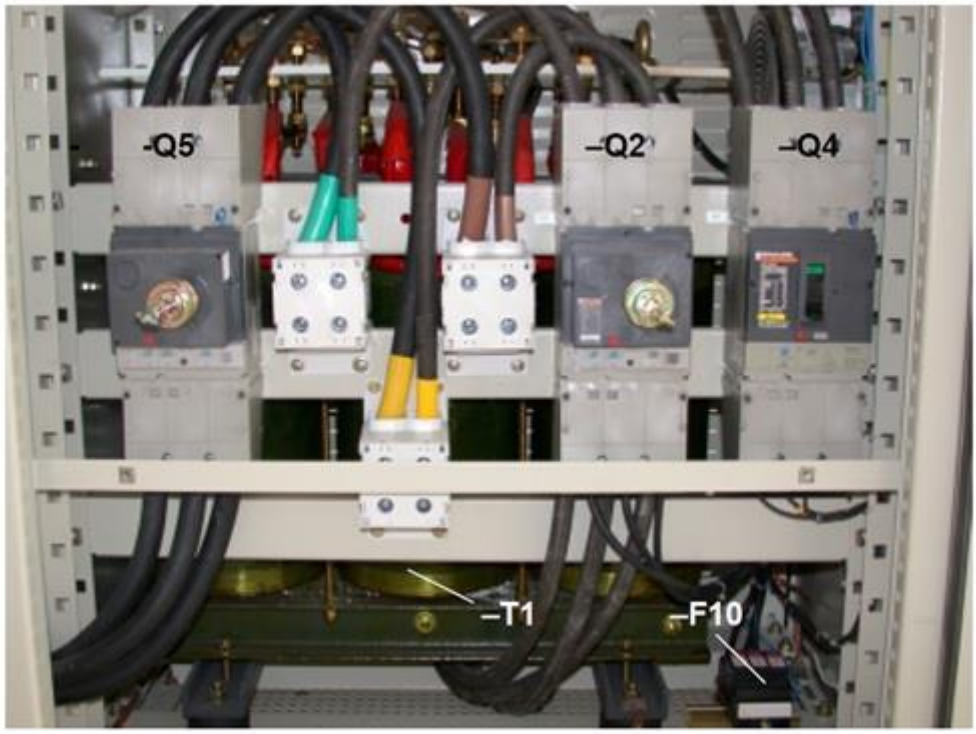

Figure 92 Photograph of compartment G. The photograph is courtesy of INDRA.

9.3 Power converter RCM data acquisition and sensors

The RCM equipment used by INDRA and INGETEAM for data acquisition and the types of sensors employed were very similar in both cases. Both power converter RCM systems were installed at the bottom of the wind turbine tower and measured a number of parameters of interest including current, voltage, humidity, temperature and vibration. Both systems were multi-channel with the INDRA RCM system for example having 16 input channels for current measurements with configurable ranges, 3 channels for PT-100 probes conditioning and 2 channels of 4-20 mA measurement. Sampling for current and voltage was continuous whilst temperature and humidity where measured at intervals. Sampling rates used were relatively low.

For both wind turbines 9 channels were used for current measurements, 5 for voltage measurements, 3 for temperature and 2 for humidity, hence a total of 19 channels. The photograph in figure 93 shows the data acquisition cabinet of the INDRA RCM system.

Figure 93 Data acquisition cabinet of the INDRA RCM system installed in one of the ACCIONA 1.5 MW wind turbines. The photograph is courtesy of INDRA.

The specifications of the sensors employed are discussed next. For the voltage measurements voltage sensors model LEM DVL 2000 were employed. The LEM DVL 2000 voltage sensors were connected to the bus wires of the power converter and measured the DC voltage of the bus. The schematic diagram in figure 94 shows the LEM DVL 2000 basic configuration and its specifications are summarised in Table 8.

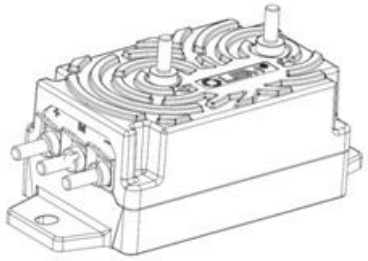

Figure 94 The LEM DVL 2000 configuration. The schematic diagram is courtesy of INDRA.

Table 8 Voltage sensor LEM DVL 2000 specifications

Primary nominal r.m.s. voltage	2000 V
Primary voltage, measuring range	±3000 V
Secondary nominal current rms	50 mA
Sensitivity	25uA/V (50 mA for 2000 V)
Supply voltage	±13,5V - ±26,4V
Current consumption	25mA + Secondary nominal current

LEM DVL 150 voltage sensors were connected to the output of the voltage transformers (2 phases). The LEM DVL 150 voltage sensors were used to measure the generated voltage. The specifications are summarised in Table 9.

Table 9 Voltage sensor LEM DVL 150 specifications.

Primary nominal r.m.s. voltage	150 V
Primary voltage, measuring range	±225 V
Secondary nominal current rms	50 mA
Sensitivity	333.33 uA/V (50 mA for 150 V)
Supply voltage	±13,5V - ±26,4V
Current consumption	25mA + Secondary nominal current

Voltage sensors LEM AV100-150/SP3 were connected to the output of the voltage transformers (2 phases) for measuring the grid voltage. The specifications of LEM AV100-150/SP3 are summarised in Table 10.

Table 10 Voltage sensor LEM AV100-150/SP3 specifications.

Primary nominal r.m.s. voltage	150 V
Primary voltage, measuring range	±225 V
Secondary nominal current rms	50 mA
Sensitivity	333.33 uA/V (50 mA for 150 V)
Supply voltage	±12V - ±24V
Current consumption	50mA + Secondary nominal current

Current sensors LEM LF 305-S were connected to the generator wires to measure the current of the stator. The photograph in figure 95 shows the current sensor LEM LF 305-S. The specifications are summarised in Table 11.

Figure 95 Photograph of LEM LF 305-S. The photograph is courtesy of INDRA.

Table 11 Current sensor LEM LF 305-S specifications.

Primary nominal r.m.s. current	300 A
Primary current, measuring range	±500 A
Secondary nominal current rms	150 mA
Conversion ratio	1:2000
Supply voltage	±12V - ±20V
Current consumption	26mA + Secondary nominal current

Current sensors LEM LF 2005-S shown in figure 96 were connected to the input of the inverter and the rectifier output for measuring the current of the inverter and the rectifier. The specifications are summarised in Table 12.

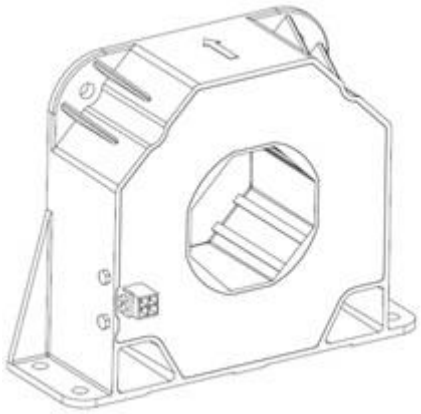

Figure 96 Schematic diagram of the current sensor LEM LF 2005-S. The schematic is courtesy of INDRA.

Table 12 Current sensor LEM LF 2005-S specifications.

Primary nominal r.m.s. current	2000 A
Primary current, measuring range	±3000 A
Secondary nominal current rms	400 mA
Conversion ratio	1:5000
Supply voltage	±15V - ±24V
Current consumption	33mA + Secondary nominal current

Humidity sensors OMEGA ® HX71-MA were used to measure humidity inside the IGBTs and CCU compartments of the power converters. The OMEGA® HX71 Series Relative Humidity Transmitter shown in the photograph of figure 97 provides a linearised and temperature compensated output signal of 4 to 20 mA which after calibration is scaled from 0% to 100% Relative Humidity. The specifications of the humidity sensor is shown in Table 1.

Figure 97 Photograph of the OMEGA HX71-MA humidity sensor. The photograph is courtesy of INDRA.

Table 13 Humidity sensor OMEGA HX71-MA specifications.

Measuring Range	5 - 95% (non-condensing)
Output	4 to 20 mA (Scaled for 0 to 100% RH)
% RH	(Current measured in milliamps – 4) ÷ 0.16 EXAMPLE: (11.04 mA – 4) ÷ 0.16 = 44% RH
Power	8 – 12 Vdc @ 20mA

For measuring the temperature within the IGBT, CCU and BAR compartments of the power inverter CORREGE PS6/60/PT100/CLA/FLSSIL/2500 temperature sensors were employed shown in the photograph of figure 98. The specification of the temperature sensors are summarised in Table 14.

Figure 98 CORREGE PS6/60/PT100/CLA/4FILSSIL/2500 temperature sensor. The photograph is courtesy of INDRA.

Table 14 Temperature sensor specifications.

RANGE	-20°C / +200°C
Type	PT100Ω thermic element A Class – 1x4 wires
Wire section	Cable 4 conductors, section 0.22mm

9.4 Instrumentation of the power converters

The current, voltage, humidity and temperature sensors used to monitor the condition of the power converter where installed without any effects induced in the operation of the INGECON power inverter. The data acquisition was installed nearby, and data acquired were retrieved remotely using a 3G connection. The photograph in figure 99 shows the location where the INDRA data acquisition unit was installed.

Figure 99 INDRA data acquisition unit. The photograph is courtesy of INDRA.

The sensors used and the locations they were installed are summarised in Table 15.

Table 15 Sensors used and installed locations

Signal	Value	Sensor	Quantity	Position
VCC BUS	1350Vcc	DVL 2000	1	Connected to the bus wires
Generated voltage	110VAC	DVL 150	2	Connected to the output of the voltage transformers (2 phases)
Grid voltage	110VAC	AV100-150/SP3	2	Connected to the output of the voltage transformers (2 phases)
Stator current	125A	LF 305-S	3	Connected to the wires generator
Rectifier current	2000A	LF 2005-S	3	Connected to the rectifier input
Inversor current	2000A	LF 2005-S	3	Connected to the inverter output
Temperature	-20 - 50ºC	PT-100 (4 wires)	3	IGBTs, BAR and CCU compartments
Humidity	0-90%	OMEGA HX71-MA	2	IGBTs and CCU compartments

The following photographs show some of the locations of the sensors.

Figure 100 Photograph showing the BCC Bus sensor. The photograph is courtesy of INDRA.

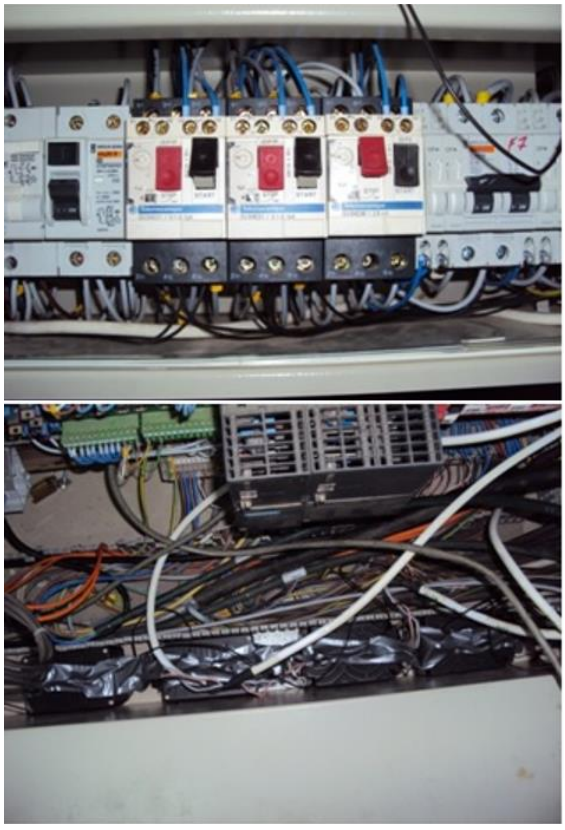

Figure 101 Generated and grid voltage sensor. The photograph is courtesy of INDRA.

Figure 102 Stator current sensor installation. The photograph is courtesy of INDRA.

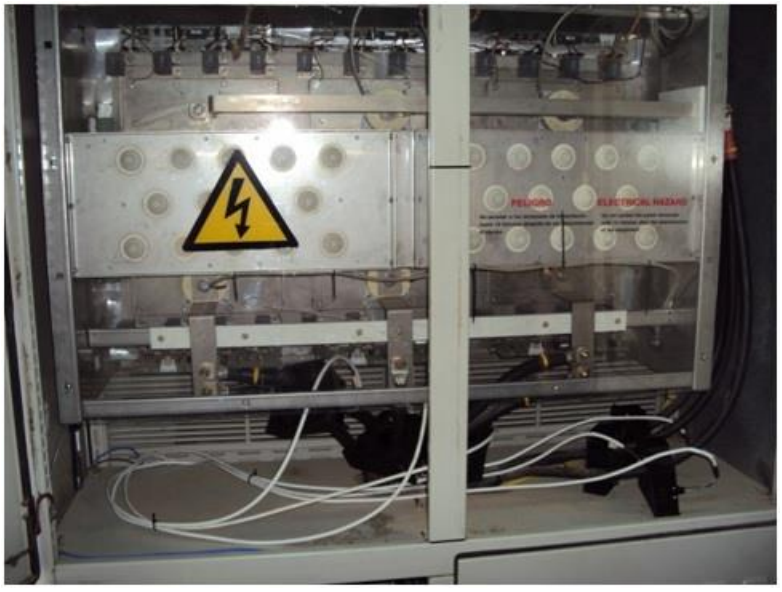

Figure 103 Rectifier current sensor. The photograph is courtesy of INDRA.

Figure 104 Inverter current sensor. The photograph is courtesy of INDRA.

Figure 105 Temperature sensor. The photograph is courtesy of INDRA.

Figure 106 Humidity sensor. The photograph is courtesy of INDRA.

9.5 Measurements and analysis for power electronics

Data were collected from the two instrumented ACCIONA 1.5 MW wind turbines over a period of approximately 30 months. During the monitoring period no faults were identified from the measurements carried out using the two RCM systems installed on the power converters nor any power electronics-related failures were reported by the wind farm operator.

However, an example of possible use of the rainflow counting algorithm on actual RCM data retrieved from the power converters are presented next. The plot in figure 107 shows the actual temperature history of one of the IGBTs monitored over a period of time. The measurements have been carried out every 3 minutes.

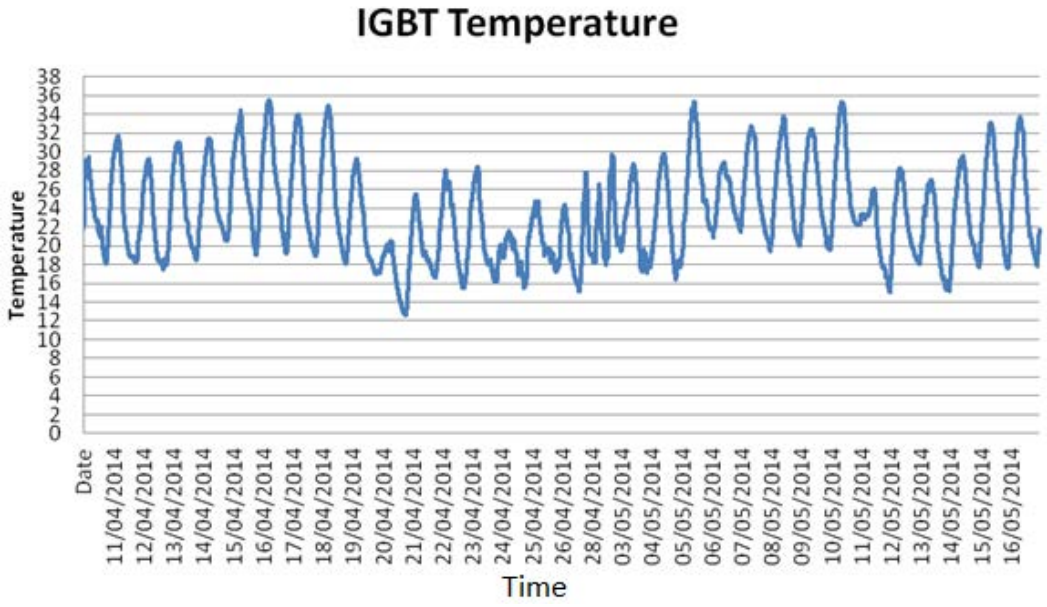

Figure 107 Raw IGBT temperature data history.

In order to use rainflow algorithm to analyse the temperature data, the data ranking number has replaced the date of the measurement as in one particular day over hundreds of data has been measured. Therefore, the plot in figure 108 demonstrates the data and data ranking number in a graph format.

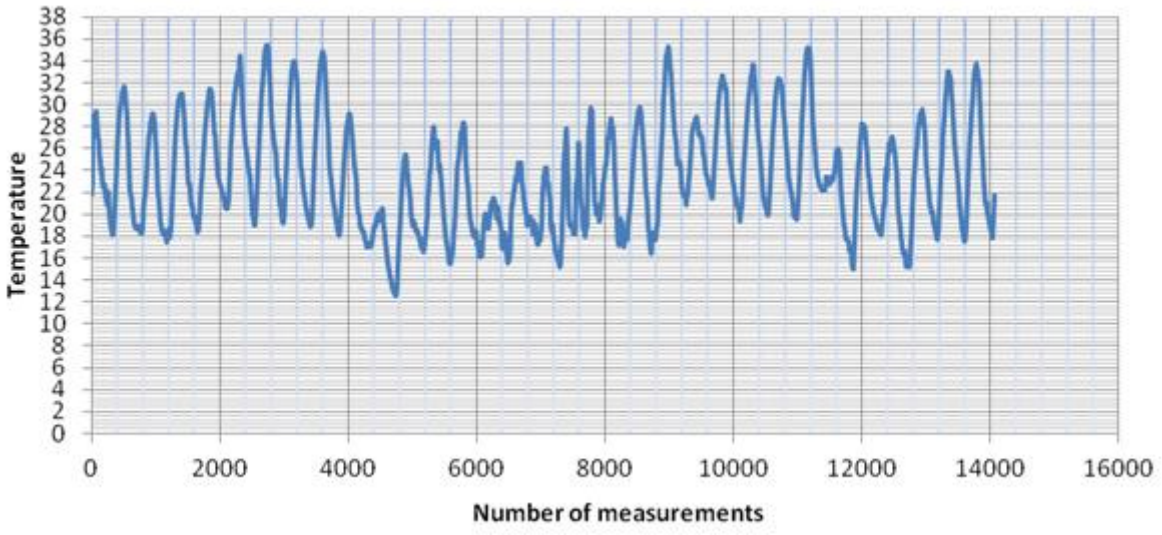

Figure 108 Temperature of IGBTs by number of measurements taken over time.

As many cycles occur over a long period of time based on the temperature measurements, therefore; the smaller cycles (small amplitude) are not much of an importance and would not have noticeable effect nor cause damage on the IGBTs if neglected. Thus, by reducing the number of cycles of the IGBTs temperature data, better condition monitoring is achieved. The derived rainflow matrix is shown in figure 109.

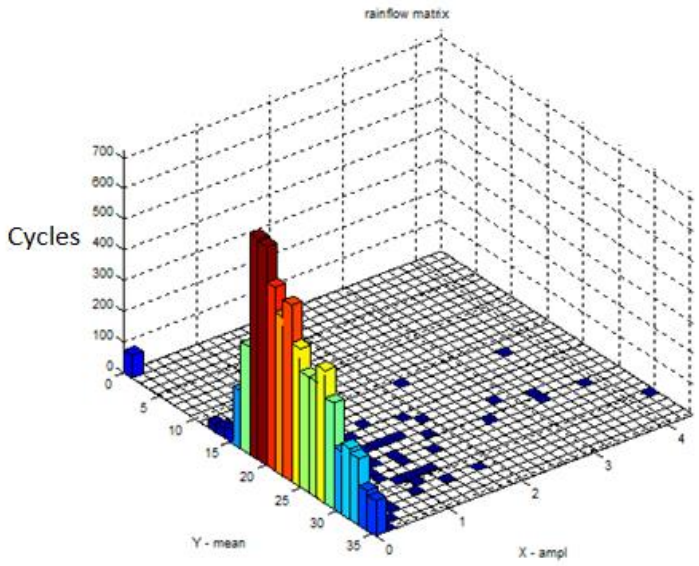

Figure 109 The rainflow matrix obtained from the data set plotted earlier.

From the matrix above, it is possible to obtain the histogram of the rainflow cycles mean value and the number of cycles as shown in figure 110.

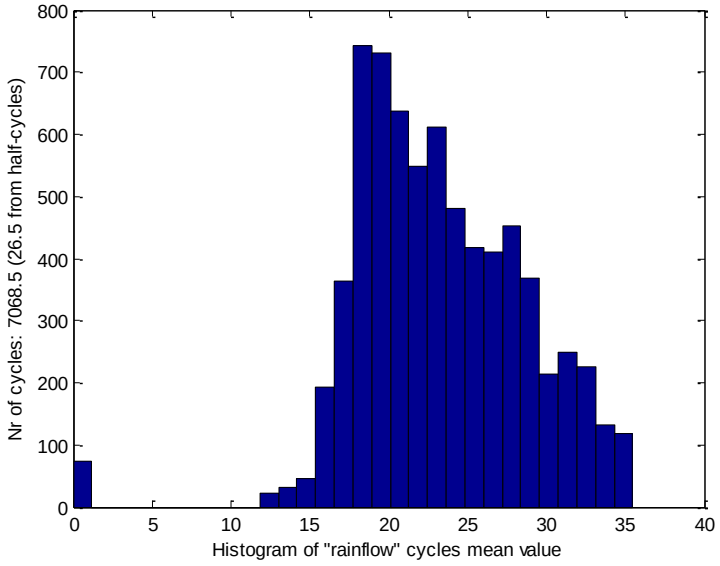

Figure 110 histogram of the rainflow cycles mean value

In figure below shows the rearrange the temperature data using rainflow algoritm, so In this graph show that, the smaller cycles that are not really important are removed using the rainflow method.

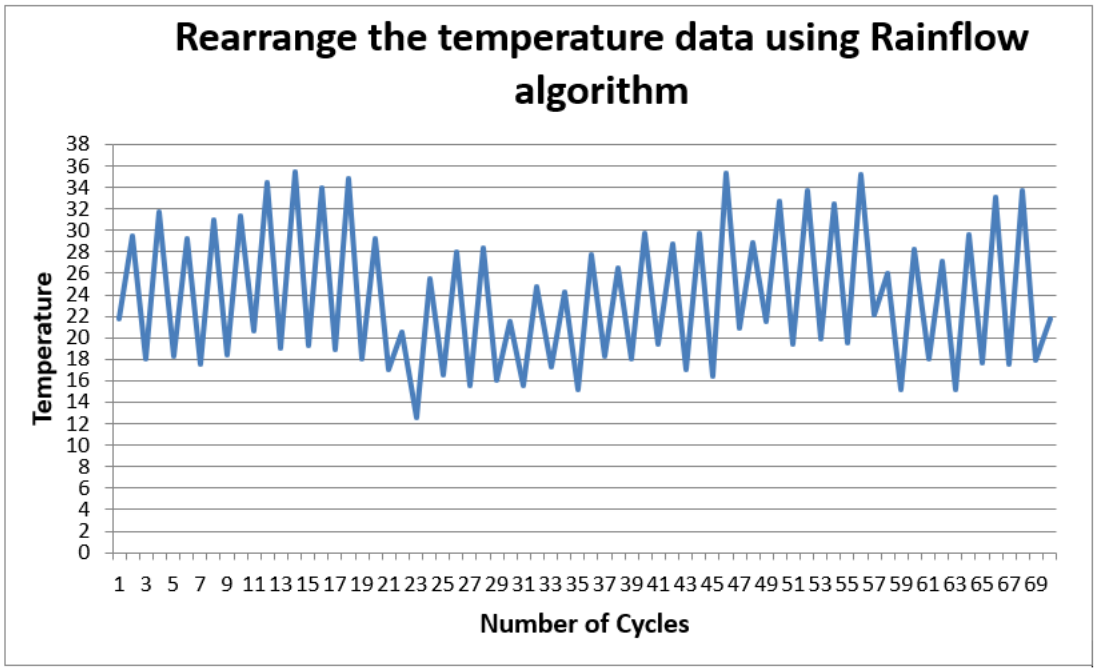

Figure 111 Rearrange the temperature data using rainflow algorithm

Therefore, using the rainflow counting algorithm it is possible to obtain the number of important events that can actually contribute to the degradation of power electronics components. Unfortunately, this approach does not compensate for the time that the events actually occur in history, so it is difficult to predict their exact contribution to damage evolution. This is a serious limitation of this approach which should always be taken into account when attempting to estimate the remaining lifetime of power converters in wind turbines.

9.6 Data trending

Data trends of different data sets are presented next. None of them shows any incipient faults or faults that have occurred.

Trend 1: The trend graph of the voltage generated in one of the phases is shown in the plot of figure 112. From the plot it is possible to verify when the turbine has been coupled to the grid and when it has been disconnected. As might be expected, the turbine has mainly been coupled and injecting current into the grid.

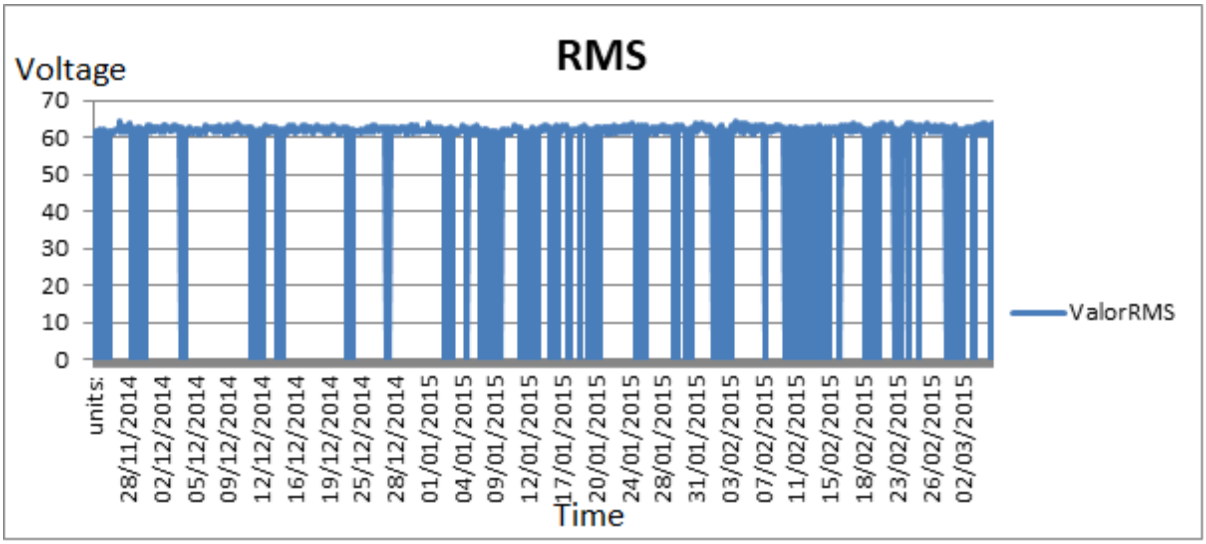

Figure 112 Trending voltage value indicating connection of the wind turbine to the grid.

Trend 2: The graph in figure 113 show a comparison of the trends in the temperature trends in the different compartments of the cabinet converter. Similar temperature is detected in the three compartments of the wind turbine at low load, but if the power produced increases, the temperature of IGBTs compartment increases relative to the other two cabinets. Red trace compartment temperature corresponds to bars, Blue trace corresponds to the temperature in the compartment CCU and Green trace corresponds to IGBTs compartment.

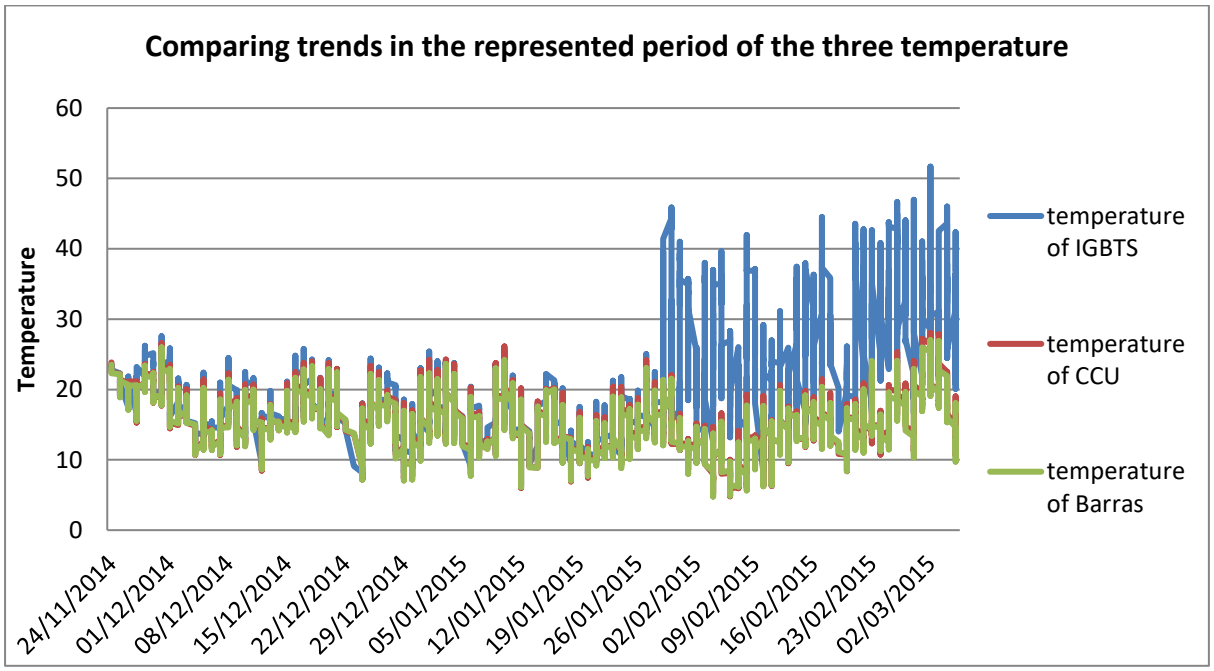

Figure 113 Temperature trends in IGBT, CCU and Bar cabinets.

Trend 3: Figure 114 shows a comparative trend graph between the intensity of stator captured in three phases over the period represented. High similarity is detected in the intensity produced in the three phases.

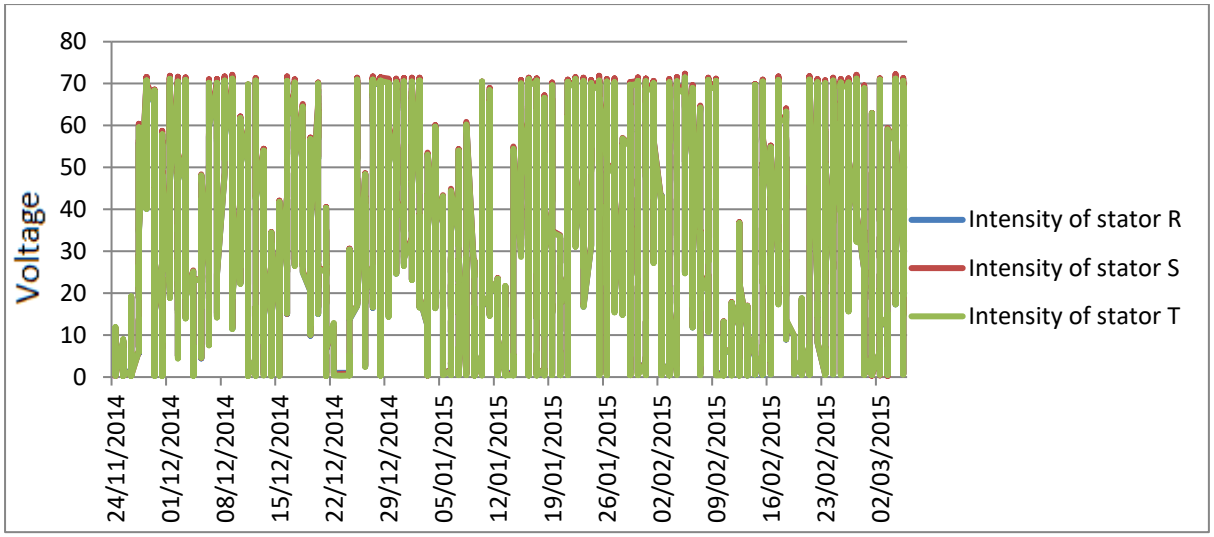

Figure 114 Stator intensity for the different phases with time.

Trend 4: Figure 115 shows a comparative trend graph between the intensity of the inverter captured in three phases over the period represented. The three trends are similar, appreciating higher amplitude in T phase captured values.

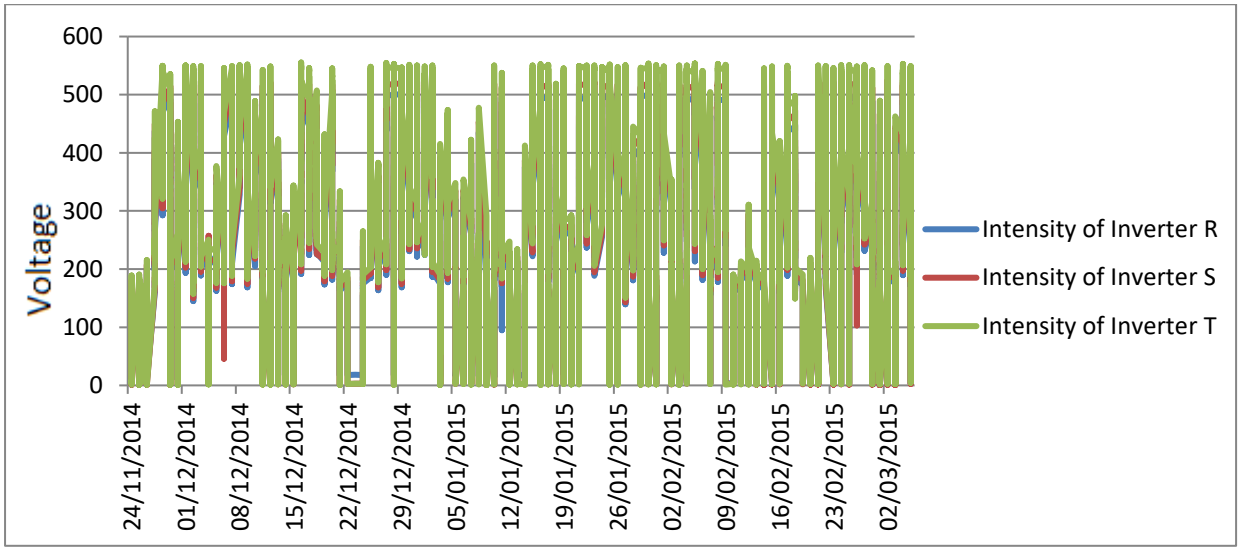

Figure 115 Trends for inverter intensity at different phases.

Trend 5: Figure 116 shows a comparative trend graph between the intensity at Rectifier captured in three phases over the period represented. The three trends are similar, appreciating higher amplitude in T phase captured values.

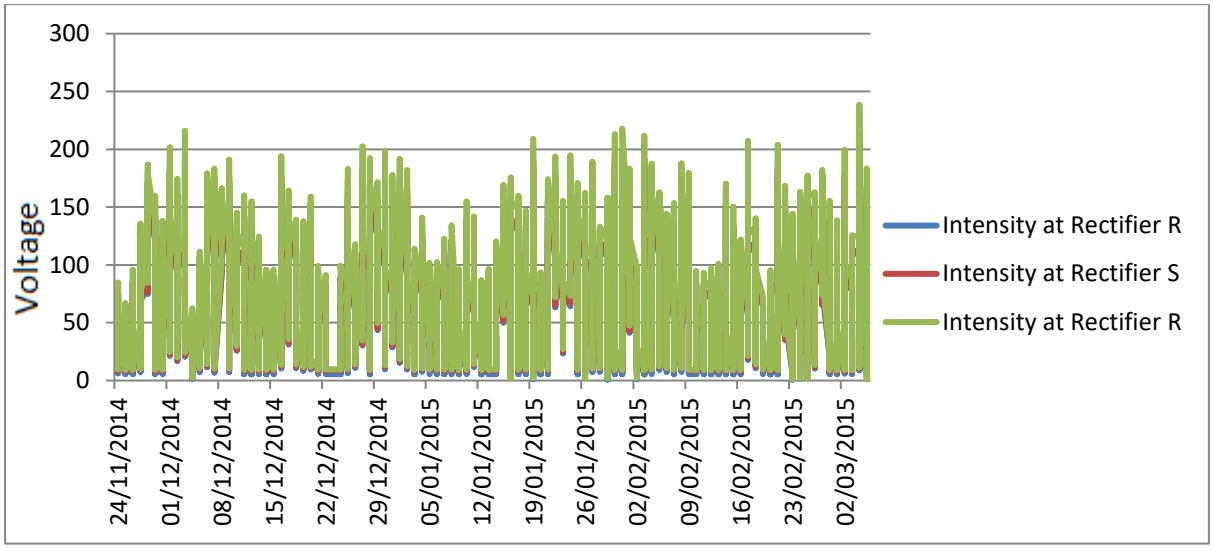

Figure 116 Trend for rectifier intensity at different phases.

Trend 6: Figure 117 shows the data trend for the DC bus voltage during the period analysed. There is no abnormal fluctuation observed in the Bus voltage, as indicated by the low amplitude variations.

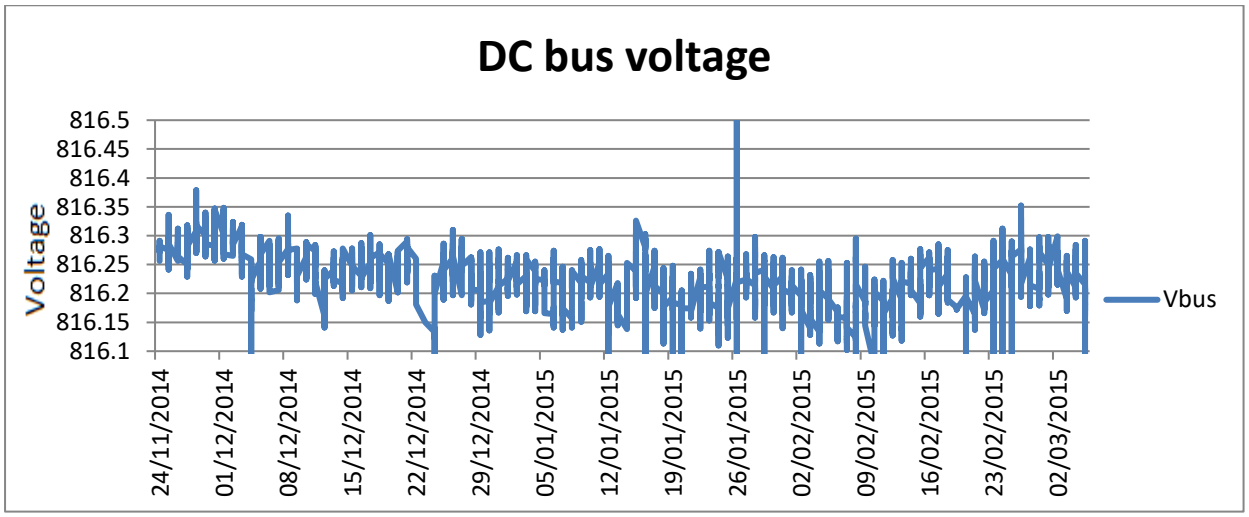

Figure 117 DC bus voltage trend with time.

Trend 7: Figure 118 shows the comparative trend graph between grid voltages captured at the two monitored phases. A slight fluctuation between each phase is detected. The amplitude of the scale values is very close which means that there is no fault present.

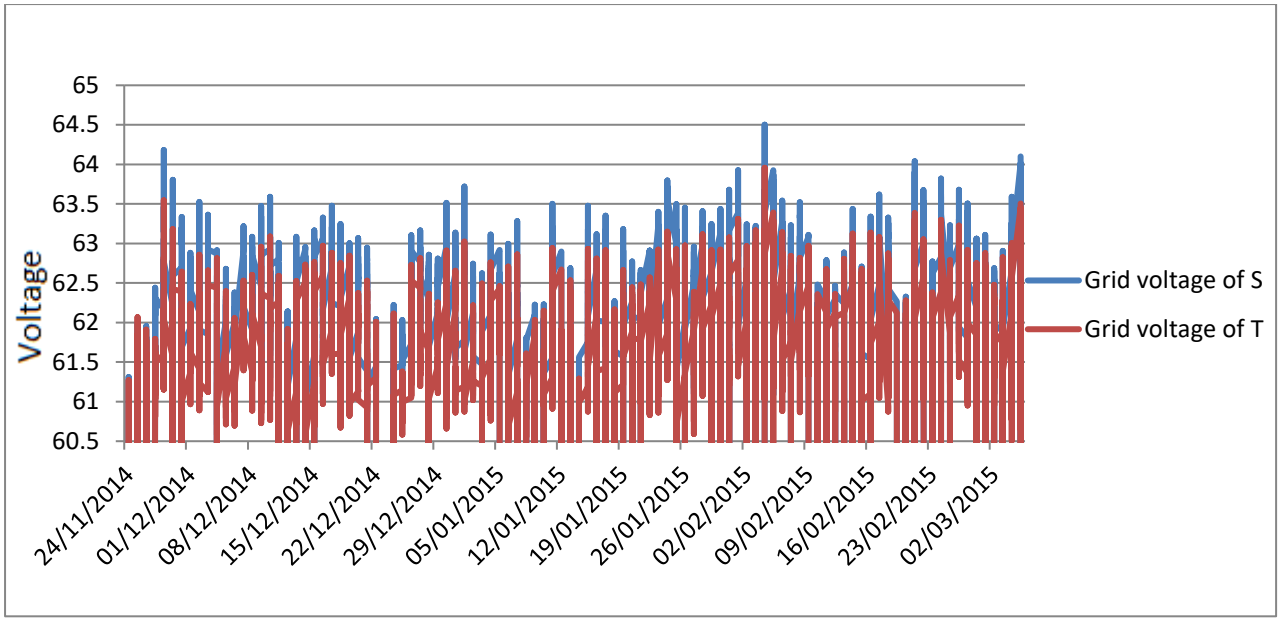

Figure 118 Grid voltage trends at different phases with time. No fault is evident.

Trend 8 – As shows in below figure comparative trend graph between generated voltages in the two monitored phases. Slightly higher amplitude is detected in S-phase, the amplitude of the scale values are very close which proves it is a small matter. Sample values to zero when the turbine is decoupled.

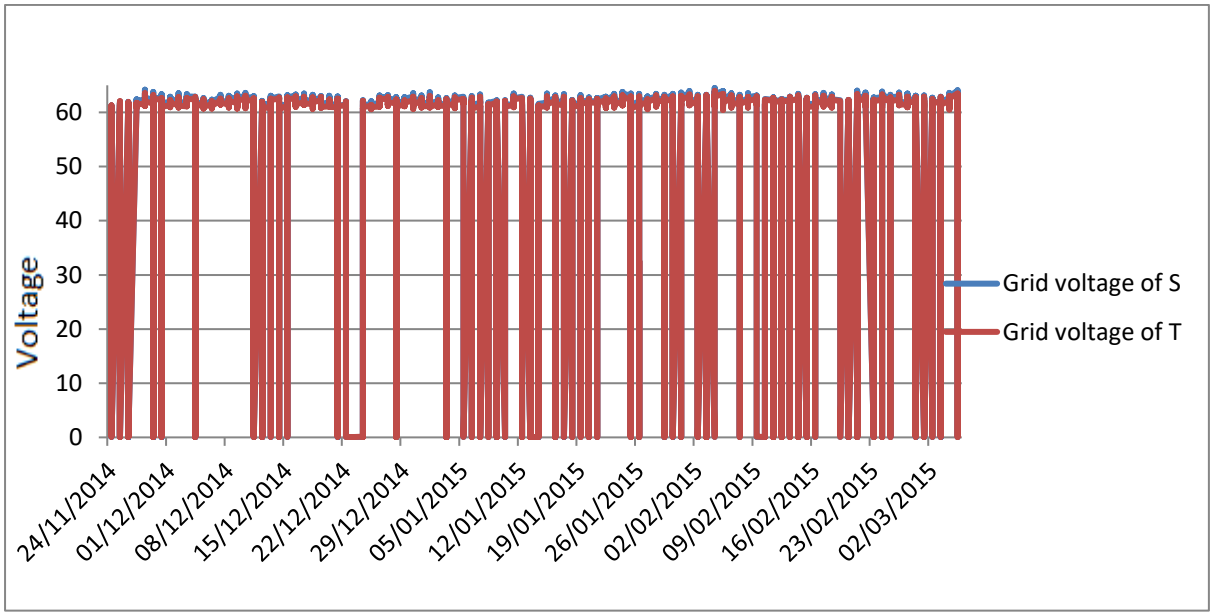

Figure 119 comparative trend graph between generated voltages in the two monitored phases

9.7 Summary

Data were collected from the two instrumented ACCIONA 1.5 MW wind turbines over a period of approximately 30 months. During the monitoring period no faults were identified from the measurements carried out using the two RCM systems installed on the power converters nor any power electronics-related failures were reported by the wind farm operator. The fact that it was impossible to record any power converter failures during the RCM of the industrial wind turbines considered in this study has been a drawback. In order to address this further data over a larger number of wind turbines and over a longer period of time will be necessary.

CHAPTER 10

WIND TURBINE GEARBOX REMOTE CONDITION MONITORING RESULTS AND ANALYSIS

10.1 Background

The consistency of the lubrication quality is an important factor influencing fatigue lifetime of wind turbine gearboxes. With gradual wear, debris in the form of particles will accumulate in the lubricant oil. Such particles will contribute to the fatigue damage accumulation on bearings and gears. Oil samples retrieved from maintenance engineers and RCM can be used to evaluate the overall particle population present in the lubricant of a particular machine as well as their average size and type. Misalignment can further contribute to excessive fatigue as it can increase the contact angles of rolling elements resulting in much higher stresses than normal. Misalignment and lubricant problems such as oil whirl and oil whip are fairly easily identifiable using existing vibration condition monitoring systems. Oil analysis data can provide useful insight with respect to the extent and type of wear sustained.

Vibration analysis based on different signal processing methodologies allows the identification of the components that have sustained damage. Having also knowledge of the exact loading conditions and operational history of a particular machine it is possible to predict the risk of failure and extent of structural damage with reasonable probability of success. The results of visual assessment can further increase the confidence levels in predicting the risk of failure.

Paris-Erdogan law, Miner's rule or better specifically adapted power laws can be used in combination in order to estimate the remaining lifetime of rotating components showing evidence of damage in the vibration signal. Nonetheless, it is important to understand that even in this case where several of the variables needed to estimate the remaining lifetime of a particular component are known, the available metal fatigue data commonly present significant scatter. Therefore, it is possible to refer only to a minimum fatigue damage threshold which

can subsequently be related to the probability of failure. Hence a statistical approach needs to be employed in order to assess the remaining lifetime of such components.

Offshore wind turbines have been in several cases experiencing excessive number of failures at much earlier times than expected or predicted by the standards. Unfortunately, the available data for offshore wind turbine failures have so far been very scarce and do not consider these failures directly. There has been a tendency to ignore them due to the fact that the wind turbines concerned had been under warranty. Thus, failed gearboxes were replaced at no cost to the operator and sometimes before actual failure had yet occurred. Nevertheless, taking into account global data for both onshore and offshore wind turbines it can be safely assumed that failure would have very likely occurred much more rapidly than anticipated in the IEC-61400-4 standard. Since the loading conditions offshore are normally much more severe than onshore, damage propagation can also be expected to progress more rapidly than onshore.

A more careful look into various offshore wind farms based on a small number of publicly accessible news releases, industrial reports and scientific articles published in journals and conferences do show the extent of the problems the wind energy currently faces. It is possible to use this information to build an overall trend of the problems faced by offshore wind turbines, but this does remain fragmented at best.

It should also be taken into consideration that all previous studies have focused on different types and makes of wind turbines. The fact that wind turbines have also been increasing in size and complexity with time, further intensifies the problem of correctly analysing the failure data available from these studies. Moreover, there seems to be no effort to correlate failures with environmental parameters prevailing at local level such as average wind speed, turbulence,

terrain morphology, icing conditions, maximum wind speed, time spent at maximum power output, etc. It should be stressed that these parameters are only a small fraction of the considerations that need to be taken into account to fully describe the problem of assessing accurately the remaining lifetime of structural and rotating components in industrial wind turbines.

In conventional fatigue testing a sinusoidal loading pattern where the loading-unloading ratio is normally defined as R=0.1 or the minimum load is equal to 10% of that of the maximum. The mean load can be calculated by simply using the following equation:

$$S_m = \frac{S_{maximum} + S_{minimum}}{2} \qquad (10\text{-}1)$$

Different loading and unloading frequencies can be used but in most cases these are defined at no higher than 5Hz. It is well known that both the loading-unloading ratio and frequency of the loading-unloading sequence have an observable effect on crack growth rate.

It should be emphasised that crack growth is not linear even if the load level remains constant. This is due to the fact that the stress intensity factor is also a function of the crack length. Hence, as the crack propagates a higher stress intensity factor (ΔK) will be applicable at a constant fatigue loading pattern, resulting in more rapid crack propagation with time. Therefore, Paris-Erdogan law describes a linear crack growth rate increase with increasing ΔK but in logarithmic scale. If we plot the actual Δα/Δn-ΔK curve, then it is easily seen that crack growth rate grows exponentially. However, in logarithmic plots this becomes practically linear

up to stage 3 at which point the crack becomes unstable and failure is imminent at a very low number of subsequent loading cycles.

As mentioned earlier wind turbines are not steady-state systems and operate constantly at variable loads. This means that during operation a spectral loading pattern is applicable. Unfortunately, this pattern cannot be predicted. Although the minimum and maximum range of loading can be established more safely it is impossible to accurately determine the frequency that the loading changes occur as well as the level of change. Both these parameters have been known to have an effect on fatigue lifetime and hence its estimation. Figure 120 shows typical loading-unloading patterns in fatigue testing. Spectral loading is of interest in wind turbines.

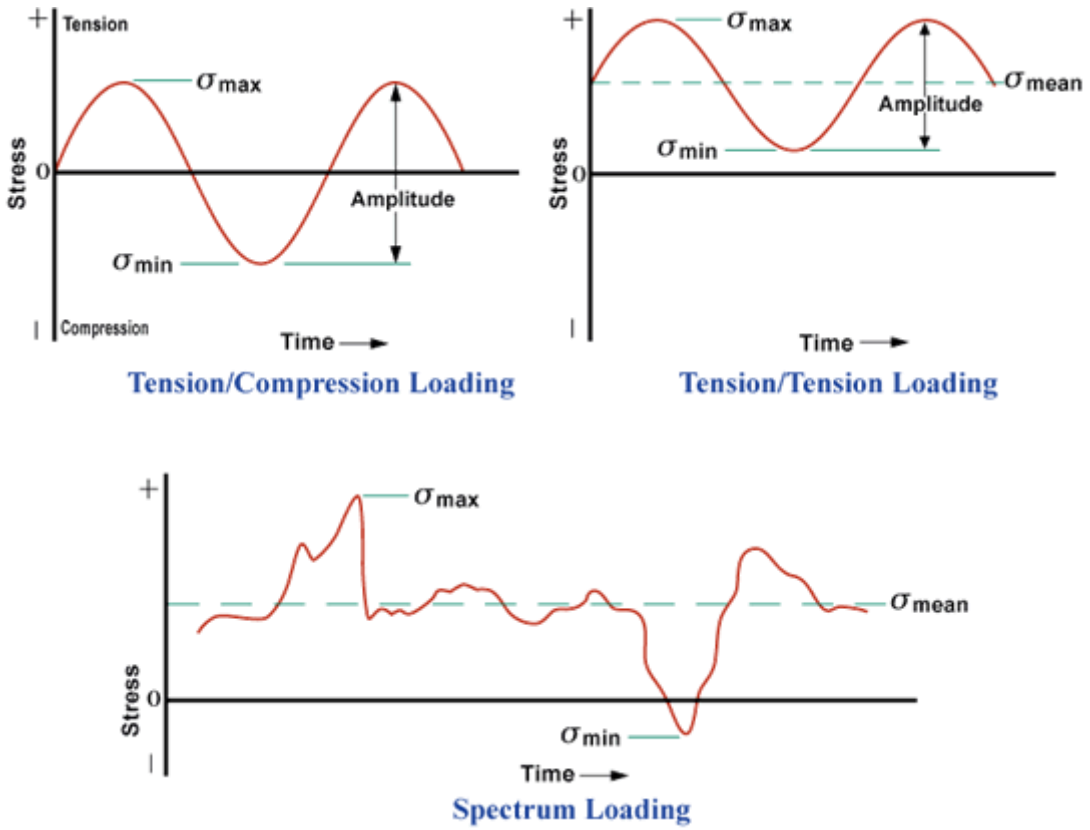

Figure 120 Fatigue loading patterns. Spectrum loading is of interest in wind turbines due to the variability of the wind. The direction of the wind should be taken into consideration since the nacelle may not be aligned to the optimum angle [Source of plots: NDE-ed.org].

The fatigue limit of different materials is described by the stress-number of loading cycles (S-N) curves. S-N curves can be severely affected by environmental conditions or in the case of rotating components lubrication quality. Figure 121 shows an example of how much the S-N plot can be altered in the presence of a corrosive medium. Similar or even more substantial effects can be anticipated in poor lubrication conditions.

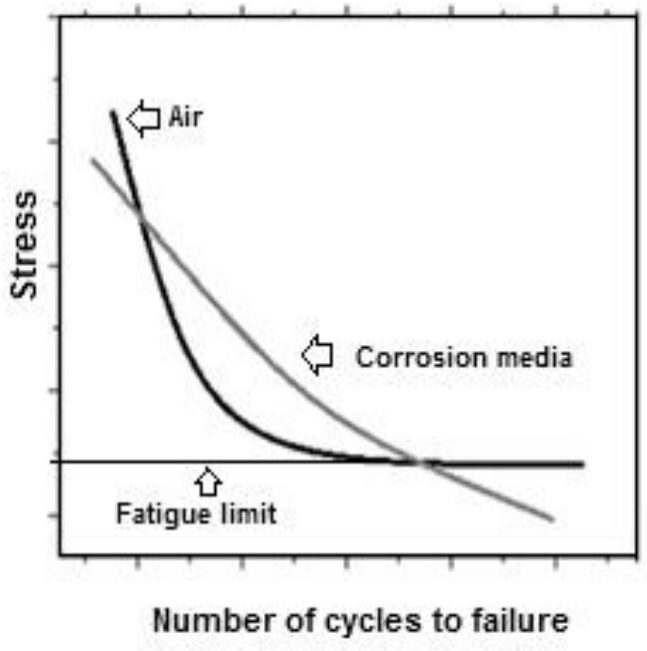

Figure 121 Figure 10.2: The effect of corrosion media in the S-N curve of a metal alloy [Source: Narciso Acu a-Gonz lez, Jorge A. Gonz lez-S nchez, Luis R. Dzib-P rez and Aar n Rivas-Mench].

10.2 RCM of wind turbine gearboxes

Since wind turbines operate under continuously variable loads and power output, it is very difficult to prognose the remaining lifetime of a particular component. Nonetheless, using acoustic emission, vibration and oil analysis it becomes possible to diagnose the location of the damage and its severity in a semi-quantitative manner.

The very well-known Miner's rule which popularised in 1945 Palgrem's hypothesis on linear damage originally suggested back in 1910 is inadequate for estimating the lifetime of gearbox

components or power converters. This is due to the inherent limitation of this algorithm in taking into account the sequence of events among other shortcomings.

Obviously considering Paris-Erdogan law and stress intensity factor calculation, a higher load at an early stage of damage initiation will have a completely different effect to the growth of a crack at a different time. Moreover, fatigue damage propagation is highly non-linear albeit in some cases, not concerning wind turbines, it may seem to be accumulating nearly linearly. This is due to the fact that events that cause damage in such cases are so scarce in time that damage accumulation does appear to be linear.

In reality in order to safely conclude even with a limited margin of accuracy the remaining lifetime the exact type of the material used and its surface treatment, its cleanliness, the quality of lubrication and wind load variability provided that the wind turbine is also pointing in the optimum direction need to be known.

Given the current knowledge gained from this project we have observed that AE is highly efficient in detecting and identifying damage much quicker and without the need for trending data as in vibration. Moreover, fewer positions are required in order to assess the entire drive-train. Another advantage is that low-speed components such as the main bearing and the main shaft especially in larger machines can be more readily monitored with AE sensors instead of accelerometers which need to be very low frequency in such cases.

Several wind turbine gearboxes have been monitored with the assistance of TERNA Energy also participating in the OPTIMUS FP7 consortium. The presence of defects and their severity have been successfully assessed and identified. However, to estimate the exact remaining

lifetime has been proven impossible at this stage. An example of one of the wind turbine gearboxes measured with AE is given next.

A three-stage planetary gearbox of an 850kW industrial wind turbine owned by TERNA Energy installed on the island of Crete, Greece, was instrumented using a customised 4-channel AE condition monitoring system. The customised data logger was created using Labview® developed by National Instruments. The acquired AE data were subsequently analysed using Matlab®.

Data were acquired over a period of time extending to a few days. Acquisition intervals were preset to take place every 10 minutes. The acquisition period was 12 seconds. The AE signal sampling rate was set at 500 kSamples/s. One Physical Acoustics Corporation (PAC) R50A AE sensor was installed on the main bearing. Ultrasonic coupling and adhesion of the sensor to the test surface were achieved simultaneously with the use of araldite. Three more R50A AE sensors were installed on the gearbox itself at the planetary, intermediate and high-speed stages. The AE signals were amplified using pre-amplifiers and amplifiers procured from PAC. The total gain was set at 58 dB. The photographs in figure 122 show the wind turbine and gearbox instrumented.

Figure 122 The 850 kW wind turbine and gearbox monitored using AE.

Figure 123 shows a raw AE signal acquired from the sensor installed at the planetary stage. From the numerous peaks present in the signal it is readily obvious that a defect is present.

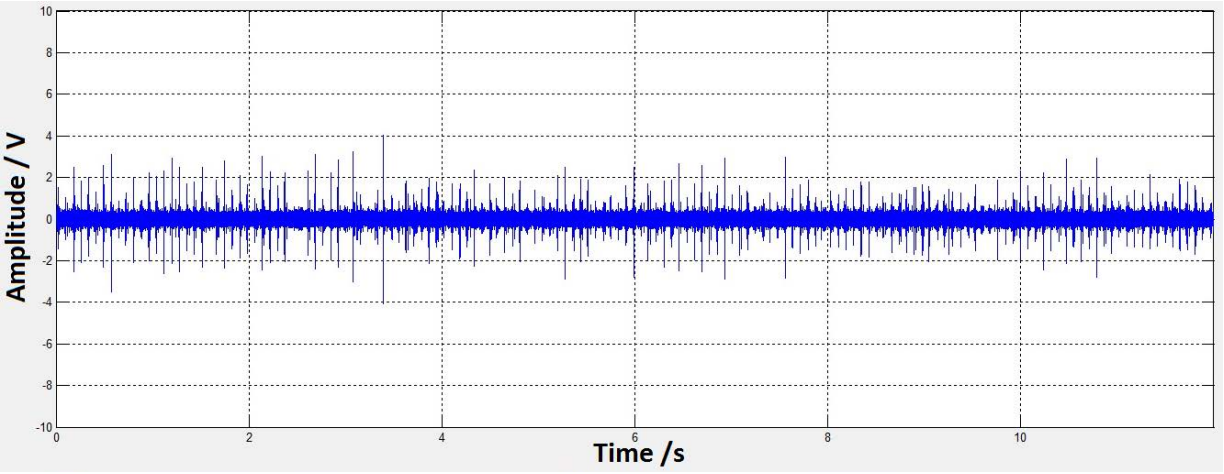

Figure 123 Raw AE signal acquired from the planetary stage sensor showing multiple regular peaks. This is an indication of a possible defect.

By looking into the power spectrum of the demodulated signal in figure 124 it was possible to ascertain that the planetary bearing had been damaged. This finding was later verified by the wind farm maintenance personnel.

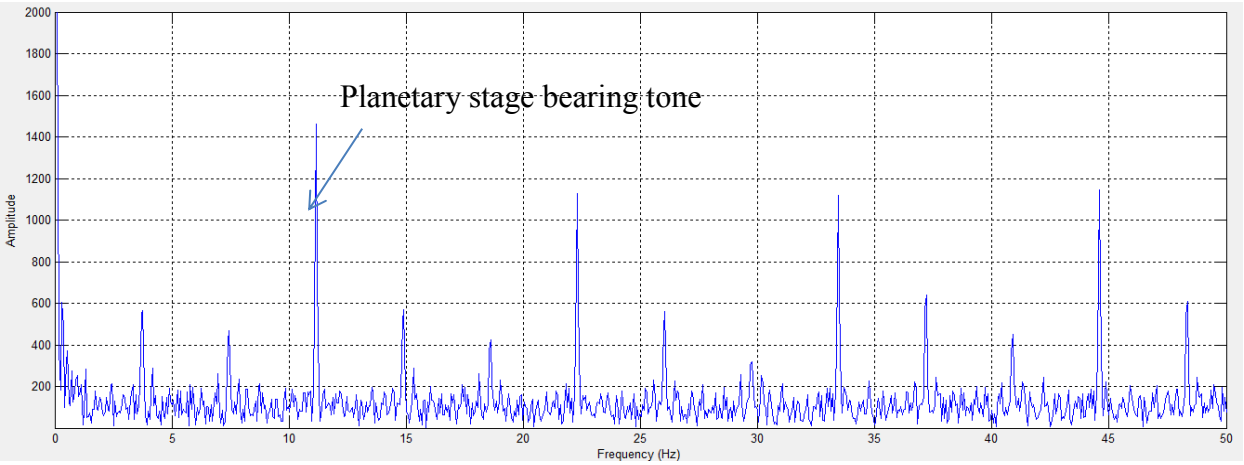

Figure 124 Low frequency power spectrum of the demodulated AE signal showing a planetary stage bearing defect with sidebands.

10.3 Wind turbine gearbox lifetime prognosis and approach to diagnosis

During their entire operational lifetime wind turbines are exposed to variable loading conditions which make extremely difficult prognosis. Although, it is possible to successfully establish the diagnosis methodology required and trend damage evolution, far more investigation is required in order to assess the remaining lifetime of wind turbine components that are subject to variable loading conditions.

It is thought that estimation of the risk of failure is more realistic enabling wind farm operators to choose proactive or semi-prognostic maintenance strategies during the low wind seasons. This can be achieved perhaps coupled with assessment of damage of removed spare parts.

AE combined with oil analysis may prove to be far more effective in assessing the drive-train damage than conventional vibration analysis. Misalignments identified in the drive-train should always be corrected as rapidly as possible. The problem of lubrication needs to be revisited more extensively by wind turbine manufacturers and gearbox designers. The effects of a defect to the rest of the system should be taken into account.

MHI-VESTAS V164 is a geared 9.5 MW wind turbine which has been designed specifically for offshore projects (figure 10.6). The basis of the MHI-VESTAS V164 wind turbine has been the V-112 machine. The V164 is currently the largest wind turbine ever built and has the highest power rating of all wind turbines commercially available. MHI-VESTAS V164 has already been selected for the 400 MW wind farm in the Horns Reef 3 project which is located off the coast of Denmark. Discussions to employ the MHI-VESTAS V164 model in other projects are ongoing. It is generally agreed that the decreasing electricity prices agreed for offshore wind farms will lead to larger devices being implemented widely by 2025. It is

expected that by 2025 the average cost per MWh produced will drop below €80. Dong recently agreed a sale price of €72.5/MWh in the Netherlands when a few years ago prices were more than double. For Borssele 1 & 2 Vattenfall gave an even lower price at €60/MWh. As prices drop, optimisation of OPEX will become critical for the future success of onshore and particularly offshore projects.

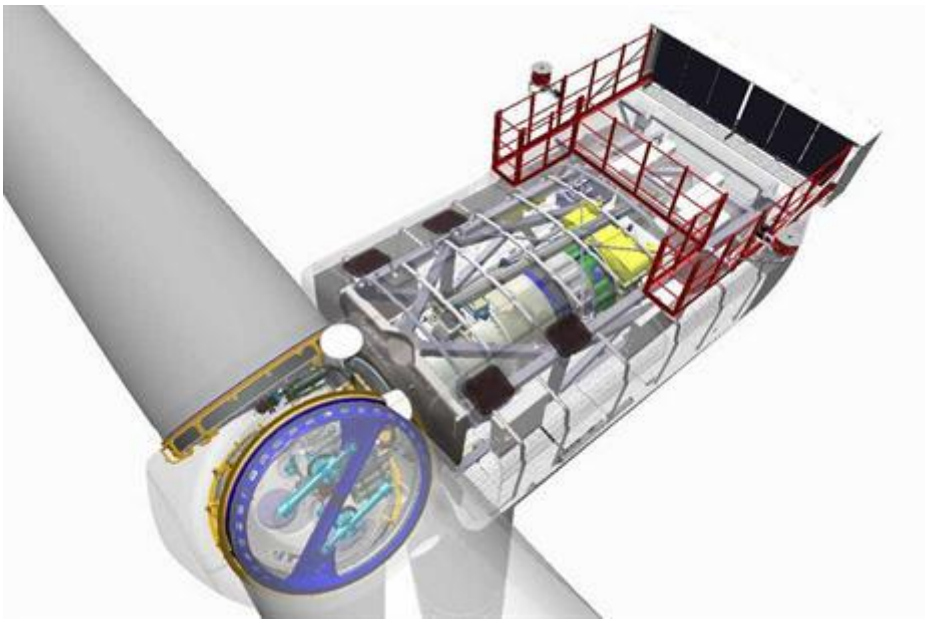

Figure 125 The MHI-VESTAS V164 nacelle [106]

The standards for RCM of wind turbines are considered to be somewhat vague. There is apparently not clear definition of what constitutes diagnosis and prognosis since the term condition-based maintenance is used to describe both. Unfortunately, several industrial stakeholders are unable to understand the difference between diagnosis and prognosis. For this reason, they also fail to understand the requirements that prognosis has in comparison with diagnosis. It is very important to clearly define what constitutes preventive, condition-based and predictive maintenance and the information required in order for these approaches to be implemented successfully. At the moment the industry largely relies on corrective and preventive maintenance approaches.

With reference the MHI-VESTAS V164 wind turbine it has been concluded based on the results obtained that for the instrumentation of the drive-train the following sensors will be required to monitor its operation:

For the main bearings, front and back, 2 AE sensors (one located on each bearing) with and operational frequency range of 100 - 700 kHz and optional 2 accelerometers (one for each bearing) with an operational frequency range of 0.05 Hz – 5 kHz. The selection of accelerometers should be based on the rotational speed of the component being measured. Since the rotor of the V-164 rotates very slowly (4.8-12.1RPM with nominal speed 10.5 RPM or 0.175 Hz) vibration measurements will only be satisfactory if the accelerometer has an appropriate low-end frequency range. The AE sensor does not have this limitation since it detects noise rather than vibration. Furthermore, AE measurements do not require trending of data. Therefore, vibration measurements are not really needed for the main bearing as the AE will perform better.

For the three-stage planetary medium speed gearbox (maximum RPM at generator ~400) 3 AE sensors (operational frequencies as main bearings), each placed at the planetary stage, intermediate and high-speed shaft and optional 5 accelerometers (various operational frequencies can be employed depending on the RPM) with 2 placed at the planetary stage, 1 at the intermediate stage and 1 at the high-speed stage.
For the generator 1 AE sensor and 2 optional accelerometers each placed on either side.

For automatic analysis, as long as the kinematics of the drive-train are known, from the AE measurements it is possible to immediately reveal whether there is a problem or not in any of

the rotating components. In case where the severity needs to be ascertained AE is particularly effective although the exact failure time cannot be estimated. However, the risk of failure within an operational period of six months could be ascertained within a reasonable level of confidence. In the case of vibration measurements alone, data trending will be required to process the available data and compare them with the good condition. The level of confidence is substantially increased by integrating vibration measurements with AE results. By trending maxima over time and using the slope information it is possible to estimate the level of deterioration with time. The CMS information can be supplemented with oil data where these are available. Further, improvement in the reliability of the analysis can be achieved by incorporating maintenance information as well as information regarding the actual materials used in the drive-train.

10.5 Summary

The gearbox of industrial wind turbines has been successfully monitored using both vibration analysis and acoustic emission techniques. In this chapter, a faulty gearbox using acoustic emission sensors only has been identified together with the component affected. The results obtained clearly demonstrate the capability of acoustic emission for monitoring large-scale industrial wind turbine gearboxes using less sensors than what would be required if vibration analysis was used instead. Moreover, the results also demonstrate that it is not necessary to employ traditional vibration measurements since acoustic emission can successfully detect defects of interest in the various bearings and gears in different stages. Finally, the signal processing methodology used for analysing acoustic emission data does not differ to the analysis methodology employed for vibration data.

CHAPTER 11

CONCLUSIONS AND FUTURE WORK

11.1 Conclusions

The importance of wind energy as a key renewable energy source in supporting the gradual decarbonisation of the global economy is undeniable. Hundreds of GW of installed capacity have already been realised whilst more projects are underway. Offshore wind farms are becoming more commonplace and their contribution to the energy mix more evident. However, wind turbines are complex systems and technologically they are still evolving.

Several studies investigating wind turbine failures and their cause have shown clearly that the power converter and the gearbox are two of the key components resulting in downtime and loss of production. Therefore, any unpredicted faults coupled with the remote locations that wind farms are normally built can incur significant amounts of additional expenditure in order to repair the faults and restore production. In extreme cases gearbox faults can cause catastrophic failure of the entire nacelle.

The importance of RCM is obvious in ensuring that faults can be diagnosed in time, so maintenance actions can be planned ahead. Although prognosis is desirable the stochastic nature of the operational conditions of wind turbines means that predictability is a complex tasks particularly when additional variables are taken into account.

In this study the failure modes and RCM methodology for wind turbine power converters and gearboxes have been investigated. Test rig simulations have been carried out to assess the effect of different damage modes to the RCM signals obtained for both power electronics and gearboxes. It has been revealed that failure occur randomly and with little or no warning in the case of power converters making life prediction estimation currently very challenging. However, in the case of gearboxes effective diagnosis appears to be within reach although the

effects of variable loading conditions can cause false alarms of overestimation of defects. The fatigue modes involved in the degradation of different materials used for the manufacturing of power electronics components such as IGBTs, and gearbox components such as bearings and gears need to be understood in more depth.

The present study also investigated RCM approaches for industrial wind turbines and compared the results obtained with those gathered from the simulations. Unfortunately, no faults were identified or detected in the two power converters monitored over a thirty month period using INDRA and INGETEAM commercial RCM systems. However, in the case of gearbox RCM the results have shown clearly the potential of the AE technique for effective diagnosis and the variables that need to be known in order to generate predictable meaningful lifetime models have been identified.

The experimental methodology employed under laboratory and field conditions has been presented and the limitations in current technology have been discussed. The link between laboratory simulations and field measurements has been analysed. The elusiveness of prognosing remaining lifetime has been proven and the variables that need to be considered have been qualitatively assessed. However, their contribution and link among them towards gradual degradation of power converter and gearbox components is yet to be quantitatively investigated. The importance of RCM has been clearly emphasised in ensuring the higher operational reliability of wind turbines.

11.2 Future work

Although significant aspects regarding the damage modes affecting power converter and gearbox components have been investigated in this study the quantification of the parameters leading to their gradual degradation is yet to be realised. The fact that it was impossible to

record any power converter failures during the RCM of the industrial wind turbines considered in this study has been a drawback. In order to address this further data over a larger number of wind turbines and over a longer period of time will be necessary.

The efficiency of the diagnostic methodology has been shown for assessing the actual condition of the wind turbine gearbox. However, in order to reach to the point where the remaining lifetime can be safely predicted far more information is required. Thus, future work should look into the link between materials quality in terms of mechanical properties, mechanisms of degradation, effect of variable loading conditions and inconsistent lubrication quality, RCM data and macroscopic and microscopic investigation of failed components.

The aforementioned work cannot be the subject of a single study and it should rather be conducted as a portfolio of several studies whose results can then be linked together in order to provide a better understanding of lifetime estimation. This study although it has demonstrated these aspects qualitatively, it has also shown the magnitude of the task that will need to be accomplished in order to enable prediction of the remaining lifetime at an acceptable level of accuracy. However, as the importance of wind energy increases further, the need to increase the reliability, availability, maintainability and productivity of wind farms will rise further. It is therefore imperative that the RCM capability continues to evolve as wind turbines also do with new models being rolled in every year capable of producing higher amounts of power but still facing similar technical challenges as older models.

References

1. P. Tchakoua, R. Wamkeue, M. Ouhrouche, F. Slaoui-Hasnaoui, T. A. Tameghe and G. Ekemb, "Wind Turbine Condition Monitoring: State-of-the-Art Review, New Trends, and Future Challenges," Energies, Vol. 7, pp. 2595-2630, 2014.
2. B. K. Bose, "Global Warming: Energy, Environmental Pollution, and the Impact of Power Electronics," IEEE Industrial Electronics Magazine, Vol. 4, No. 1, pp. 6-17, March 2010.doi: 10.1109/MIE.2010.935860
3. M. Asif, T. Muneer, "Energy supply, its demand and security issues for developed and emerging economies", Renewable and Sustainable Energy Reviews, Volume 11, Issue 7, 2007, Pages 1388-1413, ISSN 1364-0321
4. UN Framework Convention on Climate Change on Kyoto Protocol Reference Manual on Accounting of Emissions and Assigned Amount, January 2009.
5. G. Corbetta and T. Miloradovic, "Wind in Power, 2013 European statistics," EWEA Report, February 2014.
6. https://www.quora.com/How-do-wind-turbines-work. [Accessed 24 10 2017].
7. United Nations Climate Change Ad Hoc Working Group Report on Further Commitments for Annex I Parties under the Kyoto Protocol (AWG-KP), Bali, 2007.
8. J. Liu, Influence of Fluid Shear on Primary Nucleation of Organic Compounds in Solution, Ph.D. Thesis, Royal Institute of Technology, Stockholm, Stockholm, Sweden, 2002.
9. Juan Bueno Gayo, "Reliability-focused research on optimizing Wind Energy system design, operation and maintenance: Tools, proof of concepts, guidelines & methodologies for a new generation," RELIAWIND, 2008.
10. M. Papaelias, S. Hillmansen, P. Tricoli, J. Zhou, G. Fernando, F. P. G. Marquez, P. Diego and S. Kerkyras, "OPTIMUS D.1.1 report," OPTIMUS, 2014.

11. R. W. Hyers, J. G. Mcgowan, K. L. Sullivan, J. F. Manwell and B. C. Syrett, “Condition monitoring and prognosis of utility scale wind turbines,” Energy Materials, Vol. 1, pp. 187–203, September 2013.
12. R. Janssen, “Renewable Energy into the Mainstream,” IEA Renewable Energy, Netherlands, 2003.
13. Graham Sinden, Characteristics of the UK wind resource: Long-term patterns and relationship to electricity demand, Energy Policy, Volume 35, Issue 1, 2007,Pages 112-127, ISSN 0301-4215
14. S. Matthew, Wind Energy, Fundamentals, Resource Analysis and Economics, Springer-Verlag Berlin Heidelberg, 2006.
15. S. M. Kvarn, “panoramio,” 2006. [Online]. Available: http://www.panoramio.com/photo/34742170. [Accessed 21 01 2014].
16. R. W. Righter, Wind energy in America a History, Oklahoma: Oklahoma University, 1996.
17. K. Faitatzoglou, “Wind energy in Greece,” in Wind energy in Greece, CRES Presentations at ENERGYRES, Athens, 2008.
18. thefutureofthings.com, “The future of things,” [Online]. Available: www.thefutureofthings.com. [Accessed 25 4 2017].
19. “Wind turbine size increase 1980-2015.,” Wikimedia, 2015 5 20. [Online]. Available: https://commons.wikimedia.org/wiki/File:Wind_turbine_size_increase_1980-2015.png. [Accessed 2017 10 24].
20. M. A. Telles, Wind Energy: Technology, Commercial Projects and Laws, USA: Nova Science Publishers, 2006.

21. Kids, Alliant Energy, 2013. [Online]. Available: http://www.alliantenergykids.com/EnergyandTheEnvironment/RenewableEnergy/022397. [Accessed 23 01 2014].
22. "WWEA World Wind Energy Association," [Online]. Available: http://www.wwindea.org/technology/ch01/en/1_2_1_1_1.html. [Accessed 26 07 2014].
23. F. Katharina, S.Thomas, R. Hans and K. Robert, "Investigation of converter failure in wind turbines," Elforsk report, November 2012.
24. P. Musgrove, Wind Power, Cambridge: Cambridge University Press, February 2010.
25. K. Garus, "Sun and Wind energy," 16 02 2016. [Online]. Available: http://www.sunwindenergy.com/record-chinese-installations-drive-global-market-past-63-gw. [Accessed 24 10 2017].
26. P. Tchakoua, R. Wamkeue, M. Ouhrouche, F. Slaoui-Hasnaoui, T. A. Tameghe and G. Ekemb, "Wind Turbine Condition Monitoring: State-of-the-Art Review, New Trends, and Future Challenges," Energies, pp. 2595-2630., 22 April 2014.
27. L. Deyuan, Y. Zhiquan, B. Nengsheng and C. Yan, "Vibration modal analysis of the rotating rotor of horizontal axis wind turbine," Acta Energiae, vol. 25, pp. 2-77, 2004.
28. P. A. Joosse, M. J. Blanch, A. G. Dutton, D. A. Kouroussis, T. P. Philippidis and P. S. Vionis, "Acoustic emission monitoring of small wind turbine blades," Journal of Solar Energy Engineering, Vol. 124 (4), p. 456, 2002.
29. A. Hamilton and F. Quail, "Detailed state of the art review for the different online/inline oil analysis techniques in context of wind turbine gearboxes," Journal of Tribology, Vol. 133(4), p. 44001, 2011

30. Z. Hameed, Y. S. Hong, Y. M. Cho, S. H. Ahn and C. K. Song, “Condition monitoring and fault detection of wind turbines and related algorithms: A review”, Renewable and Sustainable energy reviews, Vol. 13(1), pp. 1-39, 2009.
31. E. Bossanyi, “Wind turbine control for load reduction,” Wind Energy, Vol. 6(3), pp. 229-244, 2003.
32. R. Raišutis, E. Jasiūnienė and E. Žukauskas, “Ultrasonic NDT of wind turbine blades using guided waves,” Ultrasound, Vol. 63, pp. 7-11, 2008.
33. G. Simone and F. Morabito, “NDT image fusion using eddy current and ultrasonic data”, COMPEL-The international journal for computation and mathematics in electrical and electronic engineering, Vol. 20(3), pp. 857-868, 2001.
34. F. P. rquez, A. Tobias, J. M. P rez and Mayorkinos Papaelias, “Condition monitoring of wind turbines: Techniques and methods”, Renewable Energy, Vol. 46, pp. 169-178, 2012.
35. Li Zhen, He Zhengjia, Zi Yanyang, Chen Xuefeng, “Bearing condition monitoring based on shock pulse method and improved redundant lifting scheme”, Mathematics and Computers in Simulation, Volume 79, Issue 3, 2008, Pages 318-338, ISSN 0378-4754
36. Anca D. Hansen, Gabriele Michalke, “Fault ride-through capability of DFIG wind turbines”, Renewable Energy, Volume 32, Issue 9, 2007, Pages 1594-1610, ISSN 0960-1481
37. J. Rafiee, F. Arvani, A. Harifi and M. H. Sadeghi, “Intelligent condition monitoring of a gearbox using artificial neural network,” Mechanical systems and signal processing, Vol. 21(4), pp. 1746-1754, 2007

38. Andrew Kusiak, Anoop Verma, “Analyzing bearing faults in wind turbines: A data-mining approach, Renewable Energy”, Volume 48, 2012, Pages 110-116, ISSN 0960-1481
39. B. Lu, Y. Li, X. Wu and Z. Yang, "A review of recent advances in wind turbine condition monitoring and fault diagnosis," 2009 IEEE Power Electronics and Machines in Wind Applications, Lincoln, NE, pp. 1-7, 2009.
40. H. Arabian-Hoseynabadi, H. Oraee and P. J. Tavner, “Failure modes and effects analysis (FMEA) for wind turbines,” International Journal of Electrical Power & Energy Systems, Vol. 32(7), p. 817_824, 2010.
41. F. Zare, "EMC and modern power electronic systems Section 1: Introduction," 2008 IEEE International Symposium on Electromagnetic Compatibility, Detroit, MI, 2008, pp. 1-10.
42. K. Fischer, T. Stalin, T. Stalin, H. Ramberg and R. Karlsson, “Investigation of converter failure in wind turbines: A pre-study,” Elforsk report, November 2012.
43. M. Boettcher and F. W. Fuchs, "Power electronic converters in wind energy systems — Considerations of reliability and strategies for increasing availability," Proceedings of the 2011 14th European Conference on Power Electronics and Applications, Birmingham, 2011, pp. 1-10.
44. J. B. Gayo, “Reliability-focused research on optimizing Wind Energy system design, operation and maintenance: Tools, proof of concepts, guidelines & methodologies for a new generation,” Gamesa Innovation and Technology, 14 March 2011.
45. M. Sahnoun, F. Bagui and M. Messaadia, “Failure analysis of onshore wind farms based on experimental data,” in Mediterranean Conference on Information & Communication Technologies’2015, Morocco, 2015.

46. A. Karyotakis, “On the Optimisation of Operation and Maintenance Strategies for Offshore Wind Farms,” Ph.D. Thesis, Department of Mechanical Engineering University College London, London, 2011.
47. M. Wilkinson, “Final Publishable Summary of Results of Project ReliaWind,” RELIAWIND, Brussels, March 2011.
48. Jurgen Schmid, Institut für Solare Energieversorgungstechnik, Annual Institute Report,,” ISET, Development and Results for years 2002, 2003, 2004, 2005 and 2006.
49. M.Trivedi, S.Pendharkar and K.Shenai, “High temperature performance limits of IGBT modules, 33rd Industry application,” in The 1998 IEEE Industry Applications Conference, St. Louis, MO, USA, 1998.
50. K. Fischer, T. Stalin and H. Ramberg, “Field-Experience Based Root-Cause Analysis of Power-Converter Failure in Wind Turbines,” IEEE Transactions on Power Electronics, vol. 30, no. 5, pp. 2481 - 2492, November 2012.
51. F. Didactic, “PRINCIPLES OF DOUBLY-FED INDUCTION GENERATORS (DFIG),” Lt e/Ltd, Quebec, Canada, 2011.
52. R. Pena, J. Clare and G. Asher, “Doubly fed induction generator using back-to-back PWM converters and its application to variable-speed wind-energy generation,” IET, vol. 143, no. 3, p. 231 –241, May 1996.
53. M. L. Doumbia, K. Belmokhtar and K. Agbossou, “New Developments in Renewable Energy",” in Wind Diesel Hybrid Power System with Hydrogen Storage, Québec, Canada, 2013, p. chapter15.
54. Paul Gipe, Wind Power, James & James, 2004.

55. F. Blaabjerg, M. Liserre and K. Ma, "Power Electronics Converters for Wind Turbine Systems," IEEE Transactions on Industry Applications, vol. 48, no. 2, pp. 708-719, March-April 2012.
56. A. Sattar, “Insulated Gate Bipolar Transistor (IGBT) Basics,” IXYS Corporation. IXAN0063, 1998.
57. R. Alvarez, F. Filsecker and S. Bernet, "Comparison of press-pack IGBT at hard switching and clamp operation for medium voltage converters," Proceedings of the 2011 14th European Conference on Power Electronics and Applications, Birmingham, 2011, pp. 1-7.
58. Fuji electric Co., “IGBT troubleshooting and failure analysis,” [Online]. Available: http://www.fujielectric.com/products/semiconductor/technical/application/box/doc/REH984b/REH984b_04a.pdf. [Accessed 06 05 2014].
59. Nathan Valentine, Diganta Das and Michael Pecht, “Failure Mechanisms of Insulated Gate Bipolar Transistors (IGBTs),” Center for Advanced Life Cycle Engineering (CALCE), pp. 1-30, 2015.
60. M. Trivedi and K. Shenai, "Investigation of the short-circuit performance of an IGBT,” IEEE Transactions on Electron Devices, Vol. 45, no. 1, pp. 313-320, Jan 1998.
61. V. Smet et al., "Ageing and Failure Modes of IGBT Modules in High-Temperature Power Cycling," IEEE Transactions on Industrial Electronics, Vol. 58, no. 10, pp. 4931-4941, Oct. 2011.
62. Ke Ma, Marco Liserre and Frede Blaabjerg, “Thermal Loading and Lifetime Estimation for Power Device Considering Mission Profiles in Wind Power Converter,” IEEE Transactions on Power Electronics, Vol. 30, no. 2, pp. 590 - 602, March 2014

63. M. Musallam and C. M. Johnson, “An Efficient Implementation of the Rainflow Counting Algorithm for Life Consumption Estimation,” IEEE Transactions on Reliability, Vol. 61, no. 4, pp. 978 - 986, December 2012.
64. K. Mainka, “www.infineon.com/power,” POWER MODULES, 2011. [Online]. Available: http://www.power-mag.com/pdf/feature_pdf/1319730265_Infineon0611_Layout_1.pdf. [Accessed 27 07 2014].
65. Xavier Perpina, Xavier Jorda and Miquel Vellvehi, “Long-Term Reliability of Railway Power Inverters Cooled by Heat¬ Pipe-Based Systems,” IEEE Transactions on Industrial Electronics, Vol. 58, no. 7, pp. 2662 - 2672, July 2011.
66. John Wægter, “Stress range histories and Rain Flow counting,” p. 13, June 2009.
67. Julie A. Bannantine, Fundamentals of metal fatigue analysis, New Jersey: Englewood Cliffs (NJ): Prentice-Hall, 1990.
68. L. GopiReddy, L. M. Tolbert and B. Ozpineci, "Lifetime prediction of IGBT in a STATCOM using modified-graphical rainflow counting algorithm," IECON 2012 - 38th Annual Conference on IEEE Industrial Electronics Society, Montreal, QC, 2012, pp. 3425-3430
69. S. D'Arco, T. M. Undeland, M. Bohlländer and J. Lutz, “A Simplified Algorithm for Predicting Power Cycling Lifetime in Direct Drive Wind Power Systems,” in Norwegian University of Science and Technology NTNU, Trondheim, Norway, 2010.
70. S. Ariduru, “Fatigue Life Calculation by Rainflow Cycle Counting Method,”, Thesis Natural and Applied Sciences of Middle East Technical University, 2004.
71. M. A. Miner, “Cumulative Damage in Fatigue,” Journal of Applied Mechanics, Vol. 12, pp. 159-164, 1945.

72. Jesús María Pinar Pérez, Fausto Pedro García Márquez, Andrew Tobias and Mayorkinos Papaelias, “Wind turbine reliability analysis,” Renewable and Sustainable Energy Reviews, vol. 23, pp. 463-472, 2013.
73. H. Polinder, F. F. A.Van der Pijl and G.-J. de Vilder, “Comparison of Direct-Drive and Geared Generator Concepts for Wind Turbines.,” EEE Transactions on Energy Conversion, Vol. 21, no. 3, pp. 725-733, August 2006.
74. K. He, Z. Fang, D. Zhu, C. Huang and X. Yang, “The Application of Simulation Technique on Gearbox Design,” in 2009 International Conference on Measuring Technology and Mechatronics Automation, Zhangjiajie, Hunan, China, 2009.
75. P. J. Tavner and G. J. W. V. Bussel, “Machine and Converter Reliabilities in Wind Turbines,,” in In Proceedings of IET 3rd International Conference on Power Electronics, Power Electronics, Machines and Drives, Dublin, Ireland, March 2007.
76. M. Karimirad, Offshore Energy Structures For Wind Power, Wave Energy and Hybrid Marine Platforms, Springer International Publishing, 2014.
77. “olympus,” Inspections of Wind Turbine Gearboxes, [Online]. Available: olympus-ims.com/en/applications/rvi-wind-turbine/. [Accessed 27 10 2017].
78. M. A. J. Somers, K. V. Dahl and T. L. Christiansen, “Failure Analysis and Thermochemical Surface Engineering of Bearings in the Wind Turbine Drivetrain,” Technical University of Denmark, 2014.
79. W. Musial, S. Butterfield and B. McNiff, “Improving wind turbine gearbox reliability,” in NREL National Renewable Energy Laboratory, Milan, Italy, 2007.
80. K. Smolders, H. Long, Y. Feng and P. Tavner, “Reliability analysis and prediction of wind turbine gearboxes,” in European Wind Energy Conference (EWEC), Warsaw, Poland, 2010.

81. Y. Xie, Gao Zhifei, Tang Ke, Zeng Mingjie and Wang Yonghai, "Wind turbine gearbox condition monitoring system based on vibration signal," 2015 12th IEEE International Conference on Electronic Measurement & Instruments (ICEMI), Qingdao, 2015, pp. 159-163.
82. M. Laplante, Carburizing Wind-Turbine Gears, Gear Solutions, 2009.
83. D. Herring, Heat Treating Heavy-Duty Gears, Gear Solutions, 2007.
84. D. Ancona and J. McVeigh, "Wind Turbine - Materials and Manufacturing Fact Sheet," Prepared for the Office of Industrial Technologies, US Department of Energy By Princeton Energy Resources International, LLC., 2001.
85. A. Lei, Jing Lin, Ming J. Zuo, Zhengjia He, "Condition monitoring and fault diagnosis of planetary gearboxes: A review", Measurement, Volume 48, 2014, Pages 292-305, ISSN 0263-2241,
86. M. Moon, "Lubricant contaminants limit gear life", Machinery Lubrication Magazine, 2008.
87. R. Errichello and J. Muller, "Application requirements for wind turbine gearboxes", NREL Report, California, 1994.
88. M. Nie, "Review of condition monitoring and fault diagnosis technologies for wind turbine gearbox." Procedia CIRP, vol. 11, pp. 287-290, 2013.
89. X. W. PH.D and B. Fang, "Vibration-based Health Monitoring of Damaged Bevel Gears Using ADAMS," in Regional User Conference, California, 2013.
90. W. M. Needelman, M. A. Barris and G. L., "Contamination Control for Wind Turbine Gearboxes," Power Engineering, vol. 11, p. 112, 2009.
91. V. J. Junior, J. Zhou, S. Roshanmanesh, F. Hayati, S. Hajiabady, X. Y. Li, H. Dong and M. Papaelias, "Evaluation of damage mechanics of industrial wind turbine gearboxes," Insight, Vol. 59, no. 8, pp. 410-414, 2017

92. R. González-Carrato, F. P. G. Márquez, K. Alexander and M. Papaelias, “Demonstration of Methods and Tools for the Optimisation of Operational Reliability of Large-Scale Industrial Wind Turbines,” PROJECT DELIVERABLE REPORT OPTIMUS, 2014.
93. J. Ribrant and L. M. Bertling, "Survey of Failures in Wind Power Systems With Focus on Swedish Wind Power Plants During 1997–2005," IEEE Transactions on Energy Conversion, vol. 22, no. 1, pp. 167-173, March 2007.
94. M. Ben-Daya, S. O. Duffuaa, A. Raouf, J. Knezevic, D. Ait-Kadi, “Handbook of maintenance management and engineering”, 2009.
95. Y. Feng, P. Tavner and H. Long, “Early experiences with UK Round 1 offshore wind farms,” Proceedings of the Institution of Civil Engineers: Energy, vol. 163, no. 4, pp. 167-181. 2010.
96. R&D Examples Presentation, May 2012.
97. H. Chen, X. Wang, H. Gao2 and F. Yan, “Dynamic characteristics of wind turbine gear transmission system with random wind and the effect of random backlash on system stability,” Proceedings of the Institution of Mechanical Engineers, Part C: Journal of Mechanical Engineering Science, vol. 231, pp. 2590-2597, 2013.
98. J. Muller and R. Errichello, “Oil cleanliness in wind turbine gearboxes.” Machinery Lubrication, vol. 4, no. 2, pp. 34-40, 2002.
99. J. L. Chacon, Estefania Artigao Andicoberry, Vassilios Kappatos, G. Asfis, Tat-Hean.Gan and Wamadeva Balachandran, “Shaft angular misalignment detection using acoustic emission,,” Applied Acoustics, vol. 85, pp. 12-22, November 2014.
100. F. Spinato, P. Tavner and G. V. Bussel, “Reliability of wind turbine subassemblies,” IET, Vol. 3, no. 4, pp. 387 - 401, 2009.

101. “automation direct,” System Integrator Program VARS & International Sales, [Online]. Available: https://www.automationdirect.com/adc/Overview/Catalog/Process_Control_-a-_Measurement/Temperature_Sensors_-a-_Transmitters. [Accessed 28 10 2017].

102. F. P. G. Marquez, “Assessment of condition monitoring systems employed,” OPTIMUS, 2014.

103. STMicroelectronics, “L6384E- High-voltage half bridge driver,” 2007.

104. L. reserves, “lA25-NP Current Transducer,” LEM, 2011.

105. D. A. I. Company, “chipKIT™ uC32™ Board Reference Manual,” July 17, 2012.

106. E. d. Vries, “wind power monthly,” 9 September 2013. [Online]. Available: http://www.windpowermonthly.com/article/1211056/close-vestas-v164-80-nacelle-hub. [Accessed 01 11 2017].

107. M. Entezami, Ph.D. Thesis, University of Birmingham, Birmingham, 2013.

108. D. Pheteplace, “Facts & Figures: Wind Turbine Power Market Report,” 2014.

109. D. I. Batarseh, “The Florida Power Electronics Center,” [Online]. Available: http://floridapec.engr.ucf.edu/workshops/nsf1999/presentations/batarseh/sld002.htm. [Accessed 04 12 2015].